Enhancement of Treatment System for Waste Activated Sludge and Methane Cogeneration Using Iron-based Nanoparticles

タレク ワ モ アメン

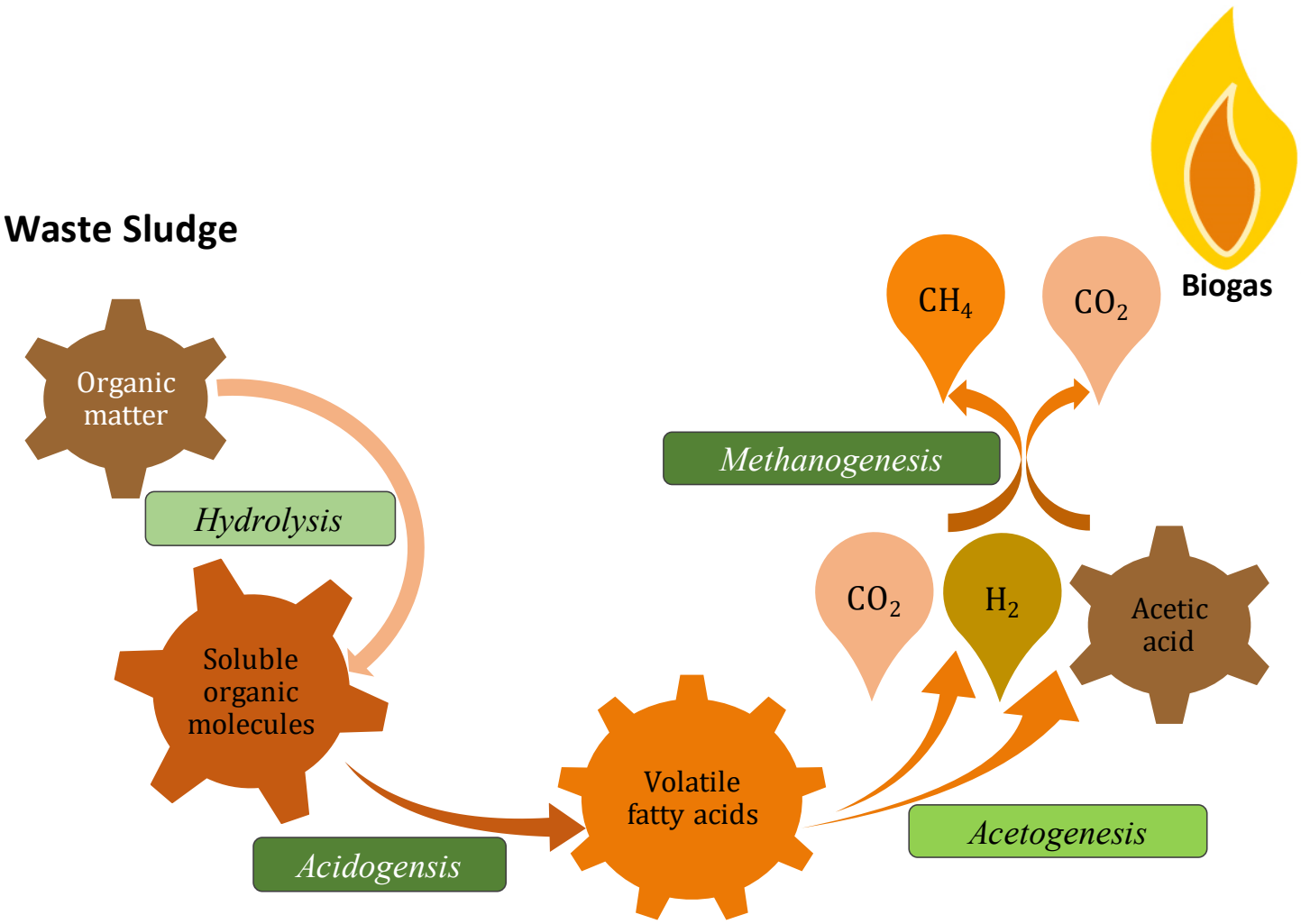

Enhancement of Treatment System for Waste Activated Sludge and Methane Cogeneration Using Iron Nanoparticles

Tareq W M Amen

九州大学
KYUSHU UNIVERSITY

Thesis on

Enhancement of Treatment System for Waste Activated Sludge and Methane Cogeneration Using Iron Nanoparticles

By

Tareq W M Amen

Supervised by

Associate Professor Osama Eljamal

A thesis submitted in partial fulfillment of the requirements for the degree of

Doctor of Engineering

Department of Earth System Science and Technology

Interdisciplinary Graduate School of Engineering Sciences

Kyushu University

Japan

September 2018

Dedication

To my family that is growing

Abstract

Employment of the nanoscale zero-valent iron (nZVI) in bioenergy enhancement is a prospective application for increasing the biogas generation process for better economy of sludge treatment. The nZVI and its modifications were applied for enhancement of the anaerobic digestion process as the core treatment process used universally to stabilized waste activated sludge. Several parameters of the sludge and the produced gas compositions have been tracked throughout the anaerobic digestion duration. These include biogas production, biogas composition as methane content and carbon dioxide content, total alkalinity, ammonium nitrogen, chemical oxygen demand, bacterial population and the emitted iron ions. The utilized nZVI stock suspension was freshly synthesized based on the optimal reduction method and the nZVI has a mean diameter less than 42 nm with an average shell thickness in a range 2-3 nm and the average surface area of 25 m^2/g, moreover, bimetallic of copper-nZVI (nZVI/Cu^0) and nZVI coated zeolite materials (ICZ) were also employed for more clarification and comparisons. Municipal wastewater and the waste activated sludge samples were collected from a domestic wastewater treatment plant with domestic manure as the substrate.

Synthesized additives were characterized and its kinetics and adsorption capacities were determined, subsequently, the toxicity effects on the wastewater microbial life, kinetics of phosphorus, ammonia stripping and the reduction of chemical oxygen demand were examined by the addition of different concentrations of nZVI and nZVI/Cu^0 under both aerobic and anaerobic operation conditions. Anaerobic laboratory scale bio-digester system was assembled and operated to study the effects of iron-based nanoparticles on biogas generation and methane content. The results show that high concentrations of nZVI/Cu^0 nanoparticles added to the wastewater mixed cultures enhance the bacterial life indicated that the copper, which planted onto the nZVI produce more Fe^{2+} ions which play a crucial role in the limitation of ammonium production and phosphorus concentrations during biological and chemical degradation processes of the domestic wastewater.

Moreover, the addition of nZVI stimulates the biogas production and methane gas content, and can accelerate the sludge fermentation. However, according to the experimental results, it is advisable to dose the optimum nZVI/Cu^0 bimetallic not more than 1500 mg/L, while the cell disruption will occur and other gases such as hydrogen will be rapidly

produced hence, the methanogenesis inhibition will be intentionally turned up. The addition of ICZ causes a lag period before starting to produce a significant biogas cogeneration that reached a maximum value compared with the other bioreactors. The higher the iron particles coated zeolite were added, the more the biogas was generated. Finally, the nZVI presence in a bio-digester could effectively improve the performance of sulfate-containing sludge digestion because it can serve as an electron donor that could mitigate the competition between sulfate-reducing bacteria and methanogenic bacteria for the same substrates. Also, it can precipitate the content of un-dissociated hydrogen sulfide that is the main factor inhibiting anaerobic digestion of sulfate-containing sludge.

Taken as a whole, it is predicted that this kind of treatment technology may hold promise to be applied in the anaerobic treatment of waste activated sludge and decrease the high costs of construction and operation of normal treatment plants. These outcomes are very interesting for carrying out the full-scale treatment of sludge substrates.

Acknowledgments

I would like to start by acknowledging the significant contribution that associate professor Osama Eljamal has made to my work and my life in Japan. Professor Eljamal was an example of work-life balance and was extremely supportive in the more difficult parts of my studies.

I wish to express my gratitude to those who have contributed to the completion of this thesis work in one way or another:

- Professor Nobuhiro MATSUNAGA, who is the head of environmental and fluid sciences, for unlimited support.
- All my former and present colleagues both Japanese and international students for sharing expertise, collaborating and supporting, especially, Dr. Ahmed Khalil who is now an assistant professor at Cairo University, Eygpt, for technical help during the experiment works; Seiya TAKAMI, and many other graduate students, for sharing the pleasant working atmosphere.
- All my friends in Japan, for always being friendly and helpful, especially Fukuoka Muslims community for accepting me as one of the community members.

I would like to acknowledge the Japanese Ministry of Education, Culture, Sports, Science, and Technology (MEXT) for financially supporting the PhD study and for the opportunity and support they gave me.

I'm ever thankful to my loving family for their constant understanding and support. I'm especially thankful for my supportive and wonderful wife, whose her patience and love is a constant source of happiness and renewal, Thanks for always believing in me.

Tareq W M Amen

Fukuoka, Japan

Acronyms, Abbreviations, and Notations

AD	Anaerobic Digestion
Ar^{3+}	Arsenite
Ar^{5+}	Arsenate
BET	Brunauer, Emmett and Teller
BOD_5	5-day Biological Oxygen Demand (composition measurement)
CCD	Charge Coupled Device
CFU	Colony Forming Unit
CH_4	Methane (chemical compound)
CO_2	carbon dioxide (chemical compound)
COD	Chemical Oxygen Demand
Cr^{2+}	Chromium (II)
DNA	Deoxyribo Nucleic Acid
E^0	Electrode Potentials
EDX	Energy-Dispersive X-ray Spectroscopy
e.g.	for instance, for example
Eq.	Equation
Fe^{2+}	Iron in reduced form (ferrous) (chemical compound)
Fe^{3+}	Iron in reduced form (ferric) (chemical compound)
FEG	Field Emission Gun
GC	Gas Chromotography
HAADF	High Angle Annular Dark Field
HRT	Hydraulic Retention Time
i.e.	id est, in other words
IMZ	Iron mixed zeolite
ICZ	Iron coated zeolite ICZ
MLSS	Mixed liquor suspended solids
µZVI	Microscale Zero Valent Iron
N	Nitrogen (chemical element)
NH_4^+	Ammonium (chemical compound)
NO_3^-	Nitrate (composition measurement)
nZVI	Nanoscale Zero Valent Iron
$nZVI/Cu^0$	Iron/Copper Bimetallic Nanoparticles

ORP	Oxidation/Reduction Potential
PNP	p-nitrophenol
PO_4^{2-}	Ortho-phosphate (chemical compound)
PRB	Permeable Reactive Barrier
R^2	Regression Coefficient of Determination
R1 to R7	Anaerobic, anoxic reactor (process unit)
Redox	Reduction-oxidation
ROS	Reactive Oxygen Species
S_D	Standard Deviation
SO_4^{2-}	Sulfate (chemical compound)
SRB	Sulfate Reducing Bacteria
SSA	Specific Surface Area
T	Temperature
TCE	Trichloroethylene
TEM	Transmission Electron Microscopy
TCD	Thermal Conductivity Detector
TS	Total Solids
USA	United States of America
US EPA	American Environmental Protection Agency
VS	Volatile Solids
WAS	Waste Activated Sludge
WHO	Water Health Organization
WWTP	Wastewater Treatment Plant
XRD	X-Ray Diffraction
ZVI	Zero Valent Iron
<	smaller than
>	larger than

Table of Contents

List of Figures

List of Tables

Thesis Declaration

I'm, Tareq W M Amen, hereby declare that all the data described in this thesis are results of my research work unless otherwise acknowledged or referenced. This thesis is submitted in partial fulfillment of the requirements for the award of Doctor of Engineering, in the department of Earth System Science and Technology (ESST) at Interdisciplinary Graduate School of Engineering Sciences (IGSES), Kyushu University, Japan.

Preface

This thesis is the results of my PhD study conducted at the laboratory of environment and fluid sciences at the department of earth system science and technology of Kyushu University from October 2015 to Septemeber 2018. The research studies were carried out under the supervision of associate professor Osama Eljamal.

The following manuscripts list was prepared during the study.

❖ Publications in Journals

1. **Amen, T.**, Eljamal O., Khalil, A., Matsunaga, N., Evaluation of nano zero valent iron effects on fermentation of municipal anaerobic sludge and inducing biogas production, IOP Conference Series: Earth and Environmental Science, Vol. 67, article number 012004, (June, 2017).
2. **Amen, T.**, Eljamal O., Khalil, A., Matsunaga, N., Biochemical methane potential enhancement of domestic sludge digestion by adding pristine iron nanoparticles and iron nanoparticles coated zeolite composition, Journal of Environmental Chemical Engineering, Vol. 5, Issue. No. 5, 5002-5013. (Oct., 2017).
3. **Amen, T.**, Eljamal O., Khalil, A., Matsunaga, N., Wastewater degradation by iron/copper nanoparticles and the microorganism growth rate, Journal of Environmental Sciences, Accepted, Corrected proof, Available online 7. (Feb, 2018).
4. **Amen, T.**, Eljamal O., Khalil, A., Matsunaga, N., Methane yield enhancement by the addition of new novel of iron and copper-iron bimetallic nanoparticles, Chemical Engineering and Processing: Process Intensification Journal, Vol. 130, 253-261. (June, 2018).
5. **Amen, T.**, Eljamal O., Khalil, A., Matsunaga, N., Evaluation of sulfate-containing sludge stabilization and the alleviation of methanogenesis inhibitation at mesophilic temperature, Journal of Water Process Engineering, Vol. 25, 212-221. (October, 2018).

❖ Conference presentations

1. **Amen, T.**, Eljamal O., Application of bimetallic nanoparticles during activated sludge digestion at high iron concentrations, International Symposium on Earth Science and Technology, Fukuoka, Japan, December, 2017.

2. **Amen, T.**, Eljamal O., Anaerobic Digestion Enrichment by Iron-Coated Zeolite, The 19th cross straits symposium on energy and environmental science and technology (CSS-EEST19), Fukuoka, Japan, November 2017.
3. **Amen, T.**, Eljamal O., Khalil, A., Matsunaga, N., Potential catalytic effect of bimetallic nanoparticles on digestion of anaerobic activated sludge, 3rd International Exchange and Innovation Conference on Engineering and Sciences (IEICES), Fukuoka, Japan, October, 2017.
4. **Amen, T.**, Eljamal O., Khalil, A., Matsunaga, N., Evaluation of nano zero valent iron effects on fermentation of municipal anaerobic sludge and inducing biogas production, 7th International Conference on Environment and Industrial Innovation (ICEII), Kuala Lumpur, Malaysia, April 2016.
5. **Amen, T.**, Eljamal O., Khalil, A., Sugihara Y., Matsunaga, N., Functionality of nanoscale zero-valent iron into domestic wastewater treatment and the role of microorganisms, IV. International Chemical Engineering and Technologies Conference (CHEMTECH '16), Istanbul, Turkey, November 2016.
6. **Amen, T.**, Eljamal O., Khalil, A., Sugihara Y., Matsunaga, N., Effects of iron metal on the chemical oxygen demand removal, phosphorus adsorption, and viable bacteria in domestic wastewater, 2nd International Exchange and Innovation Conference on Engineering and Sciences (IEICES), Fukuoka, Japan, October 2016.

CHAPTER 1

INTRODUCTION

Chapter 1. Introduction

1.1 Background

Anaerobic digestion is a complicated biochemical process that converts complex organic wastes or sludge into a mixture of methane, carbon dioxide gas and other residuals, this mixture is called biogas [1]. Biogas is considered as a renewable energy, which ensures more energy supply as clean, secure and continuous resource. It can be used instead of fossil fuel in various engineering applications as generate electricity and can decrease the running cost of wastewater treatment plants (WWTPs).

During the treatment of wastewater, municipal WWTPs generate sludge as a by-product of the physical, chemical and biological processes used during the treatment. Sludge usually contains mainly water (95%-99%) and separates that mostly putrescible organic matter. The stabilization and disposal of sludge is a problem which representing more than 50% of the operation costs of WWTPs. The generated sludge must subject some treatment in order to eliminate its volume, to reduce the associated health hazardous problems and to improve its character to meet the disposal acceptance regulations. The sludge treatment means, (i) firstly, reduce the water content of the raw sludge, and (ii) transform the biodegradable organic matter into inert or relatively stable organic and inorganic residue. The digesters as one of the crucial facilities inside municipal wastewater treatment plants are used for treating the sludge, which is capable of stabilizing the sludge and producing biogas as a clean renewable energy source [2, 3].

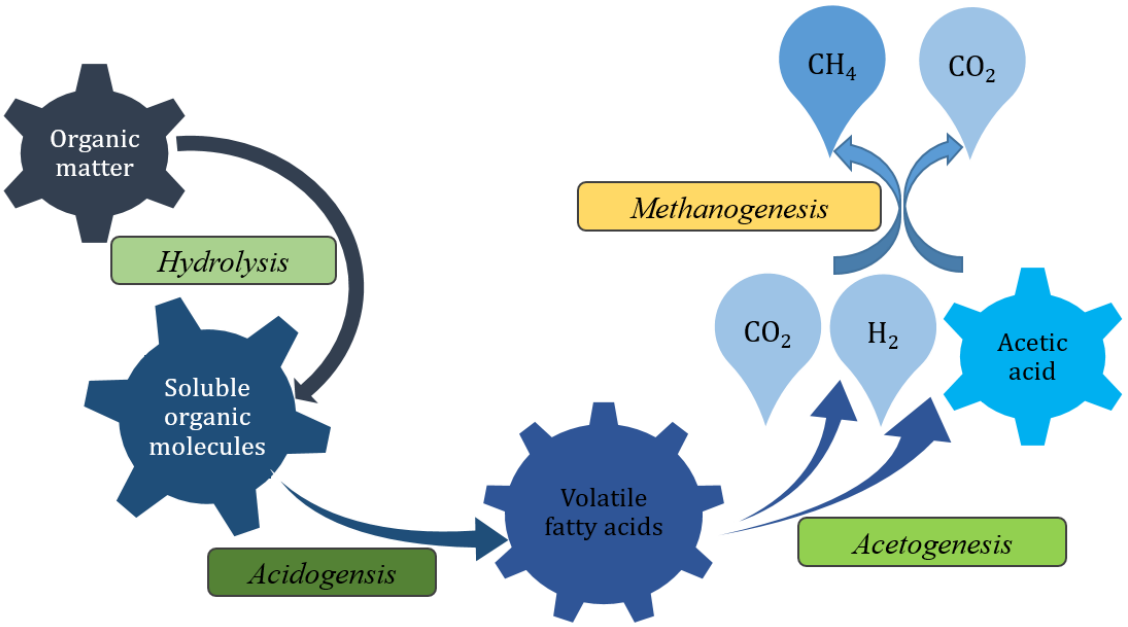

Figure 1.1 Anerobic digestion process (redrawn)

Anaerobic digestion is a sludge stabilization process consists of four microbial sequential steps (Figure 1.1): the first process is hydrolysis in which biodegradable organic matters like carbohydrates and proteins are decomposed into amino and fatty acids, these components are converted into intermediates volatile fatty acids (VFAs), like propionic acid and butyric acid during the second step that called acidogenesis. Acetogenesis as the third step converts the intermediates components into acetic acid, carbon dioxide, and hydrogen. In the final step, the biogas that mainly contains methane and carbon dioxide is produced by acetoclastic and hydrogenotrophic methanogenic bacteria [4-6].

Therefore, bacteria play a significant role in biodegradation of sludge and it was evidenced that bacteria affect the function and performance of overall wastewater and sludge treatment [1].

1.2 Wastewater treatment and sludge disposal

Conventionally, WWTPs consist of three treatment levels: a preliminary treatment in which physical removal of solids was performed whereas the secondary treatment was mainly configured based on activated sludge process and the tertiary treatment as the final treatment level. The whole preliminary treatment can remove about 50% of suspended solids and decrease the biological pollutants by 30%. The biological treatment, which consists of bioreactors and secondary clarifiers follows the preliminary treatment and it controls removing of the biodegradable pollutants as nitrogen and phosphorus that commonly removed concurrently. The produced waste sludge which generated from the secondary clarifier, partly recycled in order to ensure minimum microorganisms concentration and the rest of waste sludge is bailed up to the sludge treatment units [7].

Nowadays, activated sludge process is the most common method used for the treatment of the wastewater. During the activated sludge process, the biodegradable pollutants and nutrients like phosphorus are degraded by the function of bacteria. The biodegradable substrates can be defined as how much of a given substrate is actually utilized during the anaerobic digestion process [8].

Wastewater disposal to water bodies without removing these nutrients was the primary cause of eutrophication. Redundant algae growth rate in the surface of coastal waters is the main negative result of eutrophication phenomenon [9]. Therefore, enhancement and reaching the optimal process of activated sludge technics still interesting research point.

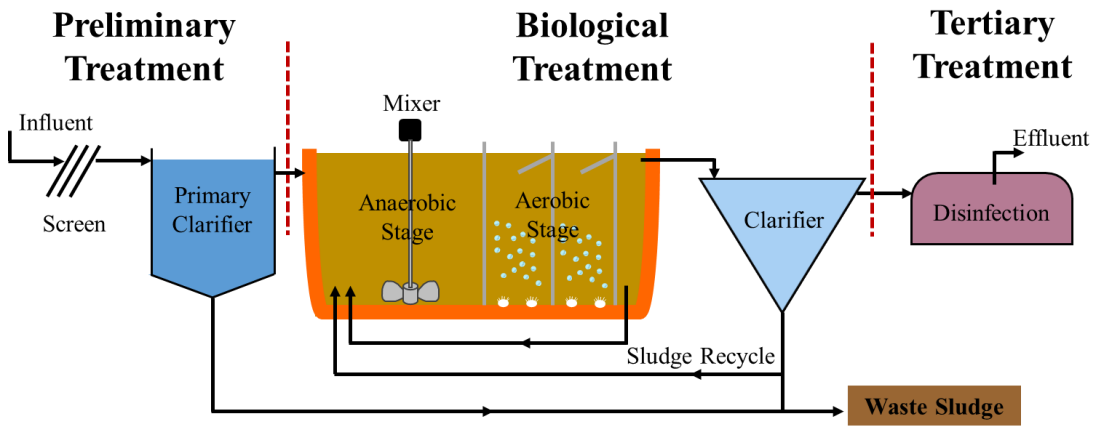

Figure 1.2 Schematic representation of the activated sludge process

Throughout the activated sludge process, the sludge is recycled through anaerobic and aerobic (or anoxic) phases in order to take up the substrate. The biological removal process of activated sludge system is comprising of the biological reactor and the secondary clarifier (Figure 1.2), which is applied widely as the secondary treatment for the municipal wastewater [10].

The present solids during the wastewater treatment is called waste activated sludge (WAS) and its usually composed of primary sludge and secondary sludge which is collected from the preliminary and final clarifier, respectively. WAS can be partially degraded and eventually separated to keep the ratio of biomass to food supplied in balance. The separated sludge accumulates in various types of thickeners and further stabilized by digestion process in anaerobic digesters prior to disposal (Figure 1.3). The sludge will be stabilized when its organic compounds like proteins and lipids -The typical organic contents (expressed as volatile solids content in total solids, VS/TS) in domestic sludge range from 60% to 80% - converted to biogas (50–60% methane) and (25–50% carbon dioxide) under anaerobic conditions [7, 11].

Accordingly, biogas generation from the waste sludge during the anaerobic digestion process has been all over the world considered as an assured method for sludge treatment and disposal [12].

Practically, a first step for treating activated sludge is thickening it by gravity, flotation or belt filtration. In doing so, the amount of sludge can be reduced to as little as a one-third of its initial volume. The separated water is recycled to the influent of the WWTPs. Once this has been accomplished, the sludge is subject to some process of biochemical stabilization as anaerobic digestion which plays an important role for further transform organic matter into biogas. Correspondingly, the final sludge solids for disposal is also

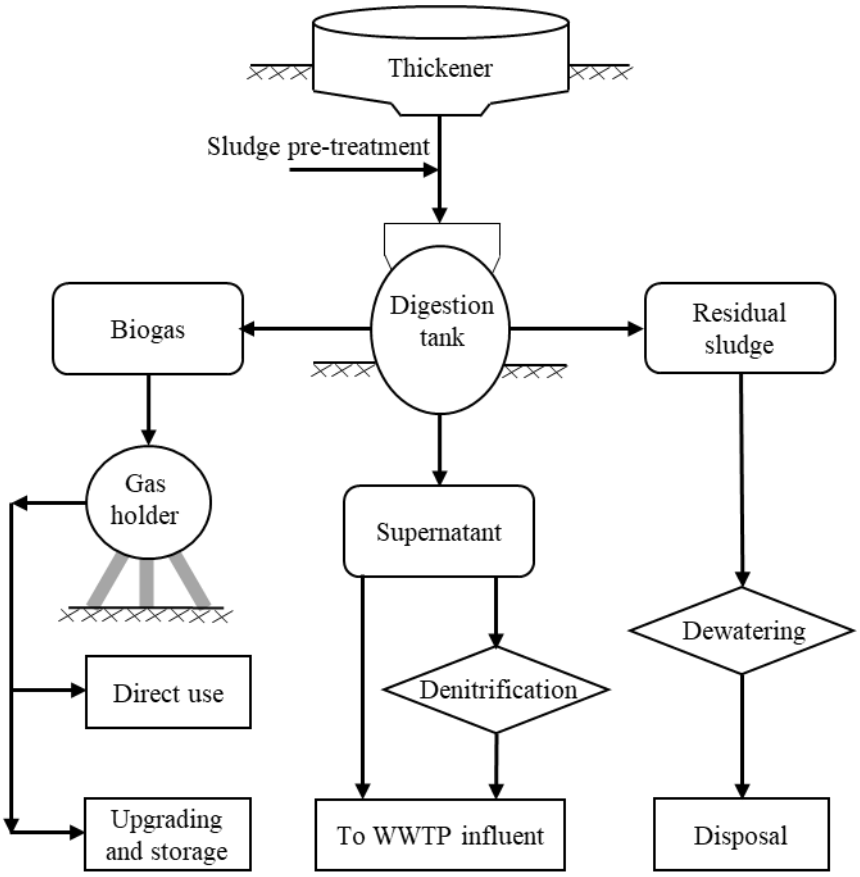

Figure 1.3 Sludge Management

reduced, destroying most of the pathogens present in the sludge, and limiting possible odour problems associated with residual putrescible matter.

Generally, the stabilized waste sludge is disposed via incineration, landfilling or ocean disposal as well as reused as a soil conditioner in agriculture. Moreover, the dried sludge or the incinerator ash is used as a primary material in the manufacturing of construction material [13]. Reuse of sludge for construction materials can not only reduce the problems of disposal but also it can offer a renewable substitute for depleting non-renewable resources, and hence provides a great potential for waste utilization [14].

In Japan for over a decade, thermal solidification of stabilized sludge was used for creating a valuable products, where the incinerator ash and dried sludge are utilized as a primary materials in producing of construction materials and other types of products can be made, such as artificial lightweight aggregates, slags, and bricks that are similar in appearance and physical properties to standard building materials [15].

Portland cement manufacturing using incinerated ash, or dried sludge powder is another way to use valuable inorganic and organic compounds of the sludge and subsequently reduce the burden from natural resources like clay and limestone (source of SiO_2 and

CaO) [16]. Artificial lightweight aggregate can also be produced using the digested sludge, these artificial aggregates were used as pavement materials as in walkways, planter soils and heat-proofing panel [17].

1.3 Basic principles of anaerobic digestion

Anaerobic digestion is a complex process which has successive steps that depend on the activity of a complex microbial association to transform biodegradable organic materials into mostly methane and carbon dioxide and it requires strict conditions to proceed (oxidation-reduction potential (ORP)<−200 mV) [18]. The digestion itself is based on a reduction process consisting of a number of biochemical reactions taking place under anaerobic conditions.

Even though the anaerobic digestion successive steps, the first step -hydrolysis- is generally considered as rate limiting step [7]. The hydrolysis process is the splitting of compounds with water, as splitting the insoluble organic material and the high molecular weight compounds such as cellulose, lipids, polysaccharides, and proteins, into soluble organic substances. Cellulose as one of insoluble organic matter make up more than 15% of the dry weight of the sludge, it involves many sugar units were joined together by chemical bonds. When the cellulose is hydrolyzed, many soluble molecules glucose are released (Eq. 1.1).

$$\text{Cellulose } (C_6H_{12}O_6)_n + H_2O \rightarrow \text{hydrolosis} \rightarrow \text{soluble sugar } n(C_6H_{12}O_6) \qquad (1.1)$$

In the second step that mainly acid-forming stage, the hydrolyzed products are further degraded through fermentative processes called acidogenesis and fatty acids and amino acids were formed. Different facultative and obligatory anaerobic bacteria are responsible to produce short chain organic acids such as butyric acids, propanoic acids, acetic acids, alcohols, carbon dioxide and hydrogen. The formed hydrogen concentration as an intermediate product in this stage influences the final product produced during the fermentation process. If the hydrogen partial pressure was too high, it would decrease the number of reduced compounds [19].

The third stage is called acetogenesis, where the organic acids produced by acidogenesis are further digested by acetogens to produce mainly acetic acid, hydrogen and carbon dioxide. The products of the acidogenic phase are consumed as substrates for the other microorganisms, active in the third phase.

In the final step that called methanogenic step, methanogenic bacteria convert the acetogenesis products into methane and carbon dioxide under a strict anaerobic conditions.

Methanogenesis is a critical step in the entire anaerobic digestion process as it is the slowest biochemical reaction process [20].

1.4 Key parameters affecting anaerobic digestion

The rate of various processes of the anaerobic digestion process is affected by different important parameters like temperature and pH.

1.4.1 Temperature

The physicochemical characteristics of the anaerobic digestion substrate are controlled directly by the medium temperature, moreover, the microorganisms metabolism and growth rate also are affected. Volatile fatty acids degradation as propionate and butyrate is most sensitive groups to temperature because it affects the partial pressure of hydrogen in the digesters, therefore controlling the kinetics of the metabolism.

The anaerobic digestion was applied in a wide range of temperature from psychrophilic (<20 °C) [21], mesophilic (25-40 °C) [22], thermophilic (45-60 °C) [21, 23], and even extreme-thermophilic conditions (>60 °C) [24]. High temperature has a negative effect due to increases the fraction of free ammonia which has been considered to have actual toxicity as a result of its free membrane permeability, thus inhibit the microorganism's activity [25]. However, the thermophilic operation is popular in anaerobic digestion applications where the ammonia inhibition is not a major consideration. On the other hand, the temperature has several advantages on anaerobic digestion, B Kanokwan (2006) listed these advantages in his doctoral thesis, as follow [26]:

1. Increasing the solubility of organic compounds to become more accessible to the microorganisms.
2. Increasing chemical and biological reaction rates, thus, accelerates the conversion process.
3. Decreasing the hydraulic retention time, so the reactor size can be smaller.
4. Increasing death rate of pathogenic bacteria especially under thermophilic conditions, which decreases the retention time required for pathogen reduction.
5. Improving the diffusivity of the soluble substrate and increase liquid-to-gas transfer rate due to lower gas solubility.
6. Decrease liquid viscosity which makes less energy required for mixing and also improve liquid-solid biomass separation.

It is important to maintain the operational temperature in the digester stable, since frequent fluctuations in the temperature affect the methanogens and process failure can occur at temperature changes in excess of 1 °C/day; and changes in temperature of more than 0.6 °C/day should be avoided [27].

1.4.2 pH and buffering capacity

Each microorganisms group has an optimum pH range, specifically methanogenic bacteria are quite sensitive to pH and it can function in a quite narrow pH interval from 5.5-8.5 with an an optimum from 6.5 to 7.2, whereas the fermentative microorganisms groups are relatively less sensitive with a more wide range of pH between 4.0 and 8.5 [28]. The main products at high pH of 8.0 are propionic acids while at a low pH mainly acetic and butyric acid are produced. Additionally, at high pH, free ammonia can cause weak base inhibition, whereas, at low pH, free volatile fatty acids can cause weak acid medium [29].

The solution resistance to pH change, that known as buffering capacity is an important factor for the anaerobic digestion process stability. Bicarbonate is the main buffer in anaerobic digesters and the volatile fatty acids are the main generated acid and sludge digesters normally have high feed bicarbonate buffering capacity and a high ammonia content which makes the pH around 7.5-8.0 [30].

1.5 Biogas as resource of renewable energy

The worldwide expanded energy demand and the environmental problems of fossil fuels with the unstable energy prices require utilization of bioenergy as a renewable energy. Among others bioenergy production technologies, biogas generation during the anaerobic digestion process attempts major advantages and it has been considered as one of the most environmentally beneficial and efficient technology for bioenergy production [31].

Due to its high methane potential, WAS as biomass has already been considered as a very desirable substrate for anaerobic digestion. Biomass under specific operating conditions will commit to methane generation. Naturally, WAS is considered to be attractive feedstock due to its high nitrogen content, high buffering capacity, and the high nutrients range utilized by methanogenic bacteria (methanogens).

The biogas as the main product of anaerobic digestion is a renewable energy resource therefore, enhancement the biogas production will reflect to increase the sustainable energy because the biogas can be predicted and works as an alternative to fossil fuels.

The potential biogas yield of various substrates mainly depends on the waste composition and the rate of biodegradability [32].

1.6 Nanotechnology

The concept of nanotechnology is referred to the application of materials on the nanoscale in the field of applied science. It is one of the rapidly growing areas of technology development and scientific research worldwide [33]. Professor Mihail C. Roco who is the chair of US National Science and Technology Council refers nanotechnology as the "Next Industrial Revolution" [34] and it is distinguished by the application or use of such material of particle size range between 1 to 100 nanometers (nm), about one hundred thousand times smaller than the diameter of a human hair. Figure 1.4 illustrates the scale of objects in the nanometer range. There are two different processes that the nanoscale particles can be formed, the first pathway that called top-down process like grinding in which the nanoscale particle can be formed mechanically from milling the macro or micro scale particle counterparts whereas, the second pathway or bottom-up processes can create the nanoscale particles from its molecules and atoms.

Commonly when the particles size decreases to be in nanoscale, the physical and chemical characterizations will be changed dramatically and at least particles in nanoscale have more mobility and reactivity in nature.

Recently, materials in nanoscale have been proposed as environmentally-friendly and cost-effective alternatives compared with the existing bulk or microscale materials based on its successes in remediating the environment [33, 35].

Nanoparticles can be also classified into organic nanoparticles like carbon nanoparticles, inorganic magnetic nanoparticles like iron nanoparticles, and semiconductor nanoparticles like zinc oxide.

The nanosize of particles can facilitate a fascinating level in the versatility of remediation and it can make the current treatment technologies more and more energy efficient by utilizing reactive nanoscale particles which can remove the chemical and biological pollutants.

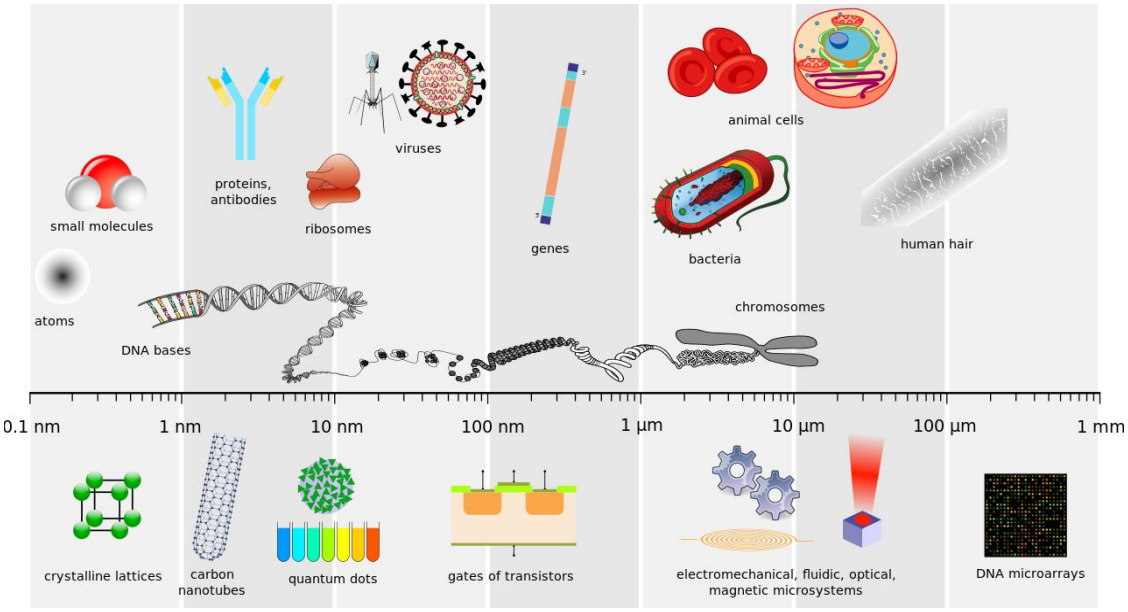

Figure 1.4 Diagram indicating relative scale of nanosized objects [36]

1.7 Zero-Valent Iron as a catalytic material

1.7.1 Zero-valent iron

During last two decades, ZVI has been used in order to remediate contaminated groundwater because it is an abundant and non-toxic material, and its redox potential ($E^0 = -0.44$ V). Thus, the directional electrons transfer from the ZVI particles to the contaminants is considered the main contaminants removal mechanism [37].

The ZVI can be obtained chemically using a reducing agent of sodium borohydride ($NaBH_4$), according to the following reaction (Eq. 1.2) [38].

$$Fe(H_2O)_6^{3+} + 3BH_4^- + 3H_2O \rightarrow Fe^0 \downarrow + 3B(OH)_3^- + 10.5H_2 \quad (1.2)$$

Details about ZVI synthesis will be clarified in research experimental work methods chapter.

ZVI in aqueous solutions can donate two electrons to produce ferrous (Fe^{2+}) plus hydrogen peroxide (H_2O_2) (Eq.1.3).

$$Fe^0 + O_2 + 2H^+ = Fe^{2+} + H_2O_2 \quad (1.3)$$

H_2O_2 then reduced with another two donated electrons to produce water (H_2O), (Eq.(1.4)

$$Fe^0 + H_2O_2 + 2H^+ = Fe^{2+} + 2H_2O \quad (1.4)$$

The combination of the Fe^{2+} and H_2O_2 can generate ferric (Fe^{3+}) with hydroxyl radicals (.OH) that is capable to oxidize various types of organic compounds, (Eq. (1.5)).

$$Fe^{2+} + H_2O_2 = Fe^{3+} + OH^{\cdot} + OH^- \quad (1.5)$$

Figure 1.5 Core shell structure on nZVI

Recently, ZVI was successfully used for degrading heavy metals [39], dyes [40], nitrate [41], nitroaromatic compounds [42], and phenol [43]. In these uses, ZVI works as electrons donor from its surface to reductive the pollutants.

In addition, another important characteristic of reactive nanoparticles is their strong tendency to aggregate in solution.

1.7.2 Nanoscale zero-valent iron

nZVI particle size is less than 100 nm, typically within a range of 1 to 100 nm, and the form of pure nZVI mainly comprises of a spherical core surrounded by a tiny shell layer (Figure 1.5). The formation of a thin shell is essential to the reactivity of nZVI as the shell layer allows electron donation for reducing pollutant and, at the same time, facilitates efficient adsorption sites for different contaminants due to the surface complexation and electrostatic interactions. Additionally, nZVI shell overcomes the rapid oxidation of the ZVI [44], and numerous studies have documented remarkable contaminants degradation rates by nZVI compared to ZVI particles.

nZVI has large surface-to-volume ratio compared with other sizes of ZVI, and the increase in the proportion of surface area promises benefits for a wide variety of environmental applications and offers unique chemical, electronic and magnetic properties. The chemical reactivity of nZVI is high and it has a long reactive lifespan and high mobility with porous media.

The laboratory and field applications of using nZVI have demonstrated that it can be used as a reactive material to remediate pollutants including chlorinated organic compounds, nitroaromatic compounds, chromium, nitrates, and phosphorus. Moreover, its reactivity

and performance are affected clearly by the composition of media, ionic strength in the contaminated water, and the geochemical properties such as pH, dissolved oxygen, and ORP [45]. The main mechanisms of contaminant removal by nZVI application follow reduction, adsorption, and co-precipitation [46]. These mechanisms are constituted according to ferrous and ferric iron ions, leading the released electrons to become available for the contaminants.

1.7.3 Nanoscale zero-valent iron copper bimetallic

Basically, the iron copper bimetallic nanoparticles (nZVI/Cu^0) are from a modified technique of nZVI, and they have the similar physico-chemical characteristics and may have a relative stronger oxidability under the aerobic condition.

As demonestrated by Li and Zhang [47], doping metals ions on nZVI that have electrode potentials (E^0) more than the nZVI E^0 value like copper (Cu^{2+}) and mercury (Hg^{2+}) will remove the pollutants principally by surface-mediated reductive precipitation. However, doping metals on nZVI that have E^0 less than or close to the iron E^0 value like zinc (Zn^{2+}) and cadmium (Cd^{2+}) will remove the pollutants basically by sorption.

Table 1 Redox couples of various metals ions with nZVI ([48])

Redox couple	Principally removal mechanism using nZVI
$nZVI + Zn^{2+} \rightarrow Zn^0 + Fe^{2+}$	Sorption/surface complexation
$Cd^{2+} + nZVI \rightarrow Cd^0 + Fe^{2+}$	Sorption/surface complexation
$Hg^{2+} + nZVI \rightarrow Hg^0 + Fe^{2+}$	Reductive precipitation
$Cu^{2+} + nZVI \rightarrow Cu^0 + Fe^{2+}$	Reductive precipitation

As shown in Table 1, there is an excess of aqueous Fe^{2+} developed from the anodic dissolution of the nZVI that can make contaminant reduction reactions more favorable. Moreover, when the bimetallic is formed, the nZVI is considered to become an anode that can protect the noble metal. Removal of pollutants by chemical reduction at the surface of nZVI bimetallic particles is considered to occur through two pathways. The first way is through the direct electron transfer with noble metal whereas, the second way is through the hydrogen produced by oxidation of nZVI.

The high potential difference between the nZVI anode and Cu cathode has reflected the acceleration of corrosion rate of nZVI and its reactivity. Therefore, adding a small amount of Cu ions directly through the nZVI synthesis to form nZVI/Cu^0 nanoparticles will have a much higher reduction rate of the pollutants than the rate obtained through the nZVI

system. It is also proved that the Cu planting onto the iron copper nanoparticles could improve significantly the p-nitrophenol (PNP) removal in aqueous solution [49].

Thereafter, adding bimetallic may sustain the methane production which might not only decrease the operation cost of sludge treatment but also promise a considerable digestion space to increase the sludge stabilization.

1.7.4 Nanoscale zero-valent iron supported onto zeolite

Zeolite is a non-cytotoxic mineral composed of silica, aluminum, and oxygen [50] and it is distinguished by its systematic structure that consists of plenty of channel and pores cavities.

Zeolite has a large number of mesoporous structures with pore size distribution ranging from 2 to 50 nm, which has high internal and external surface active sites for cation adsorption.

Owing to these properties, the zeolite can trap nanoparticles inside its pores and immobilize the nZVI particles on its surface [51]. Therefore, it can be demonstrated that the zeolite modification by nZVI could allow the nanoparticles to enter into the zeolite pores, which could mitigate agglomeration and excessive oxidation of the nZVI.

It's also considered that zeolite in presence of nanoparticles can work an inorganic cation exchanger which means can offer high ion exchange capacity, compatibility, and selectivity with the natural environment [52].

Currently, the literature focusing on the use of nZVI coated zeolite for arsenic adsorption [53], nitrate reduction [54], lead ions removal from water [55] and applied the nZVI coated zeolite into the anaerobic digestion application is limited. Planting the nZVI particles on zeolite may be a suitable pathway to enforce the contact between microorganisms and the nZVI species, and as a result, cell membrane disruptions that nZVI caused will be prevented.

Hence, coating the nZVI particles on a carrier may be a feasible strategy to increase the overall performance of anaerobic digestion process.

1.8 Water treatment by nanoscale zero-valent iron

Water resource scarcity listed in 2015 by the World Economic Forum as the largest global risk in terms of potential impact over the next decade [56]. The global water consumption has doubled every 15 years as a result of urbanization and industrialization. Meanwhile, water resources now have a wide range of contaminants due to the urban and

industrial activities and the people's health is directly affected. Therefore, water treatment is a critically important pathway to protect the world peoples.

There is an increase on the use of nanoparticles for the removal of contaminants from water, and this is reflected in the enormous journal articles published during the last decade. The journal articles focus on a range of applications of nZVI for removing several contaminants include nitrate, phosphate, arsenic, nitrobenzene and heavy metals.

1.8.1 Nitrate removal

Nitrate as pollutant can reach the water bodies mainly due to excessive use of pesticides and agricultural fertilizers causing mutation defects, methemoglobinemia and carcinoma [37]. World Health Organization (WHO) standard guidelines set 10 mg/L as nitrate-nitrogen as a maximum concentration of potable water.

ZVI has an ability to remove the nitrate by chemical reduction pathway that is allocated as the major pathway to remove nitrate by the addition of ZVI particles. During the chemical reduction of nitrate, ammonium is to be the main product as detected by Eq. (1.6) and also ZVI can react with nitrate then nitrite was formed and finally converted to nitrogen gas Eq. (1.7) and Eq. (1.8) [57].

$$4Fe^0 + NO_3^- + 10H^+ = 4Fe^{2+} + 3H_2O + NH_4^+ \quad (1.6)$$

$$Fe^0 + NO_3^- + 2H^+ = Fe^{2+} + H_2O + NO_2^- \quad (1.7)$$

$$3Fe^0 + 2NO_2^- + 8H^+ = 3Fe^{2+} + 4H_2O + N_{2(g)} \quad (1.8)$$

1.8.2 Chromium and nickel as heavy metals

The seriousness of heavy metals in the water beside is allocated to its toxicity and carcinogenic trends, it can not be biodegradable and it can easy to accumulate on living organisms causing potential short term and long term hazards. Recently, ZVI has been demonstrated as an effective catalytic for removing chromium (Cr) and nickel (Ni).

ZVI can control chromium by instantaneous adsorption of Cr^{5+} on the surface of ZVI, meanwhile, pricipitate the mixture of Cr^{3+} and Fe^{3+} following Eq. (1.9) and Eq. (1.10).

$$Cr_2O_7^{2-} + 2Fe + 14H^+ = 2Cr^{3+} + 2Fe^{3+} + 7H_2O \quad (1.9)$$

$$Cr^{3+} + Fe^{3+} + 6OH^- = Cr(OH)_{3\downarrow} + Fe(OH)_{3\downarrow} \quad (1.10)$$

Ni ions were uptaken by nZVI through surface precipitation as discussed in the Efecan et al. study [58]. nZVI also elucidated that the kinetics of Ni^{2+} uptakes was high and the extent of uptake was not profoundly affected by pH variations.

1.8.3 Arsenic

Arsenic in water was often found in two form arsenite and arsenate and due to its carcinogenic and toxic effects, WHO considered it as a first priority pollutant and recommended the concentration of 10 µg/L as a limited level in drinking water. Different processes are involved when using ZVI in order to remove arsenic, moreover, reduction, adsorption, and surface precipitation were the main mechanisms of arsenic removal with different nZVI species [59]. Further corrosion of ZVI increased notably the removal of arsenic from groundwater via adsorption and precipitation. In aerated water, arsenite was removed by sorption on newly formed hydrous ferric oxides and hydroxyl radicals [60].

1.9 Anaerobic digestion by nanoscale zero-valent iron and the microbial interactions

Waste sludge is stabilized by the anaerobic digestion process and this process is considered to be one of the most energy-efficient methods for sludge stabilization in parallel to produce methane which can be used as a renewable fuel [61]. The addition of nZVI or its composites may significantly affect the biodegradable organic matters of waste sludge into volatile fatty acids and methanogenesis. Therefore, the presence of nanoparticles may imapct the function of bacteria.

nZVI has high ability to gain or lose electrons, this makes it a competitive chemical additive to the anaerobic digestion process but excess iron ions produce a toxic free radicals as presented in Eq. (1.5). Excess ions will disturb the function of microbial life of organic material media. However, the comparatively low release elector donors like nµ particles is suitable for methanogenesis bacteria during the anaerobic digestion process resulting in an increase in the methane yield and increase the biogas production volume [62].

Also nZVI when exerted iron oxide and iron hydroxide ions inhibited a specific type of bacteria by rapid coating cell [63] or due to strong electrostatic interactions between another type like *Escherichia coli* and iron nanoparticles ions, the pure nZVI was adsorbed vigorously to this type of bacteria and therefore it induces the reductive stress and disrupts cell membranes and finally inhibits the bacterial growth [64]. In addition, nZVI can penetrate the bacterial cell membrane which leads to damage whole bacteria that happen associated with the production of intracellular reactive oxygen species (ROS) [63, 65].

In Contrast, nZVI has been paid attention to increase the anaerobic degradation because ZVI can act as an electron donor to improve the anaerobic condition by decreasing the ORP and controling pH through reduction of protons to hydrogen gas.

When Su et al. [66] added 0.1wt% of nZVI on the waste sludge under 37 °C for digestion period of 17 days and the results showed that this 0.1 wt% nZVI increases the methane yield by 40.4% and biogas generation volume by 30.4%. Whereas Yang Y. et al. [67] who also examined the impact of nZVI on the anaerobic digestion of anaerobic sludge from Columbia municipal wastewater treatment plant for 14 days at 37 °C. The results showed that adding 1, 10 and 30 mM nZVI to the sludge resulted in 20%, 20% and 70% decrease in methane production respectively. The authors referred the inhibitory behavior of nZVI to the rapid hydrogen ions production that resulted from the dissolution of nZVI but the microscale-ZVI dissolution showed a slow release of hydrogen ions which enabled methanogenesis processes and increased methane production. Comparatively, Abdelsalam E. et al [5] emphasized that 20 mg/L of nZVI yielded 580 mL of biogas which means achieved the highest biogas startup and it reduce the lag phase of production and the average production of the control during the first five days of hydraulic retention time (HRT) was only 159.3 mL. Su L. [66] reported that the promotion of methane production by the addition of nZVI is attributed to the function of nZVI toward reducing the hydrogen sulfide concentration (H_2S).

In the anaerobic digestion process with the addition of iron particles, ZVI has been found able to accelerate the hydrolysis and fermentation stages due to its action as electron donor. Zhang et al. reported that the microscale of ZVI enhanced the methane yields of waste activated sludge for all concentrations. According to the authors, the microbial hydrolysis-acidification of complex matters were promoted by the reduction of ferric oxides on the surface of the iron [68]. A good digestion performance was observed when utilized ZVI bed in an UASB reactor because ZVI could act as additional electron donor to decrease the un-dissociated H_2S concentration, thereby decreasing its negative impact on the anaerobic digestion process [69]. In a posterior study, where UASB used for treating azo dye wastewater, the authors claimed that ZVI promoted the growth of methanogens due to the high degradation rates that UASB achieved at low temperature (25 °C) and HRT (12 hrs) [70].

Although ZVI has exhibited its stimulative activity to a plenty of microbes, it is considered as universally bactericidal in aquifer systems and it exerts selective pressure

on the microbial community, inhibiting some microbial groups particularly the nanoscale of ZVI [71]. nZVI due to its particular physicochemical property can easily attach to the bacterial cell surface. During their contact, some interactions could occur between nZVI and the bacteria, which may be chemical, physical, biological reaction or any combinations of them and subsequently nZVI exerts an inhibition influences onto the bacteria cells [72]. The inhibition and cytotoxicity of the nZVI include damaging the cell membrane integrity, interference with respiration, oxidative damage of various enzyme of DNA due to excess ROS generated from Fenton's chemistry. The nZVI toxicity mechanisms to the microbes involve two aspects: one is disruption of the cell membrane architectures and enhancement the membrane permeability, this aspect is recognized as physical damage. The other is biochemical damage in which an interference in energy transduction and exchange, gene and protein damage happened.

1.10 Nanoscale zero-valent iron applications

ZVI-based application technology can be generally divided into two main groups: in the first group, which use ZVI as an electron donor to convert the contaminants into less toxic compounds or induce the microbial life; and those which use the ZVI as contaminant immobilizing reagent, sorbent or co-precipitant [73].

The American Environmental Protection Agency (US EPA) grouped a list of 25 sites where nZVI was utilized for soil remediation. More than 56% of the sites have 70% as an average contaminants removal rate and all case has high dosage concentration and the most frequently applied concentration was 8 g/L. 40% of sites applied pure nZVI while 32% used bimetallic [74].

New innovative *in situ* technology has been used to remediate polluted groundwater, this new sustainable technology which called permeable reactive barrier (PRB). The concept of PRB involves perpendicular injecting of a reactive media like ZVI to the potential path of the polluted groundwater in Figure 1.6. When the polluted plume crosses the PRB, the pollutants will react with the reactive media and will be transferred to be less harmful compounds [75].

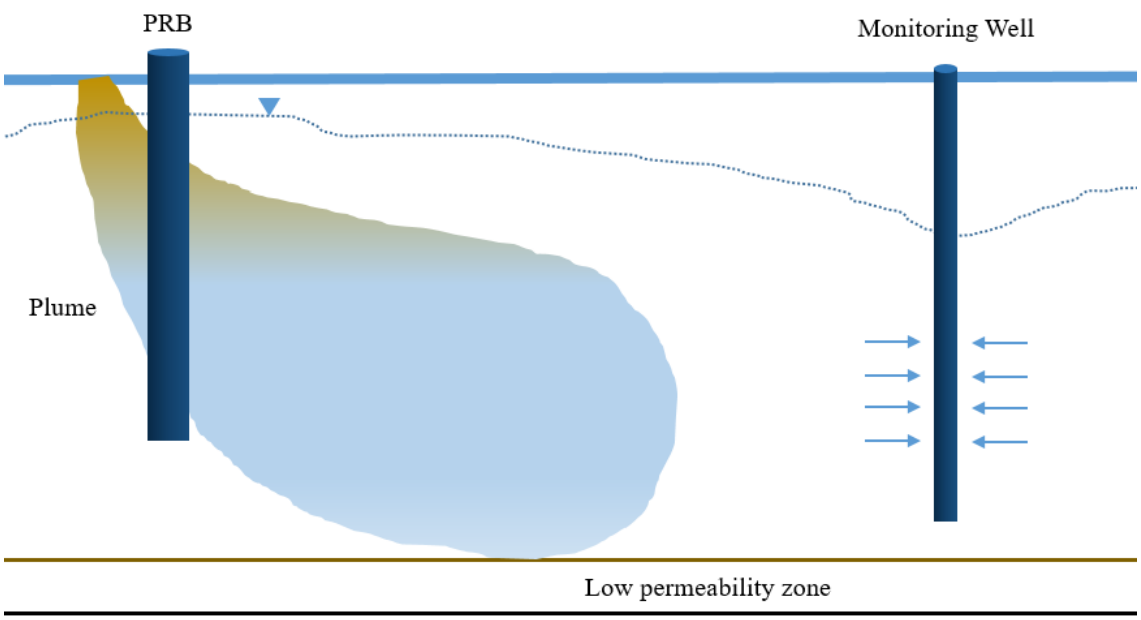

Figure 1.6 Permeable reactive barrier

On the other application, Li S. el al. [76] constructed a new nZVI wastewater treatment pilot plant in order to remove heavy metal. The nZVI treatment plant was constructed in April 2012, and served as a pretreatment to remove arsenic and metals in the wastewater. Their work demonstrated that nZVI is an ideal reagent for treating wastewater containing heavy metals, and reported a systematic approach using nZVI for wastewater treatment.

On the other side, Kumpiene et al. [77] assessed ZVI for stabilization of Cr, Cu and arsenic in soil. Controlling the bioavailability of the arsenic and Cr in contaminated soil was significantly decreased by 98% and 45%, respectively.

For the drinking water sources contaminated by arsenic, ZVI-based cleanup technologies have been developed to address the major problem of arsenic contamination in groundwater-sourced drinking water, particularly in the areas faced this problem as in West Bengal and Bangladesh, where up to 80 million inhabitants consume contaminated water with arsenic. A considerable number of field studies have been developed the removal of arsenic by ZVI, highlighting the arsenic was removed by direct adsorption processes or co-precipitation with more than 90% arsenic removal rate [78, 79].

1.11 Cost of nanoscale zero valent iron

The price of one kilogram of nZVI particles varies between 25 and 325 Euro. This variation in price is determined by the manufacture and also based on the type of nZVI (stabilised products, modified products, conservation) as listed in Table 2. As much as the micro-scale and granular ZVI are available for less than 1 Euro/kg.

Table 2 List of commercially available nZVI [80]

Producer Name	Country	nZVI Type	Price	Surface area	Particle size
Nano Iron	Czech Republic	nZVI powder	25 - 65 Euro/kg	20-25 m^2/g	50 nm
TODA KOGYO CORP.	Japan	RNIP(mainly iron oxides), powder	25-33 Euro/kg	23 m^2/g	100 nm
Polyflon company	USA, Florida	nZVI powder	Unknown	37-58 m^2/g	100-200 nm
Gotthart Maier Metallpulver GmbH	Germany	µZVI powder	1.2 euro/kg	N.A.	0–80 µm

Even though, the total cost of a particular nZVI application project is difficult to estimate while it depends on various factors, e.g. the amount used, cost of transportation and the product type.

1.12 Research aim and objectives

The goal of this research work was to develop a novel treatment enhancement system for waste activated sludge. A biochemical methane potential setup was primarily assembled and operated. In this study, nZVI was selected as a promising catalytic reactive material for wastewater treatment and sludge stabilization enhancement.

The main research objectives of this Ph.D. study were:

- Exploring the role of bimetallic nZVI/Cu^0 particles into wastewater contaminants degradation, and the toxicity of nZVI/Cu^0 to the domestic wastewater microbial community was distinguished.
- Employed nZVI/Cu^0 into laboratory scale anaerobic digestion system for improving the biogas production and methane yield through dosing wide-range bimetallic concentrations and comparison with the outcomes of nZVI influences.
- The effect of two different nZVI particles loadings have been examined and the performance on biogas production of this novel composite ICZ was tested based on modified biochemical methane potential test, and compared with that of the bioreactors exposed to only nZVI particles or zeolite material. The batch experiments were also carried out with no additive and with the mixture of both nZVI and zeolite labelled (IMZ).
- Assess the performance of anaerobic digestion process for the treatment of sulfate-containing sludge in presence of nZVI. Accurately, the impact of various

concentrations of nZVI on methanogenesis activities in anaerobic digestion will be determined.

1.13 Structure and Outline of the Thesis

The thesis consists of six chapters in addition to the conclusions and recommendations. Chapter 1 includes an introduction to the water and sludge treatment by nanoparticles. In chapter 2, the experimental work methods were systematically described. Chapter 3 involves the nZVI and nZVI/Cu^0 employment for wastewater contaminants degradation and microorganisms growth rate tracking. Whereas chapter 4 determines the methane generation stimulation by the addition of nZVI/Cu^0 bimetallic nanoparticles and chapter 5 compare between pure nZVI and nZVI coated zeolite addition toward enhancing the biomethane generation. Chapter 6 discuss and evaluate the sulfate-containing sludge stabilization by nZVI. Based on the study outcomes, main conclusions and recommendations were listed along with the future outlook and research needs.

CHAPTER 2

RESEARCH EXPERIMENTAL WORK METHODS

Chapter 2. Research experimental work methods

This chapter presents the methodology that has been used to conduct the experimental works involving chemicals preparation, nanoparticles synthesizing method, samples collections, characterization of produced nanomaterials and analytical investigations.

2.1 Chemicals

The following chemicals were used as received: ferric chloride hexahydrate salts ($FeCl_3 \cdot 6H_2O$) was used for preparing the pure or bimetallic iron nanoparticles and ICZ composites were purchased from Junsei Chemical, Japan. The reductant agent of sodium borohydride ($NaBH_4$) was purchased from Sigma-Aldrich, USA. Anhydrous copper chloride ($CuCl_2$) was also purchased from Sigma-Aldrich, USA. Commercial raw zeolite powders which have a particle size in micrometer scale was purchased from Sigma company, Germany. Sodium dithionite or Sodium hydrosulfite ($Na_2S_2O_4$) was obtained from Junsei chemical company, Japan. Ethanol (C_2H_5OH) with the concentration of 99.5% was purchased from Wako company, Japan for washing the prepared nanoparticles. For controlling the pH during experiments execution, sodium hydroxide (NaOH) with a concentration of 97% and hydrochloric acid (HCl) with a concentration of 35% were bought from Wako company, Japan. Various reactants solutions were prepared using: Potassium dihydrogen phosphate (KH_2PO_4) with the concentration of 99.5% was ordered from Kanto chemical company, Japan, while anhydrous sodium sulfate (Na_2SO_4) was purchased from Wako pure chemical industries, Japan. Nutrient agar which was used to ensure appropriate medium for bacteria inoculation was from OXOID company, England. All the chemicals used in this work were employed as delivered without further purification and all the aqueous solutions have been nitrogenized for 20 minutes prior to use.

2.2 Wastewater and waste sludge samples

Wastewater samples were taken from the entrance of Mikasagawa domestic wastewater treatment center in the city of Fukuoka, Japan. Mikasagawa wastewater treatment center has capacity to treat 300,000 m^3/day using conventional activated sludge system. The samples were pre-screened by a 2 mm mesh to remove the large particles, then kept at 4 °C to maintain its freshness. The wastewater charactrizations are listed in Table 3.

Table 3 Wastewater sample characterizations

Parameter	Value	Unit
Turbidity	4	
pH	7.3	
SS	175	mg/L
COD	424	mg/L
BOD	229	mg/L
Ammonium nitrogen	28	mg/L
Total nitrogen	37	mg/L
Total phosphorus	4.45	mg/L

As well as domestic sludge samples were collected from the influent point of the anaerobic digester at the same treatment center. The anaerobic digester of the treatment plant receives mixtures of thickened activated sludge and the samples were collected in a plastic container and immediately were analyzed and characterized.

2.3 Catalytic synthesis

2.3.1 Nanoscale zero-valent iron synthesis

nZVI stock suspension was freshly synthesised based on the optimal reduction method proposed by Glavee, G. N. et al. [81]. The reduction method due to its simplicity, is one of the most frequently used method for synthesizing the nZVI.

The nZVI particles were synthesised in a 500 mL flask reactor with four open necks using various stock solutions were purged with nitrogen for 20 minutes to eliminate dissolved oxygen before use. One gram nZVI stock suspension was freshly prepared by reducing five grams of $FeCl_3(H_2O)_6$ that were dissolved in 120 mL of deionized water with 5 grams of $NaBH_4$ that also were dissolved in another 120 mL of deionized water as presented in Figure 2.1. $NaBH_4$ solution was dropwised to the $FeCl_3$ solution under the nitrogen atmosphere while the $FeCl_3$ solution was vigorously stirred at 250 rpm. The entire synthesis was conducted at 27 ◦C by using thermostatic waterbath.

The reduction reaction was expressed in subsection 1.71. as following Eq. (1.2).

$$Fe(H_2O)_6^{3+} + 3BH_4^- + 3H_2O \rightarrow Fe^0 \downarrow + 3B(OH)_3^- + 10.5H_2 \quad (2.1)$$

After 30 mintues as an aging time, the obtained nZVI suspention was washed with deoxygenated, deionized water and ethanol. Lastly the prepared nZVI particles were

filtered by vacuum pump and collected in an oxygen-free chamber, the product obtained is characterized by a homogeneous structure that displays high reactivity [80].

2.3.2 Iron copper bimetallic synthesis

The nZVI/Cu^0 bimetallic particles used in this research were prepared by loading $CuCl_2$ (10% wt/wt) to the $FeCl_3(H_2O)_6$ solution before dropping the reducing reagent of $NaBH_4$. The mixtures were continuously stirred at 250 rpm. Subsequently, the prepared nanoparticles were separated from the aqueous solution by vacuum filtration and rinsed three times with water and absolute ethanol respectively. Eventually, the bimetallic nanoparticles slurries were anaerobically sorted prior to use. All above processes have been carried out in a nitrogen environment.

The ratio of nZVI/Cu^0 was chosen based on the successful use of nZVI/Cu^0 in nitrate reduction [57] which can facilitate movement of iron ions due to the high electric conductivity of the medium in presence of nZVI/Cu^0 [82].

$CuCl_2$ was used to deposit copper on the surface of the nZVI particles by iron-copper replacement reaction, and the Cu mass loading on the surface of iron particles could affect the catalytic activity of the prepared nZVI/Cu^0 bimetallic particles.

2.3.3 Iron coated zeolite synthesis

For preparing ICZ with two different nZVI particles loadings (500 and 1000 mg/L) to obtain ICZ 500 and ICZ 1000 composites, two $FeCl_3$ of masses (2.5 and 5 grams) were separately mixed with 2 grams of zeolite in 120 mL of deionized water. HCl was added to adjust the initial solution pH to meet the range between 3 to 4 to overcome any supposed associated interference in the liquid phase of iron concentration measurements caused by iron precipitation. The $FeCl_3$ salt and zeolite aqueous mixture was vigorously stirred for 30 minutes at ambient temperature. The prepared aqueous mixture was then placed in a four-neck flask (Figure 2.1). 120 mL of $NaBH_4$ aqueous solution was introduced drowsily to the four-neck flask at a rate of one litter per hour. The formed ICZ composites were then washed three times with deionized water and ethanol. The whole preparation steps were carried out under a nitrogen atmosphere.

For the comparison purpose, a mixture of prepared nZVI and zeolite (IMZ) was also used in this research study as it will be discussed in chapter 5.

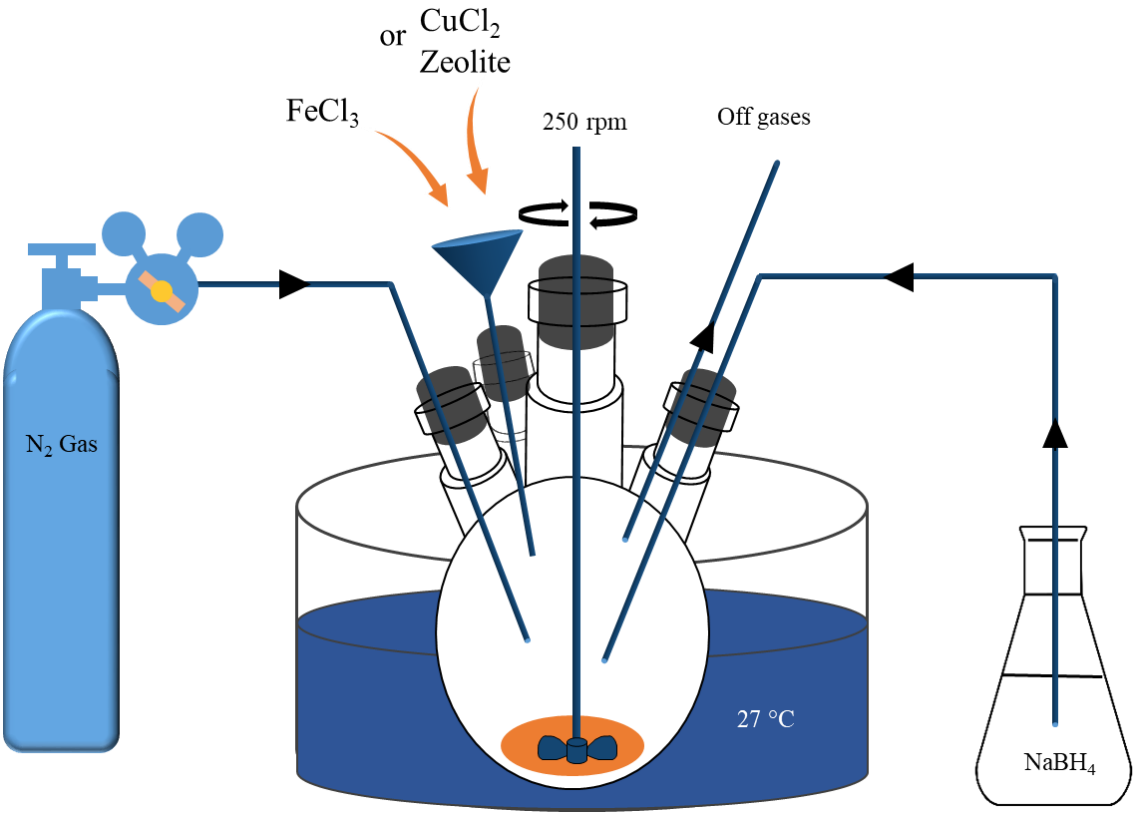

Figure 2.1 Schematic diagram for synthesis the iron based nanoparticles

2.4 Sorption kinetics study

The sorption characteristics of the research prepared additives were investigated in an aqueous system and the adsorption kinetics and sorption capacity were studied in a batch tests.

In order to examine the adsorption kinetics of zeolite, one gram of zeolite and 100 mL of 50 mg/L deoxygenated ferric solution was introduced into a plugged conical flask under 150 rpm stirring. At predetermined time intervals, samples were withdrawn from the solution and the concentrations of dissolved iron were immediately analyzed. The purposes to investigate the zeolite adsorption kinetics and capacity for the ferric ions are mainly first to determine the needed time for zeolite to reach the equilibrium time of adsorption and to determine the adsorption capacity on the equilibrium time. These purposes will be subsequently fixed in the batch experiments.

Additionally and to examine the sorption kinetics of sulfate on nZVI, sulfate solution with 500 mg/L sulfate as initial concentration was prepared. 100 mL of the prepared sulfate solution was added to Erlenmeyer flask. A concentration of 1000 mg/L of freshly prepared nZVI was added to the sulfate-contain flask. The sulfate solution in the experiment was mixed with nZVI for 1200 minutes at certain conditions (temperature

25 °C; agitation speed 200 rpm and pH 7.2). At predetermined time intervals, samples were extracted with a syringe and filtered through 0.45 μm membranes for analyzing the final concentration of sulfates.

The adsorption kinetics for adsorbent have been extensively described by the pseudo-first-order and pseudo-second-order reactions [83], and the linearized forms of both models are presented in Eq. (2.2) and Eq. (**Error! Reference source not found.**), respectively:

$$\log(q_e - q_t) = \log q_e - \frac{k_1}{2.303} t \qquad (2.2)$$

$$\frac{t}{q_t} = \frac{1}{k_2 q_e^2} + \frac{1}{q_e} \qquad (2.3)$$

where q_e and q_t (mg/g) are the amounts of iron ions adsorbed at equilibrium and at time (t), respectively, k_1 (1/min) and k_2 (1/mg×min) are the pseudo-first-order and pseudo-second-order rate constants, respectively.

2.5 Adsorption isotherm models

Adsorption isotherms models describe the distribution of the adsorbate species between liquid and adsorbent based on a set of assumptions related to the homogeneity or heterogeneity of adsorbents, and the possibility of interaction between the adsorbates [84].

For the adsorption isotherm of iron onto zeolite, the isotherm models employed to describe the relationship between the iron concentrations of a solution and the quantities of adsorbed iron on the zeolite as adsorbent at a fixed condition. The models are based on the assumption that all adsorption sites onto the adsorbent surface are dependent and equivalent. Isotherm models can also describe how the adsorbate concentration will interact with the adsorbent media. Therefore, empirical models of Freundlich and Langmuir were used for the evaluation of experimental results. Practically and to explore the adsorption capacity of zeolite, several adsorption isotherm batch inspections were conducted in order to define and to determine the highest amount of iron ions that zeolite can adsorb. Six groups of 100 ml of deoxygenized water containing $FeCl_3(H_2O)_6$ at various iron concentrations (5, 25, 100, 500, 1000 and 2000 mg/L) were prepared and pH range was fixed between 2 to 3. One gram of zeolite as adsorbent was suspended in each of the 100 mL solutions. The isotherm batch tests were checked under the ambient temperature and 150 rpm stirring. Flasks were kept sealed in order to decrease oxidation

interference and to minimize losses to the atmosphere. The concentrations of dissolved iron were determined before adding zeolite and at equilibrium time.

In addition and in order to describe the sulfate isotherm onto nZVI, groups of batch experiments were conducted within an initial sulfate concentration ranging from 0 to 500 mg/L. In Erlenmeyer flasks, each sulfate solution was mixed with nZVI at ambient temperature and 200 rpm stirring. Each flask was immediately sealed and the equilibrium concentrations of sulfate were determined at equilibrium time and the adsorption capacity of nZVI was measured.

The number of iron ions adsorbed (q_e) was calculated by Eq. (2.3):

$$q_e = \frac{(C_0 - C_e)V}{m} \qquad (2.3)$$

where q_e is in (mg/g) which equal to the amount adsorbate at equilibrium time, C_0 is the initial adsorbate concentration in the solution (mg/L), Ce is the final adsorbate concentration in solution at equilibrium (mg/L), m is the mass of adsorbent as adsorbent (g) and V is the volume of the solution in liter (L).

2.6 Batch experiments

Batch experiments were conducted to determine the potential effect of nZVI and nZVI/Cu^0 nanoparticles on the wastewater treatment process through testing the ammonia changes, phosphorus adsorption, and COD removal rates. To ensure the aerobic condition and to saturate the solutions with oxygen, the air was continuously injected in the solution for 20 minutes and the same way was used but with nitrogen gas to purge dissolved oxygen and utilize anaerobic condition. 200 mL of raw wastewater was utilized which sampled from Mikasagawa purification center. Two groups of batch experiments were conducted, six sets each. The first group was carried out under aerobic condition to examine the effects of nZVI/Cu^0 with four different dosages 10, 100, 200 and 500 mg/L in addition to the 100 mg/L nZVI dosage and to the control experiment, while the second group was accomplished under anaerobic condition. All experiments were vigorously continuously shaken at 150 rpm at 37 °C using reciprocator shaker (AS ONE Co., Japan).

2.7 Biochemical methane potential batch test setup

Batch anaerobic laboratory scale bio-digester system was assembled and operated. The anaerobic batch system was consisting of a bio-digester; 500 mL Duran bottle closed with two nozzles cap (SANSYO company, Japan). For keeping the temperature at mesophilic condition (37 ± 0.3 °C); a thermostatic water bath (SANSYO company, Japan)

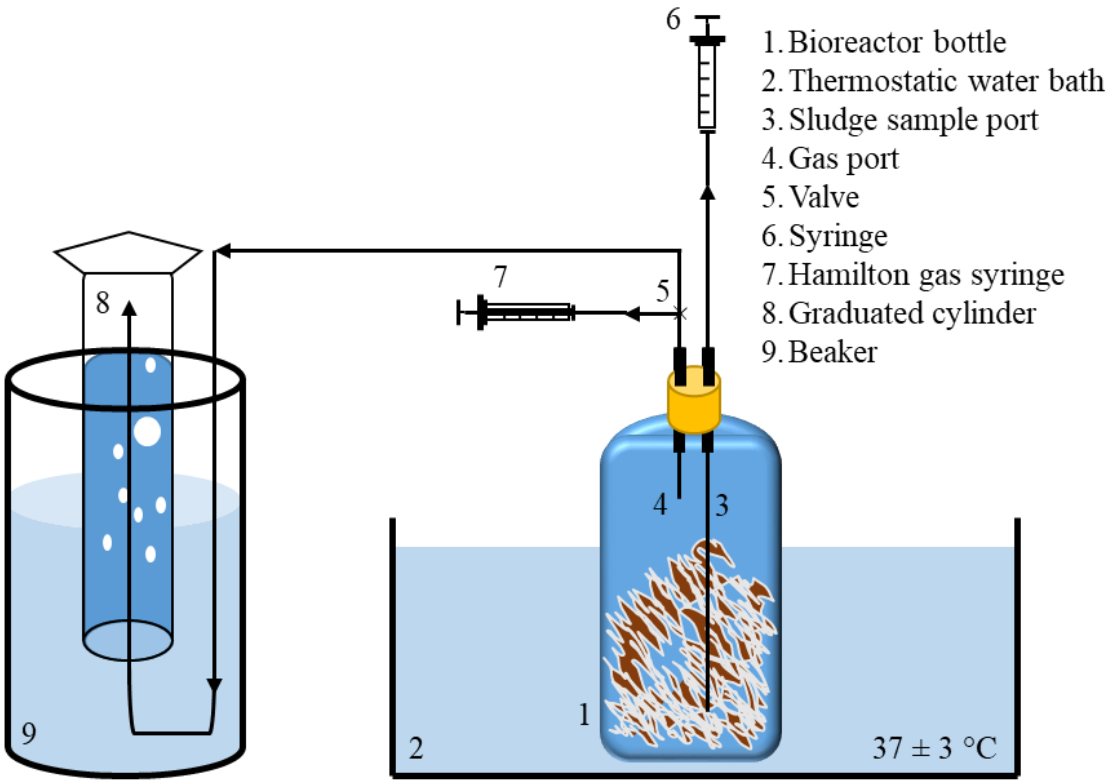

Figure 2.2 Bioreactors design and setup

was used. The municipal sludge mixture was loaded into each bio-digester, subsequently purged with pure nitrogen for 10 minutes and sealed with the two nozzles cap.

Each nozzle allows taking samples in order to characterize the biogas and sludge properties respectively. A schematic diagram of the sludge bio-digester system is shown in Figure 2.2.

Investigations of the effect of nZVI and nZVI/Cu^0 additives on the activated sludge were carried out through biochemical methane potential batch test experiments. The nanoparticles were added to anaerobic bio-digesters systems from the beginning of digestion. The sludge samples were regularly collected using a 10 mL syringe for the aqueous samples chemical and biological analysis. The volume of the produced biogas was measured on a daily basis using ultra clear glass graduated cylinder (300 ± 2 ml, AS ONE corporation, Japan) which was connected to the gas outlet nozzle by 5 mm plastic tube. The graduated cylinder was placed upside down in polypropylene beaker filled with distilled water. Moreover, the methane and carbon dioxide content was measured by sampling the gas directly from the headspace using a Hamilton gas-tight syringe and the gas compositions were classified by gas chromatography instrument (GC, GL Sciences Inc., Japan).

2.8 Chemical analysis

The pH was adjusted by the addition of HCl or NaOH solutions. All parameters were analyzed in accordance with the standard methods for the examination of water and wastewater [85] using ultraviolet-visible spectrophotometer (DR 3900, Hach company, USA). Sulfate anions were determined using power pillows reagents. COD was determined using reactor digestion method. Ammonium nitrogen (NH_4-N) was determined using a colorimetric method but the concentrations of total iron ion's and ferrous ions were determined by the FerroVer and 1,10-phenanthroline method, respectively. The ferric ions concentration was evaluated by subtracting the Fe^{2+} ions concentration from the total iron ions concentration.The pH was recorded using a pH analyzer (LAQUA, Japan).

2.9 Gas volume record and composition

The volume of produced biogas was daily recorded by reading water displacement inside the calibrated glass cylinder which was fitted to the bio-digesters (Figure 2.3).
Gas chromatography (GC) method was used to separate different types of gases because it has good sensitivity and selectivity of seperation related to column chemistries, detectors and sample introduction techniques [86]. GC is favourable to use while its high resilution, good accuracy and precision and it is still on the eminence as a first chromatographic separation techniques that has been developed. The sample is added into a stream of carrier gas called mobile phase via an injector and separated on the column

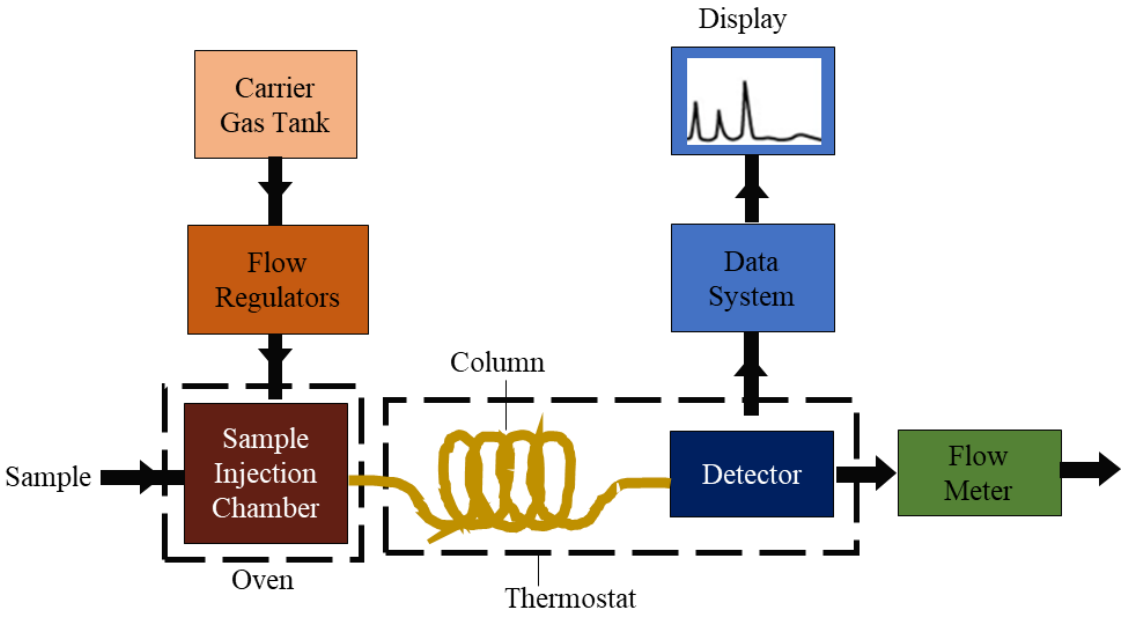

Figure 2.3 Gas chromatography fowchart

into the individual components at a stationary phase. The components of the sample are analyzed in the detector after separation on the column (Figure 2.3). Biogas compositions from the bio-digesters headspace were analyzed by GC instrument with a thermal conductivity detector (TCD), the TCD temperature was set at 80 °C and its current rate was fixed at 60 mA. For the analysis, two different stainless-steel packed columns were operated. The first column can separate methane while the second column can separate carbon dioxide. The temperatures of the GC injector, detector and column were kept at 60 °C, 100 °C, and 80 °C. Argon gas was used as the carrier gas at a flow rate of 20 and 30 mL/min for separation carbon dioxide and methane, respectively.

2.10 Culture and analysis of bacteria

Bacteria growth rate was estimated by counting the number of survival bacteria using colony forming unit (CFU) technique based on the pour plate method. Viable colonies on plates were counted after incubation using the nutrient agar. The agar was melted by dissolving 23.5 g dehydrated medium agar with typical formulas of 2.5 grams' yeast extract, 5 grams peptone, 1 gram dextrose, and 15 grams agar into 1000 mL deionized water, then the medium was heated under mixing, afterward it was sterilized at 120 °C for 20 minutes and maintained at 50 °C prior to use.

Each wastewater sample was diluted ten thousand times to obtain the final colonies between 30 to 300 then it was inoculated two times for 7 days. By Adding 15 mL melted agar to each Petri dish containing 1mL of diluted sample and mixing the medium carefully with rotating plates on the level of surface 10 times. After agar inside Petri dishes plates has hardened, the Petri dishes were inverted and immediately incubated at 37 °C for 24 hours. After incubation, the viable bacteria count was determined by counting visible colonies and was recorded in respective dilutions.

2.11 Instrumentation

2.11.1 X-Ray diffraction

For the composition analysis of the additives used in this study, an X-ray diffraction (XRD, TTR, Rigaku, Japan) was employed over the 2θ range and the goniometer scanning was from 3° to 90° covered all major species using graphite monochromatic Cu Kα radiation and scanning speed of 2° min^{-1}. XRD results reflect the crystalline structure of samples. The chemical composition of nZVI or it other composits

used in this research work can be indentified by using the set of information from the crystallographic planes of unknown materials.

2.11.2 Transmission elector microscopy

Prepared additives shape morphologies were observed by transmission electron microscopy (TEM, JEM-ARM 200F, JEOL Co., Japan). The TEM observations were performed on a FEI Tecnai G2 20 X-Twin instrument (350 kV accelerating voltage) using copper mounted holey carbon grids. A smaple amount of nZVI sample was diluted in ethanol until almost full transparency. nZVI diameter size was also measured manually by eye visual analysis of TEM pictures against the calibrated TEM scale bar. At same magnification, several representative images were taken at different spots of the TEM grid. Moreover, the elemental distribution analysis of the nZVI and nZVI/Cu^0 were performed using an energy-dispersive X-ray (EDX, EX-23000BU JEOL Co., Japan) spectroscopy. The TEM was equipped with EDX system, high angle annular dark field imaging (HAADF) detector, and field emission gun (FEG). The charge-coupled device (CCD) camera was from Gatan, Inc. Samples were prepared by dispersion in ethanol and a droplet placed upon a copper mounted holey carbon grids before drying prior to analysis.

2.11.3 Specific surface area analyzer

Brunauer–Emmett–Teller specific surface area (BET SSA) of the research additives was measured using a 3Flex surface characterization, Micromeritics, USA. For BET SSA analysis, the sample tubes were initially rinsed then dried at 110 ^oC under vacuum for 1 h using VacPrep 061 degasser (Micromeritics, USA), followed by degassing of the samples placed in these tubes at 350 ^oC for 2 h, and then the degassed solids were subjected to the nitrogen flow at 77 K.

2.11.4 Particle size analyzer

Using optional units, with the ability to precisely measure particle size distribution, the particle size analyzer (SALD-2300, Shimadzu Co., Japan) with wide a measurement range from 17 nm to 2500 µm was used to determine the particle size for the nanoparticles.

CHAPTER 3

WASTEWATER DEGRADATION BY IRON/COPPER BIMETALLIC NANOPARTICLES AND THE MICROORGANISM GROWTH RATE

Chapter 3. Wastewater degradation by iron/copper bimetallic nanoparticles and the microorganism growth rate

In this chapter, the role of bimetallic nZVI/Cu^0 particles into wastewater contaminants degradation was characterized and the toxicity of nZVI/Cu^0 to the domestic wastewater microbial community was distinguished. The nZVI/Cu^0 effects were also compared with the reactivity of pure nZVI under different atmospheric conditions of nitrogen and air.

3.1 nZVI and iron/copper bimetallic characterization results

Fresh and spent nZVI and nZVI/Cu^0 nanoparticles were tested by TEM and EDX to investigate the typical morphology, particle size distribution, the shape properties of nanoparticles and the elemental distribution analysis for each sample. Figure 3.1illustrates the morphology, particles shape, and elemental compositions of the freshly prepared nZVI.

Figure 3.1A clearly shows the agglomeration of nZVI particles. The nZVI particles aggregate and form necklace-like aggregates with particle size diameter less than 100 nm stating that the major proportion of synthesized particles are in nano size. From the EDX spectrum (Figure 3.1B and Figure 3.1C).. Meanwhile, the EDX spectrum of fresh nZVI/Cu^0 has Fe, Cu, and C as main observations, indicating most of the nZVI/Cu^0 are Fe and Cu (Figure 3.3) and the main detected signals are from Fe atoms, confirming that nZVI is mainly composed of Fe. The C atom results from polluted carbon derived from the holey carbon coated grids where the samples have been placed. The HAADF and corresponding TEM-EDX of the spent nZVI/Cu^0 nanoparticles under both nitrogen or air atmosphere observed a strong positive association of Cu with Fe abundance, consistent with phosphorus and sulfide being retained on the bimetallic nanoparticles (Figure 3.4 and Figure 3.5). In order to ensure that the synthesized nZVI/Cu^0 particles are in nano size, laser particle size analyzer was used and the results show that half of the tested synthesized particles have an average diameter of 42 nm.

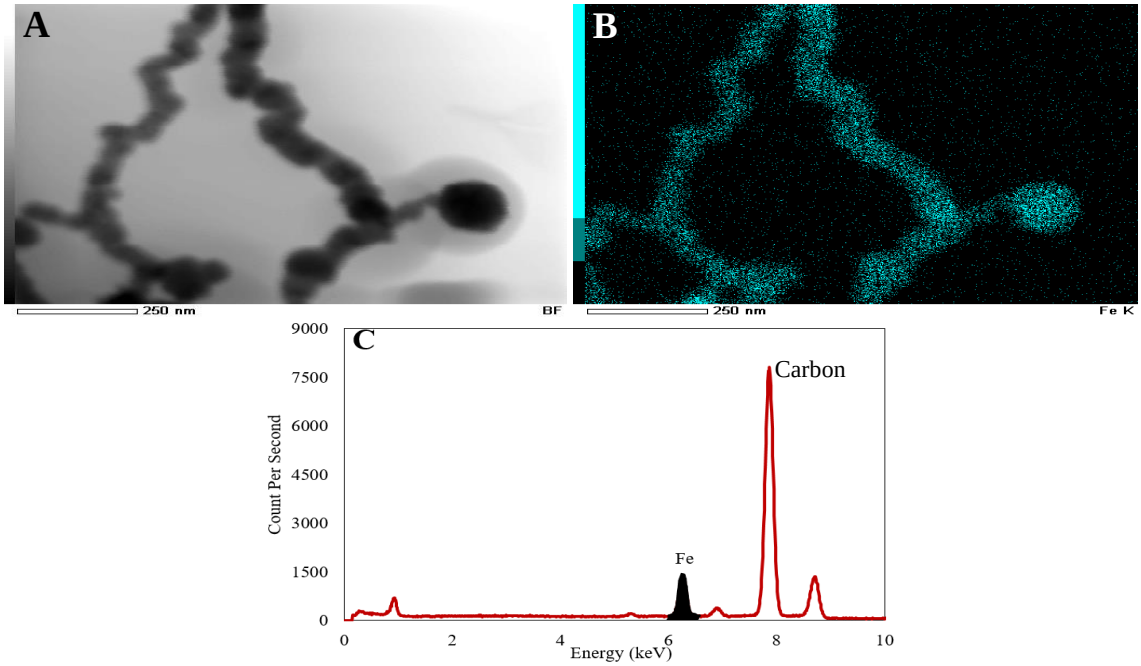

Figure 3.1 TEM HAADF images of the pure nZVI (A); (B) elemental map's observation of the presence of Fe; (C) EDX analysis of the sample, allowing to characterize composition of nZVI.

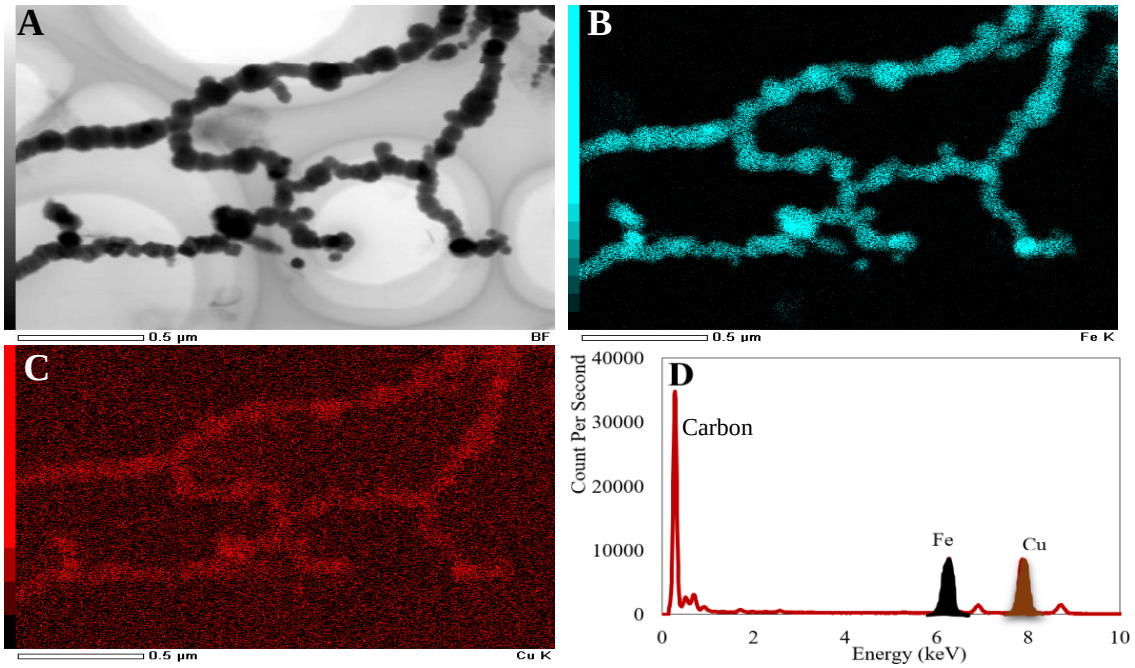

Figure 3.2 TEM HAADF images of the fresh nZVI/Cu^0 (A); (B) and (C) elemental map's observation of the presence of Fe and Cu; (D) EDX analysis of the sample, allowing to characterize composition of nZVI /Cu^0

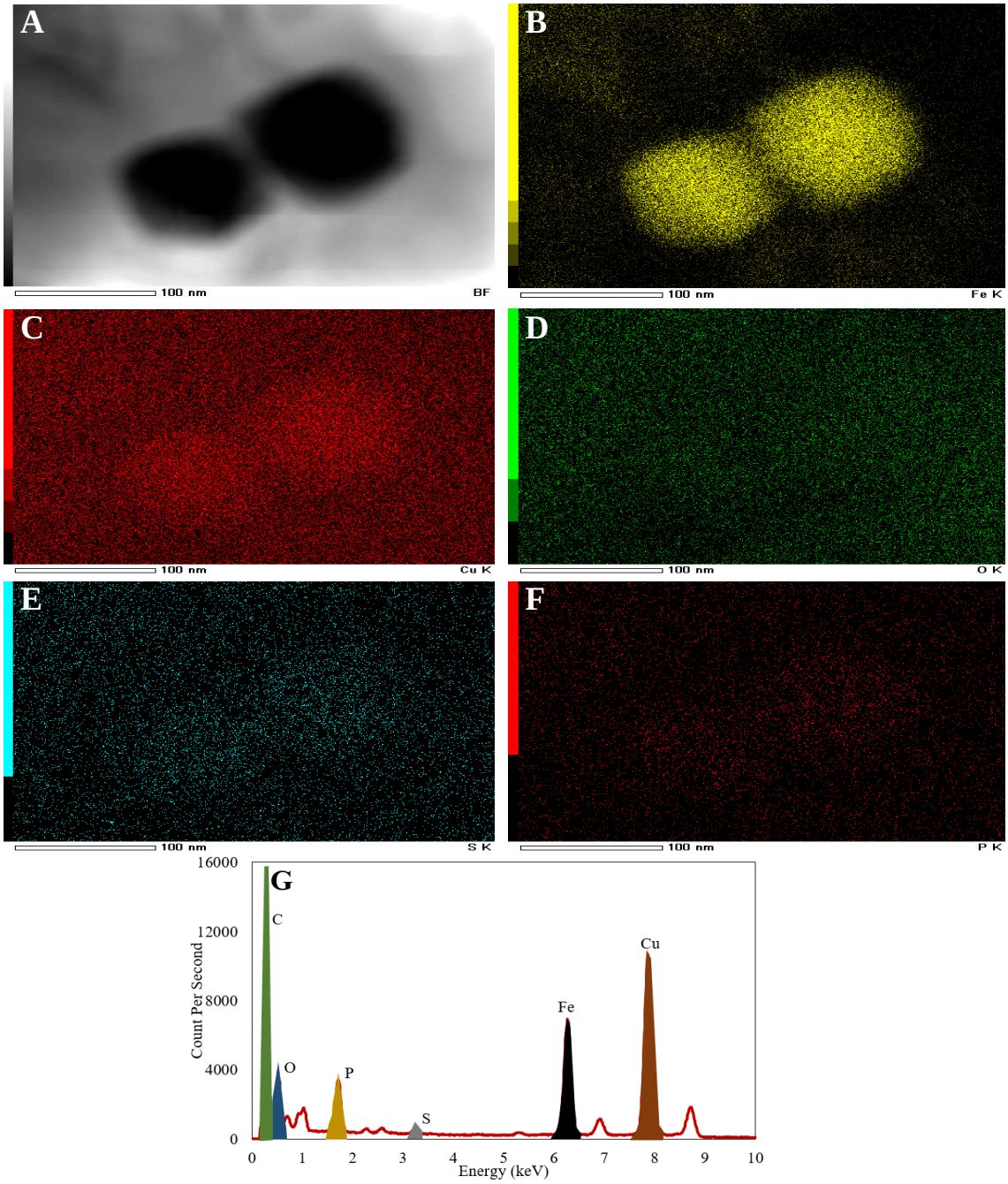

Figure 3.3 TEM HAADF images of the aerobic spent nZVI/Cu^0 (A); (B), (C), (D), (E) and (F) elemental map's observation of the presence of Fe, Cu, O, S and P; (G) EDX analysis of the sample, allowing to characterize composition of the aerobic spent nZVI/Cu^0

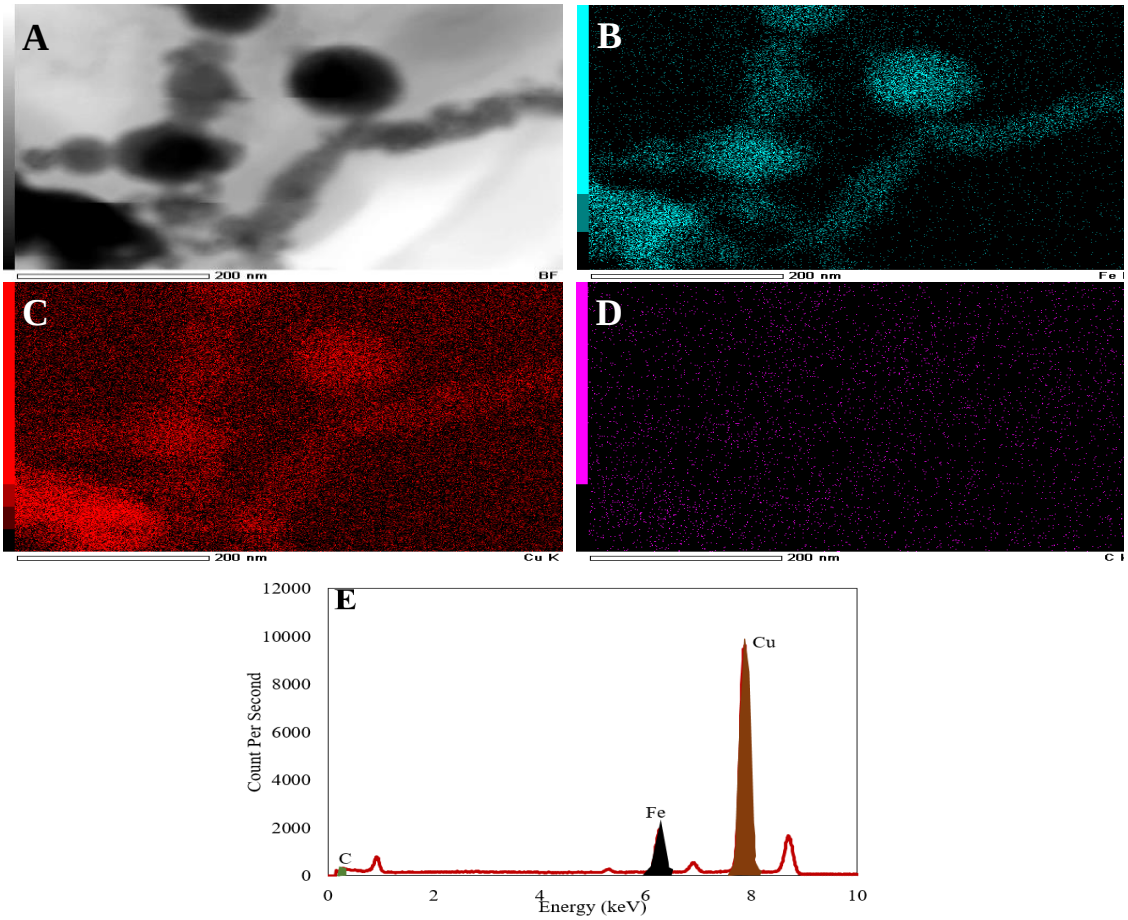

Figure 3.4 TEM HAADF images of the anaerobic spent nZVI/Cu^0 (A); (B), (C) and (D) elemental map's observation of the presence of Fe, Cu and C; (E) EDX analysis of the sample, allowing to characterize composition of anaerobic spent nZVI/Cu^0

The structure crystallinity of the fresh and used nanoparticles was checked by XRD analysis as presented in Figure 3.5. XRD spectrums of fresh nZVI/Cu^0 indicates the major peaks of Fe and Cu with the intensities at 2θ equal to 44.8° and at 65.8°, respectively, confirming that the components of nZVI/Cu^0 were primary Fe^0 and the copper-iron oxide components were evident (Figure 3.5A).

Additionally, the XRD analysis confirmed that increased oxygen content points out that iron oxides layer were formed on the metallic surface similar confirmation was also reported by Li R. et al (2015) [87].

As shown in Figure 3.5B and Figure 3.5C, the peak at 2θ = 44–45° signalize that the nZVI/Cu^0 is mainly consiste of Fe^0. However, a characteristic peak at 2θ = 34–35° is also existed, indicating that bimetallic oxide was evident. It was mainly due to the surface part of bimetallic being oxidized when it was used for the wastewater contaminants degradation. The increase of phosphorus elements after reaction suggest that nitrogen and phosphorus compositions or intermediates were absorbed onto the bimetallic particles surface.

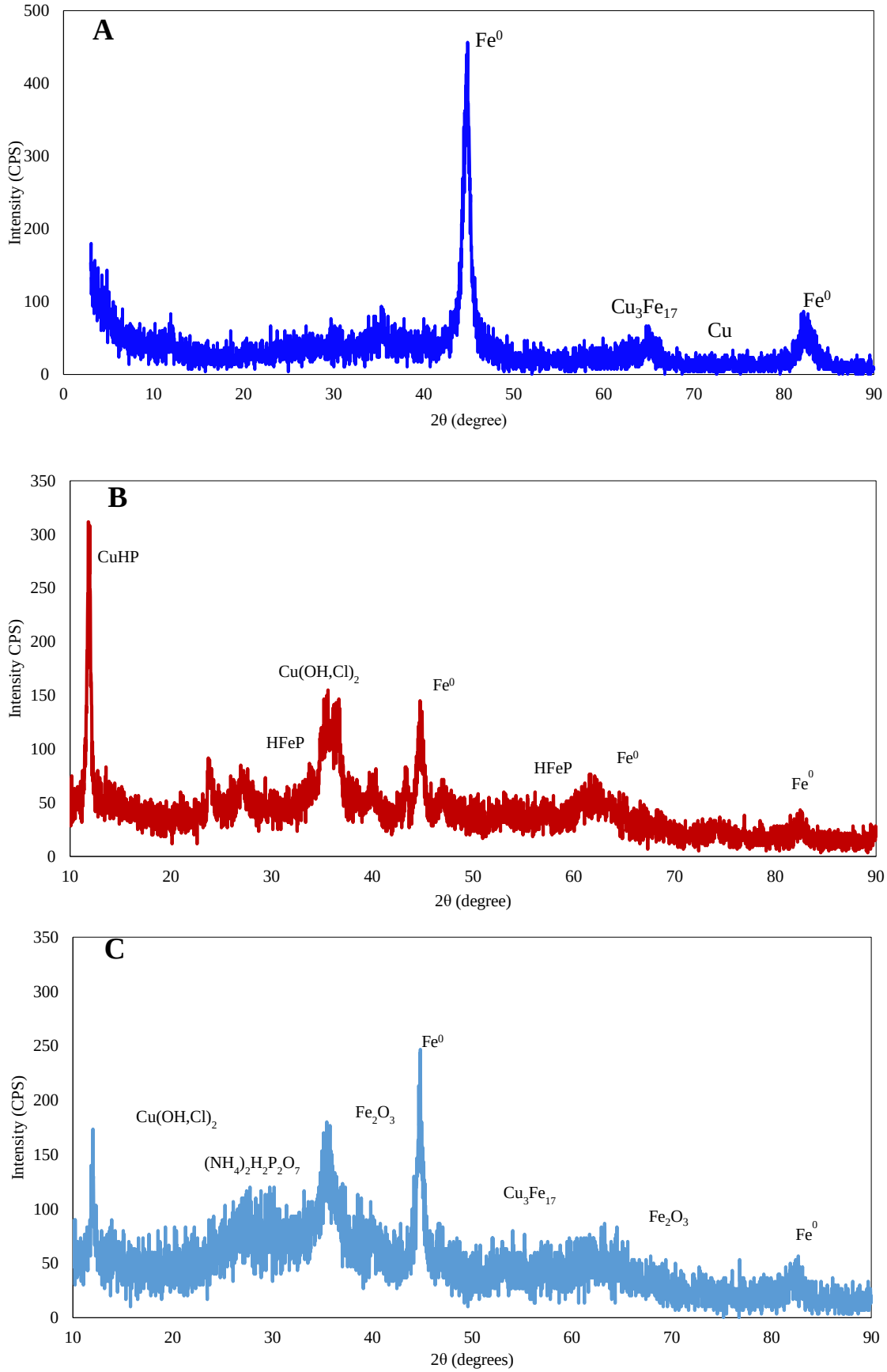

Figure 3.5 XRD analysis results: A) fresh nZVI/Cu^0, B) anaerobic spent nZVI/Cu^0 and C) aerobic spent nZVI/Cu^0

3.2 The toxicity impact of bimetallic on the microorganism's life

Tracking the survival bacteria and bacterial growth rate change is believed as one of the best ways to investigate the toxic effects of nanoparticles on the microbial life into the wastewater. During treatment of wastewater, bacteria is responsible for the degradation of nutrients and contaminations [88]. Figure 3.6 presents the bacterial growth with several nZVI/Cu^0 concentrations and pure nZVI nanoparticles under aerobic and anaerobic conditions. Under aerobic condition, both pure nZVI and the bimetallic nZVI/Cu^0 dosage comparatively inhabit the number of survival bacteria comparing with control, particularly during the first 60 hours of exposure. According to Figure 3.6A the number of bacterial colonies decreased when exposing the wastewater samples to 10 and 100 mg/L of nZVI and nZVI/Cu^0 nanoparticles. However, when the nZVI/Cu^0 concentration was 200 mg/L, the bacterial growth rate roughly was the same as control. Considerable survival numbers of colonies were depicted when dosing 500 mg/L nZVI/Cu^0. After 72 hours, which means at the end of increasing growth phase, the numbers of surviving colonies were 34, 46, 70 and 144 $\times 10^4$ CFU/mL at the nZVI/Cu^0 concentrations equal to 10, 100, 200 and 500 mg/L respectively, however, the lowest CFU was allocated for the 100 mg/L of pure nZVI. The recovery of microbial activities when inducing nanoparticles means that introduction of nZVI and nZVI/Cu^0 can have a significant impact on domestic wastewater microorganisms and the inhabitation effect can be overcome and a fast recovery of the bacterial community occurs within a time period of one hour. The reason for declining the bacterial population in the early phase can be assigned to the negative effect of chemical oxidation of nanoparticles and the Fe^{2+} generation (Figure 3.7), following the oxidation of generated Fe^{2+} to Fe^{3+} which permit the oxidizing bacteria to gain the energy and subsequently decreased total cell abundance [89].

The likely explanation for these results that increasing nZVI/Cu^0 dosage with presence of oxygen leads to increase iron metal dissolution, therefore, formation of iron oxide/ hydroxide layers of metal surface and react with contaminants iron like forming insoluble amorphous complexes and the results will reduce the inhabitation activity and increased the biological activity in presence of bimetallic nanoparticles [90].

Under the anaerobic condition in which the oxygen was replaced by nitrogen gas, as seen in the Figure 3.6B, substantial bacteria growth was observed when exposure the samples to pure nZVI or nZVI/Cu^0 despite the dosage concentrations and the significant increasing rate was observed with low nZVI/Cu^0 concentration. Survival rate was redoubled six

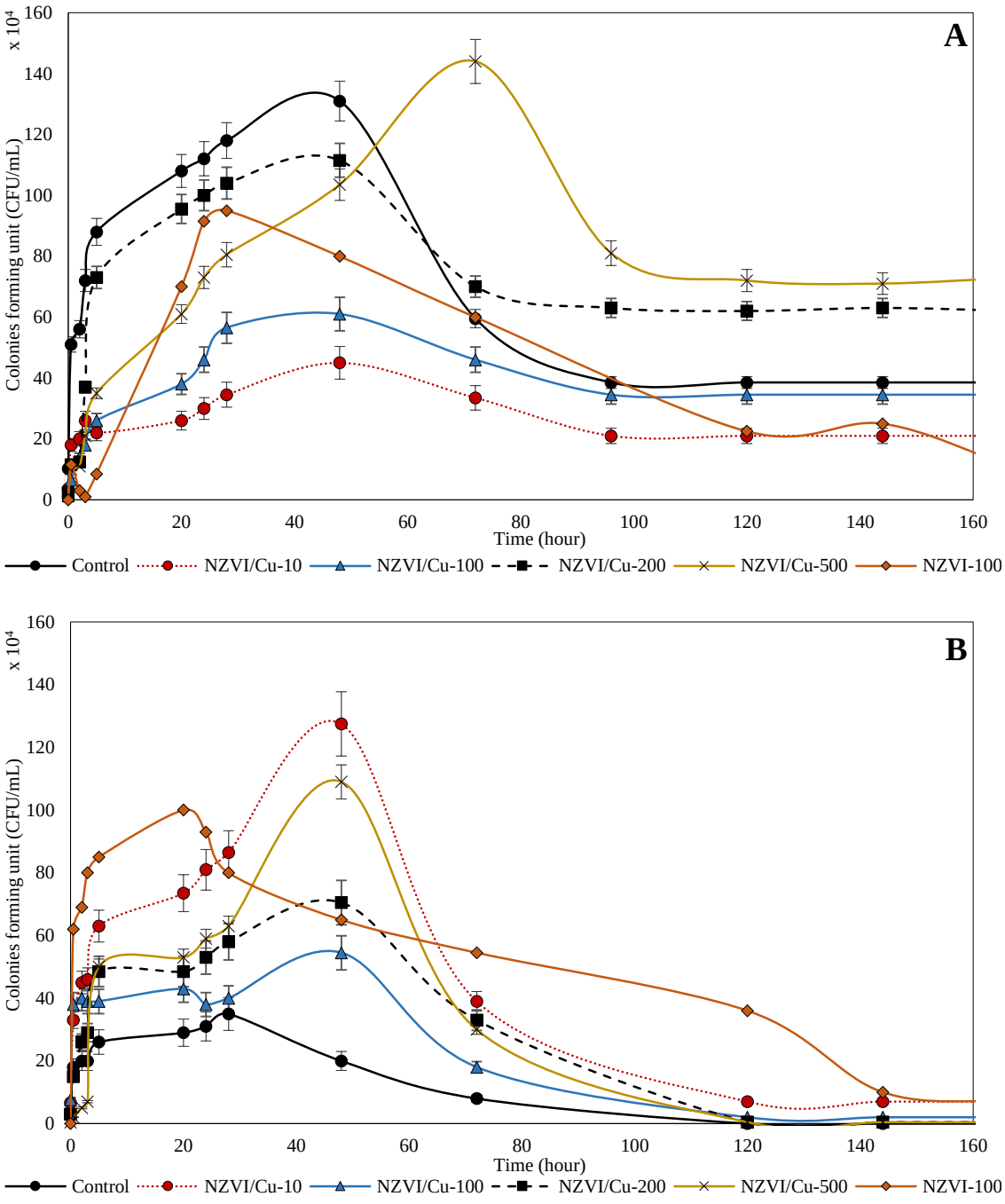

Figure 3.6 Survival counts of bacteria under different condition: A) Aerobic and B) Anaerobic

times at 10 mg/L nZVI/Cu^0 compared with control, therefore, bacterial growth was increased with decreasing of Fe^{2+} concentration (Figure 3.7B). It was pointed out that the bacteria life growth reach declining phase after 48 hours when purging samples with nitrogen gas, compared with 72 hours in presence of oxygen. Whereas, the stationary phase of the samples exposed to pure nZVI nanoparticles was ended after only 20 hours which reflect faster iron ions dissolution compared with bimetallic nanoparticles.

The numbers of bacterial colonies were 20, 55, 71 and 109 colonies after 48 hours with nZVI/Cu^0 concentrations 0, 100, 200 and 500 respectively. The raised on the number of CFU is generally because the corrosion of bimetallic nanoparticles and the generation of hydrogen gas which the bacteria use it as an electron donor for respiration [72].

Recently publications have demonstrated that the primary mechanism that the nanoparticles could easily attach to the cell of bacteria due to physiochemical properties between the nanoparticles surface and bacteria cell. These physiochemical properties were mainly because electrostatic attraction and hydrogen bonds [72, 91] and some chemical or biological interactions could occur between the bacteria and the nanoparticles.

3.3 The metal dissolution and the profiles of ferrous and ferric ions

Metals dissolution has a critical function when applying nZVI/Cu^0 to municipal wastewater contaminants removal. The catalytic capability of iron metal is strongly affected by an electrochemical corrosion and formation iron ions mostly consist Fe^{2+} and Fe^{3+} ions [92, 93]. In natural water, the primary components available for corrosion reactions are dissolved oxygen and water, with the former being, thermodynamically favored [48]. Through iron dissolution, an electrochemical corrosion of nZVI provides electrons for the reduction of pollutants. In presence of oxygen, iron reacts with oxygen and produce hydroxide and iron ions (Eq.(3.1)).

$$Fe^0 + O_2 + 4H^+ \rightarrow 2Fe^{2+} + 2H_2O \qquad (3.1)$$

In absence of oxygen, where oxygen was eliminated the iron corrosion occurred when iron reacts with water [48, 94] (Eq. (3.2)).

$$Fe^0 + 2H_2O \rightarrow Fe^{2+} + H_2 + 2OH^- \qquad (3.2)$$

Figure 3.7 prove the profiles of Fe^{2+} ions concentrations with the addition of 100 mg/L nZVI and at different nZVI/Cu^0 doses both under aerobic and anaerobic tests, respectively. As presented in Figure 3.7A the Fe^{2+} ions generation under aerobic condition was very rapid and reached the maximum within 60 minutes and the maximum generated Fe^{2+} was found with dosage only 10 mg/L nZVI/Cu^0 then subsequently the Fe^{2+} generation significantly slow down. After first 60 minutes, the concentrations of Fe^{2+} were decreased and the final amount of generated Fe^{2+} after 72 hours increased with increasing the nZVI/Cu^0 dosage. On the contrary, under anaerobic condition, the Fe^{2+} increased gradually. After 72 hours, the concentration of Fe^{2+} ions increased from 0 to 0.37, 0.49, 0.52 and 0.82 mg/L when increasing the bimetallic nanoparticles to 10, 100, 200, 500

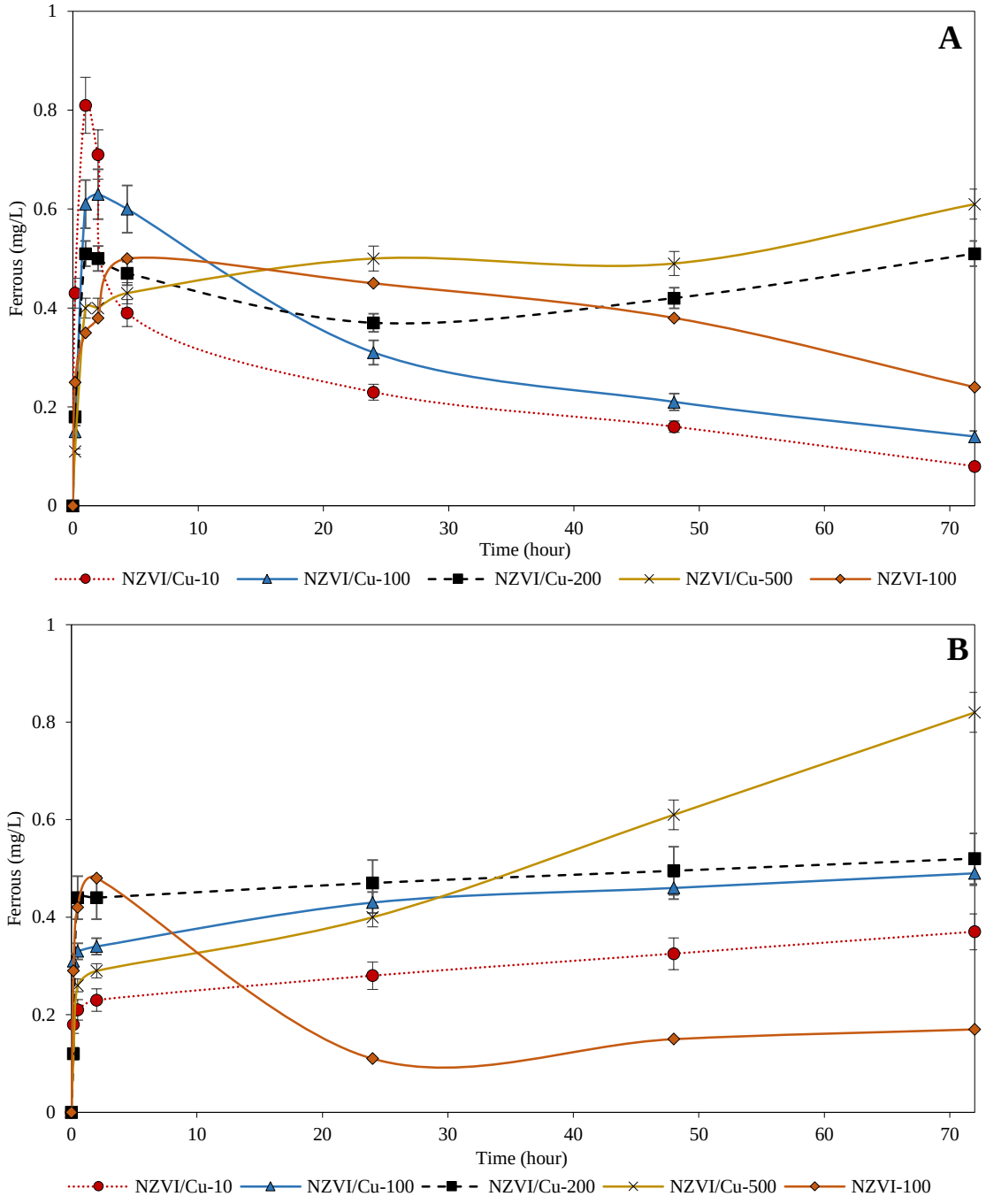

Figure 3.7 Iron dissolution (Fe^{2+} concentration): A) Aerobic and B) Anaerobic

mg/L, respectively, However the trend of Fe^{2+}generated from the nZVI experiment was increased dramatically and reach the maximum after 60 minutes, followed by decreasing trend and the final Fe^{2+} concentration was the lowest compared with the bimetallic experiments (Figure 3.7B).

Figure 3.8 illustrates the Fe^{3+} generated profiles under the aerobic and anaerobic condition. As clearly presented in Figure 3.8A the Fe^{3+} concentration was considerably lower than that of Fe^{2+} during the course of batch experiments of both nZVI and nZVI/Cu^0.

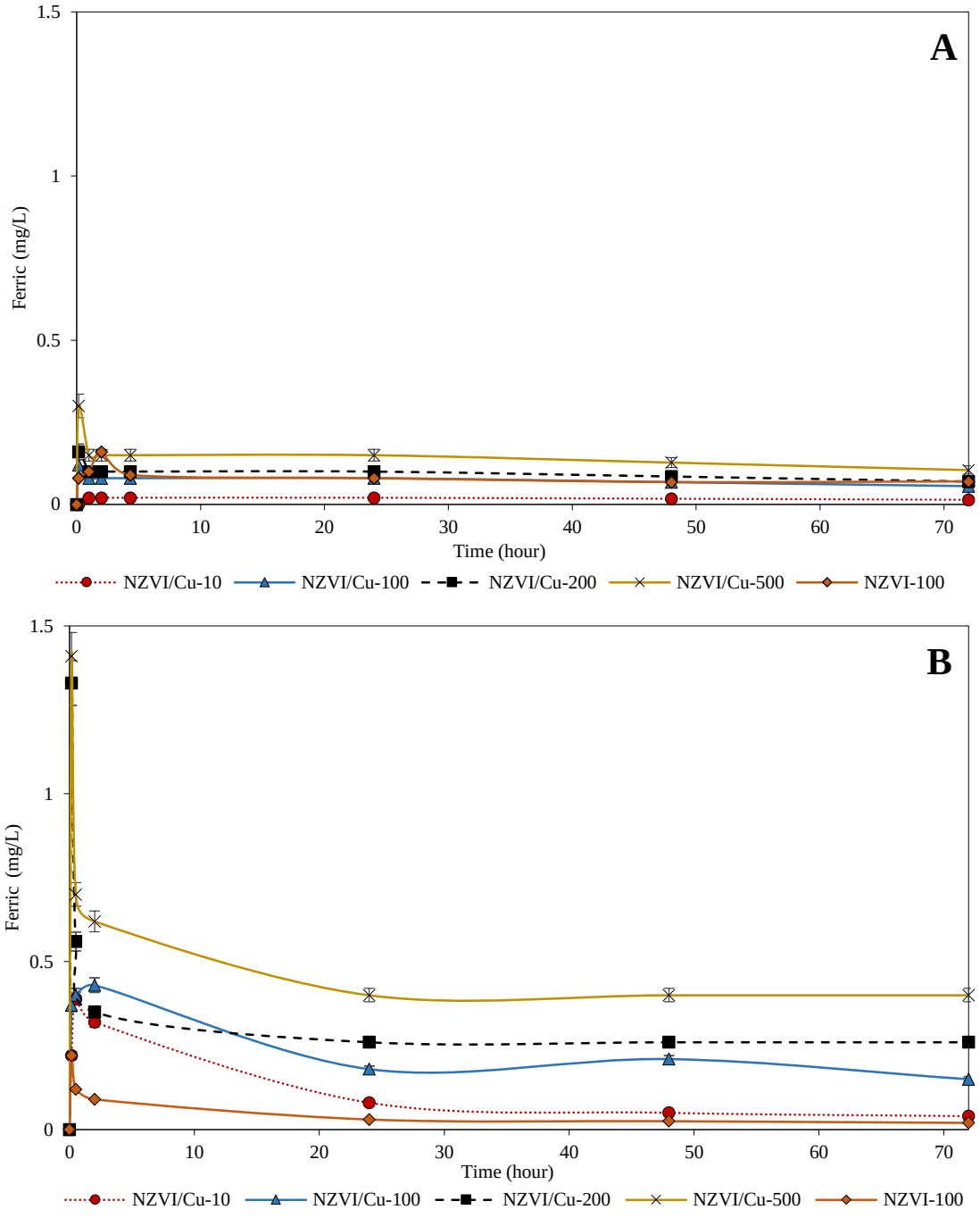

Figure 3.8 Iron dissolution (Fe^{3+} concentration): A) Aerobic and B) Anaerobic

The Fe^{3+} reduced to Fe^{2+} through the Fe^{3+} reduction (Eq. (3.3)).

$$Fe^{3+} + Fe^{0} \rightarrow Fe^{2+} \qquad (3.3)$$

As a result, the dissolved iron ions mostly consist of Fe^{2+} and the change of Fe^{2+} concentration characterized the contaminants removal from wastewater, these results are in the same line from those reported by Harada et al and Fujioka et al. [92, 93].

The dynamic transitions of Fe^{3+} under both aerobic and anaerobic conditions were very similar to each other but the Fe^{3+} generated under the anaerobic condition reached three

times higher compared with what was generated under aerobic condition. The generation of Fe^{3+} under anaerobic condition was quickly occurred within 60 minutes and decreased dramatically until 120 minutes where it decreased and remained steady-state of around 0.15, 0.28, 0.30, 0.48 and 0.1 mg/L with 10, 100, 200 and 500 mg/L nZVI/Cu^0 and 100 mg/L nZVI respectively (Figure 3.8B).

3.4 Effect of bimetallic particles on ammonia concentration

Ammonium ions as the ionic form of ammonia into the wastewater sample were checked by measuring the changes of its concentrations under the aerobic and anaerobic condition at nZVI/Cu^0 concentrations of 10, 100, 200 and 500 mg/L and at 100 mg/L nZVI. As shown in Figure 3.9. It was well-documented that ammonia is considered as the main product for the chemical reduction of nitrogen components of wastewater and nZVI or its bimetallic nanoparticles are promised to eliminate the ammonia generation when the nZVI and nZVI/Cu^0 reacts in the wastewater medium.

In absence of oxygen, it was found that increased the bimetallic dosage have an insignificant influence to decrease the ammonia concentrations. Addition of 500 mg/L under anaerobic condition has a negative effect on decreasing ammonia concentration. There are two likely explanations for the rise in the concentration of ammonium ions which appeared with high bimetallic concentrations at the beginning of the reaction that the nZVI/Cu^0 particles reduce chemically nitrogen dissolved solids into the wastewater to ammonium ions and more ammonium ions were generated at the high concentration of nZVI/Cu^0. For the second explanation, the biological process was inhibited by the high concentration of nZVI/Cu^0 particles. However, the anaerobic decreasing rates of ammonia were faster than those in the control test and at the end of bimetallic dosage course, the ammonium ions concentration was decreased by 11% compared with control suggesting that under anaerobic condition, the addition of nZVI/Cu^0 particles showed a positive effect on ammonia stripping.

The equilibrium value was reached after 48 hours of exposure in presence of oxygen regardless of the nanoparticles or concentration dosages. More ammonium ions stripping was obviously shown under the aerobic condition where the ammonium ions concentrations removal rate reached to 78% for 100 mg/L nZVI and to 75, 78, 78, and 77% at nZVI/Cu^0 concentrations of 10, 100, 200 and 500 mg/L, respectively as shown in Figure 3.9A. Whereas, under the anaerobic condition the removal rate hardly reached to 21, 33 and 37% at nZVI/Cu^0 concentrations of 10, 100 and 200 mg/L, respectively (Figure

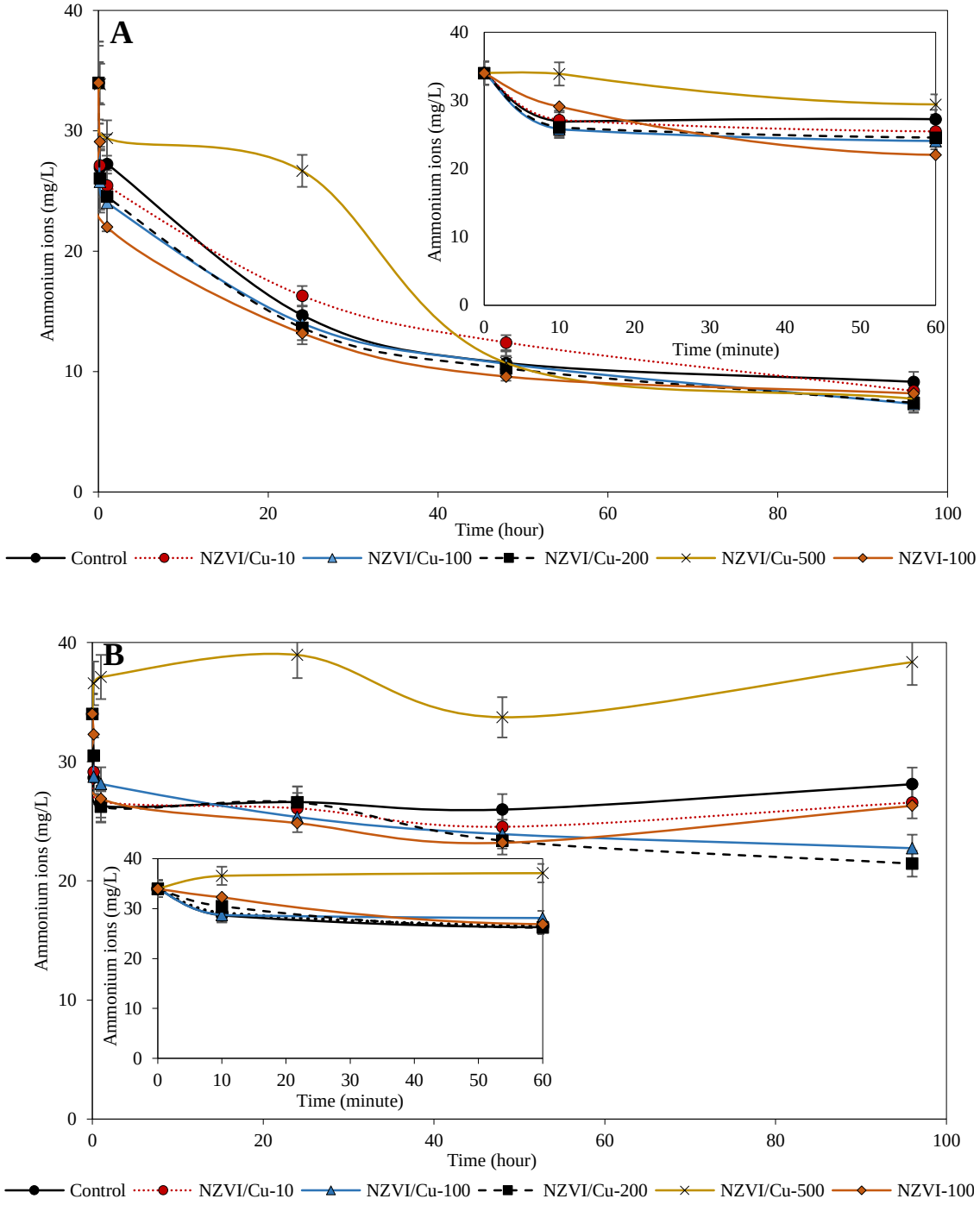

Figure 3.9 Ammonium concentration under different condition: A) Aerobic and B) Anaerobic

3.9B). Based on the results that showed decreasing of ammonia concentration in presence of nZVI/Cu^0 particles, it can be said that nanoparticles addition is a successful proposal for ammonia stripping. This is consistent with the findings of another study [95].

Moreover, decreasing the ammonia yield is considered as a primary factor to eliminate eutrophication problem of wastewater management [96].

3.5 Effect of bimetallic particles on phosphorus removal

Controlling phosphorus concentrations into the wastewater was achieved biologically through incorporating with bacteria cells and chemically through adsorption [97, 98]. As shown in the Figure 3.10, without adding nanoparticles, the removal of phosphorus concentrations in anaerobic condition was not achieved compared with considerable decreasing which clearly occurred under aerobic condition and the phosphorus concentration only was decreased from 3.12 to 2.1 mg/L in presence of air during the course of batch experiment (Figure 3.10A). Furthermore, under aerobic condition, the phosphorus removal efficiency by adding nZVI/Cu^0 particles increased significantly and the removal kinetics was increased by increasing the bimetallic concentrations, as presented in Figure 3.10A where the phosphorus concentrations decreased to 1.36, 0.96, 0.71 and 0.52 mg/L when dosing 10, 100, 200 and 500 mg/L bimetallic nanoparticles, respectively. However, the phosphorus concentration of the samples that exposed to pure nZVI was only decreased to 1.95 mg/L. These results indicated that bimetallic nanoparticles increased the phosphorus removal rate. The phosphorus removal equilibrium capacity showed a gradual increase with an increase in nZVI/Cu^0 concentration. Therefore, by raising the concentration of bimetallic particles as an adsorbent, the surface area of bimetallic particles comprise copper-iron oxides components also increased which eventually provided more vacant sites that promoted the adsorption of phosphorus [99].

It was seen from Figure 3.10 that the phosphorus sorption on bimetallic nZVI/Cu^0 surface was initially fast and more than 70% of phosphorus uptake occurred at the first 60 minutes. After that, the phosphorus adsorbed increased slowly. The adsorption equilibrium under the anaerobic atmosphere (Figure 3.10B) was approached within about 120 minutes and the phosphorus concentrations remained almost steady. Based on, the results suggest that the high reactivity of nZVI/Cu^0 bimetallic nanoparticle can be obtained under the acidic conditions due to the generation of hydrogen peroxide (H_2O_2) as a result of the interaction between the nZVI and oxygen [49] [100].

When dosing only 10 mg/L nZVI/Cu^0 concentration, the removal efficiency of phosphorus sharply increased, these outcomes were obtained as a result of microbial life activity as presented in Figure 3.6 which the bacterial growth was increased significantly at 10 mg/L bimetallic dosage and due to completely bimetallic dissolution which formed copper-iron oxides components. Copper-iron oxide components are attributed to increasing the phosphorus adsorption rate [101, 102].

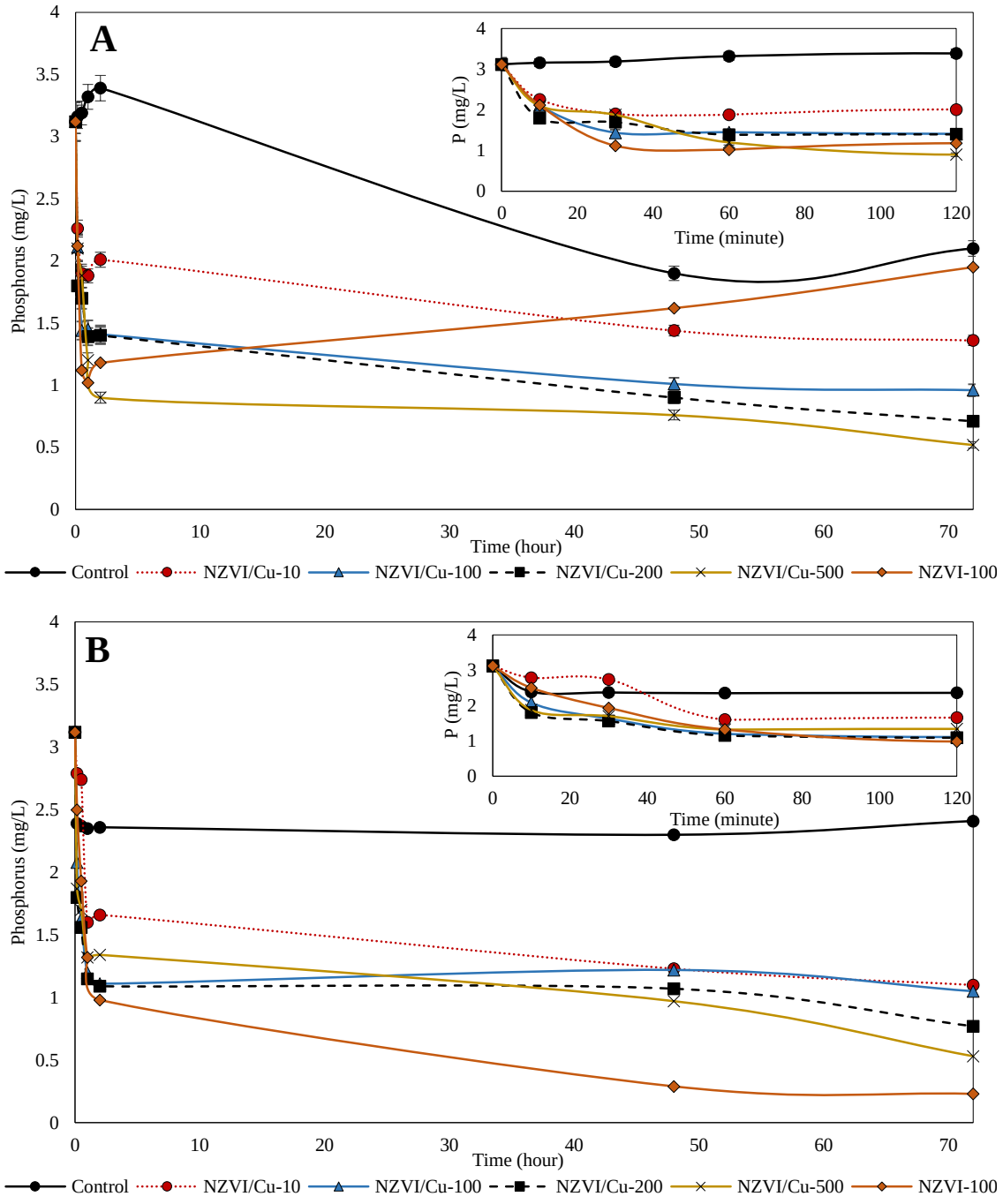

Figure 3.10 Phosphorus concentration under different condition: A) Aerobic and B) Anaerobic

However, the removal kinetics seems to be slower when increasing the nZVI/Cu^0 dosages more than 10 mg/L. After 60 minutes, it was seen that the moderate addition of nZVI/Cu^0 can support the phosphorus removal. However, further increasing of nZVI/Cu^0 until 500 mg/L did not promote the phosphorus removal efficiency, whilst dosing 500 mg/L of nZVI/Cu^0 proved superior phosphorus removal after 72 hours and the phosphorus concentrations were decreased to 0.52 mg/L for the aerobic condition.

Due to the high surface area of nZVI/Cu^0, its particles can exhibit more active site on the surface of nanoparticles and phosphorus could be adsorbed easily. Also, phosphorus concentration decreased as a result of a continuous release of Fe^{2+} and/or Fe^{3+} and subsequently do a critical influence on coagulation/precipitation process [95, 103].

3.6 COD removal

Effect of applied different concentrations of nZVI/Cu^0 or pure nZVI on COD removal were investigated. Figure 3.11 depicts the COD removal by the addition of NZVI and nZVI/Cu^0 both under aerobic and anaerobic condition. It indicates that big proportion of COD removal was obtained within 30 minutes of exposing the sample to the nanoparticles and COD concentrations decreased from 424 mg/L to 134, 98, 208 and 230 mg/L and to 71, 71, 99 and 83 mg/L when adding 10, 100, 200 and 500 mg/L nZVI/Cu^0 under aerobic and anaerobic condition, respectively and the COD concentration was decreased to 109 and 135 mg/L for the 100 mg/L nZVI experiments. It also demonstrates that after 96 hours of exposure the wastewater to 500 mg/L bimetallic nanoparticles, the COD removal efficiency reach 86% compared with 75% in control sample. More reduction of COD concentration by nZVI/Cu^0 under anaerobic condition achieved after 96 hours of applying nZVI/Cu^0 where the COD concentration decreased from 424 mg/L to 88, 111, 75, and 52 mg/L with 10, 100, 200 and 500 mg/L nZVI/Cu^0, respectively and decreased to 90 mg/L for the nZVI experiment (FFigure 3.11B). It was found that nanoparticles under anaerobic conditions can decolorize COD concentration more rapidly in comparison with those obtained under aerobic conditions unless when adding 10 mg/L of nZVI/Cu^0, the COD removal efficiency reaches 67% and 79% with the purge of nitrogen or presence of air, respectively. It can be seen that regardless of the bimetallic dosage concentration, a rapidly significant reduction of COD values occurred in the first one hour and then approximately reached equilibrium. This was due to the logarithmic rate of the bacterial population grows that was increased as shown in Figure 3.6 where new cells permit the degradation of wastewater substrates [104]. Thus, nZVI/Cu^0 is highly supposed to promise alternative cost-effective approach to improving contaminants degradation from domestic wastewater in activated sludge process.

In conclusion, it can be reported that COD decolonization could be enhanced by combined using of nZVI/Cu^0 and anaerobic microbes, and an addition of nZVI/Cu^0 can provide an effective strategy to enhance anaerobic treatment. According to the trend of COD removal, it was observed that after 96 hours of exposing the wastewater samples to

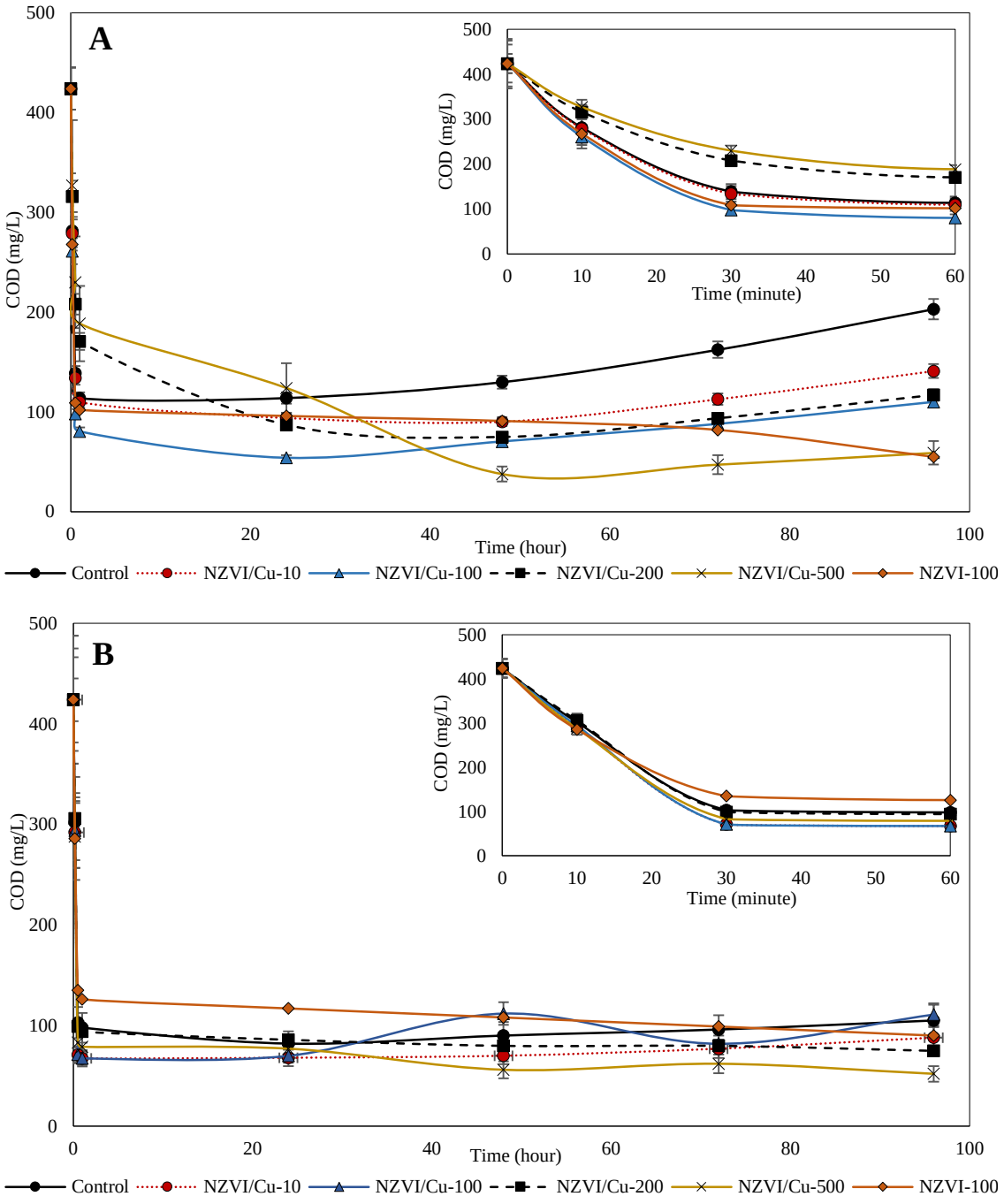

Figure 3.11 COD concentrations under different condition: A) aerobic and B) anaerobic

different nZVI/Cu^0 concentrations in absence of air a slight difference among the final COD concentrations values. Consequently, a clear dependency of bimetallic nZVI/Cu^0 on COD removal rate was not found (Figure 3.11B).

Based on the abovementioned results, two possible mechanisms for COD degradation mechanisms using iron-based nanoparticles were proposed. The two mechanisms are adsorption and reductive reaction. The first strategy involved adsorbed the organic matter onto the surface of bimetallic nanoparticles, where the oxide and hydroxide layers located

onto the nanoscale iron-based particle surface. The second strategy is attributed to the reactant of bimetallic nZVI/Cu^0 to served directly degrade of COD concentration through bimetallic corrosion reaction. The reductive reaction strategy is proposed while the corrosion of bimetallic particle emits two electrons that will be transferred to the organic matter. Therefore, the organic matter will be degraded.

3.7 Conclusions

The addition of high concentrations of bimetallic NZVI/Cu^0 particles to the wastewater mixed cultures enhances the microbial life both with oxygen or without it. The results indicated that the copper planted onto the NZVI can produce more Fe^{2+} ions under anaerobic condition and play a crucial role in limitation ammonia production and phosphorus concentrations during biological and chemical degradation processes in the domestic wastewater. The phosphorus removal efficiencies were obviously improved with the addition of only 10 mg/L NZVI/Cu^0 but this dosage concentration did not increase ammonia stripping rate compared with high dosage bimetallic concentrations. Taken as a whole, the potential ability to offer contaminants biological or chemical degradation of domestic wastewater will open many new doors for our better understanding and application of bimetallic iron-based on wastewater treatment and sustainable resource recovery.

CHAPTER 4

METHANE YIELD ENHANCEMENT BY THE ADDITION OF NEW NOVEL OF IRON AND COPPER-IRON BIMETALLIC NANOPARTICLES

Chapter 4. Methane yield enhancement by the addition of new novel of iron and copper-iron bimetallic nanoparticles

In this chapter, nZVI/Cu^0 was employed into laboratory scale anaerobic digestion system for improving the biogas production and methane yield through dosing wide-range bimetallic concentrations. To the extent of our knowledge, this is the first time to examine the effects of nZVI/Cu^0 bimetallic dosage onto anaerobic sludge and comparison with the outcomes of nZVI influences. For more than 14 days, the impact of nZVI and nZVI/Cu^0 bimetallic nanoparticles on anaerobic digestion of municipal wastewater was evaluated by determining the changes in cumulatively produced gas volume, soluble COD, pH and other chemical properties in the sludge.

The changes in microbial populations by quantitatively counting the number of colonies to describe the bacterial life through the digestion period with exposure to nanoparticles were also determined.

4.1 Comparison between nZVI and nZVI/Cu^0 additives for enhancing the biogas cogeneration

Biogas production is considered as an index used to assess the performance of anaerobic sludge digestion. During the anaerobic digestion processes, the biodegradable activated sludge was anaerobically digested to produce methane at the appropriate temperature of 37 °C [67, 105]. Accordingly, to investigate the effects of nZVI and nZVI/Cu^0 particles, the anaerobic digestion of sludge was conducted by adding nZVI and nZVI/Cu^0 particles with different concentration levels (0, 50, 100, 250, 500, 1,500, 3,000 mg/L).

The cumulatively produced biogas from the nZVI and nZVI/Cu^0 bio-digester systems during the digestion period of 14 days is presented in Figure 4.1. The average production of the control bio-digester during the digestion period reached 229 mL. Every bio-digester with the addition of nanoparticles observed in this study has biogas production more than the control, excluding the bio-digesters which were exposed to the lowest two concentrations of nZVI (50 and 100 mg/L). During 14 days long, the cumulative biogas generations were decreased from 229 mL to 192 mL and 209 mL for 50 mg/L and 100 mg/L addition of nZVI respectively, which was attributed to low dissolution of iron under these two nZVI concentrations as it discussed in the subsection of iron ions release.

The highest biogas production was achieved when the sludge was treated with high concentration of bimetallic (1,500 mg/L nZVI/Cu^0). However, by the end of digestion,

adding 3,000 mg/L of nZVI/Cu^0 bimetallic nanoparticles inhibits the biogas generation by 31.1% compared to the volume of biogas generated through 1500 mg/L bio-digester. Moreover, the nZVI/Cu^0 nanoparticles concentrations proved that adding of 50, 100, 250, 500, 1500 and 3000 mg/L of nZVI/Cu^0 bimetallic boosted the produced biogas from 229 in control bio-digester to 337, 355, 373, 516, 693, 477 mL respectively, in percentage 47.16, 55.02, 62.88, 125.33, 202.62, 108.30% respectively. In general, the addition of nZVI/Cu^0 could contribute to enhancing the biogas production from the domestic activated sludge under the test conditions, which confirm the positive effects of iron-copper bimetallic nanoparticles on the anaerobic digestion process.

For the high concentration of nZVI, and when the bio-digesters were exposed to 250, 500, 1500 and 3000 mg/L of nZVI, these iron nanoparticles significantly increased the biogas volume 1.19, 1.31, 1.73 and 2.05 times the biogas volume generated by the control respectively (Figure 4.1).

During the 14 days of anaerobic digestion duration, the biogas generated for nZVI sets were daily observed and the maximum gas production was observed at day 6. Afterwards, from day 7 to day 14, during which a much slower increase of biogas production was observed.

For comparison, contrary from day 8 onwards, the bio-digesters which were exposed to nZVI/Cu^0 bimetallic nanoparticles, it was demonstrated that there was no considerable increase of a cumulative gas and the biogas production in all bio-digesters was almost negligible. At the end of day 14, the total biogas volumes for the 1,500 mg/L and 3,000 mg/L bio-digesters were about 693 and 477 mL respectively. Therefore, the daily production rate and cumulative volume of 3,000 mg/L of nZVI/Cu^0 bimetallic addition relatively inhibited the generation of biogas. This meant that the methanogenic activity was quite low when the bimetallic dosing concentrations were increased more than 1,500 mg/L.

The likely mechanism for these results is related to activities enhancement of methanogenic bacteria in presence of nanoparticles and the ability of nZVI and nZVI/Cu^0 nanoparticles to serve as an elector donor for reducing the carbon dioxide into methane through methanogenesis according to the Eq. (4.1) and Eq. (4.2) [61]. The inhabitation was observed might be due to the fast H_2 generation under the anaerobic conditions consistently as Yang et al concluded [67].

$$CO_2 + 4Fe^0 + 8H^+ \rightarrow CH_4 + 4Fe^{2+} + 2H_2O \quad (4.1)$$

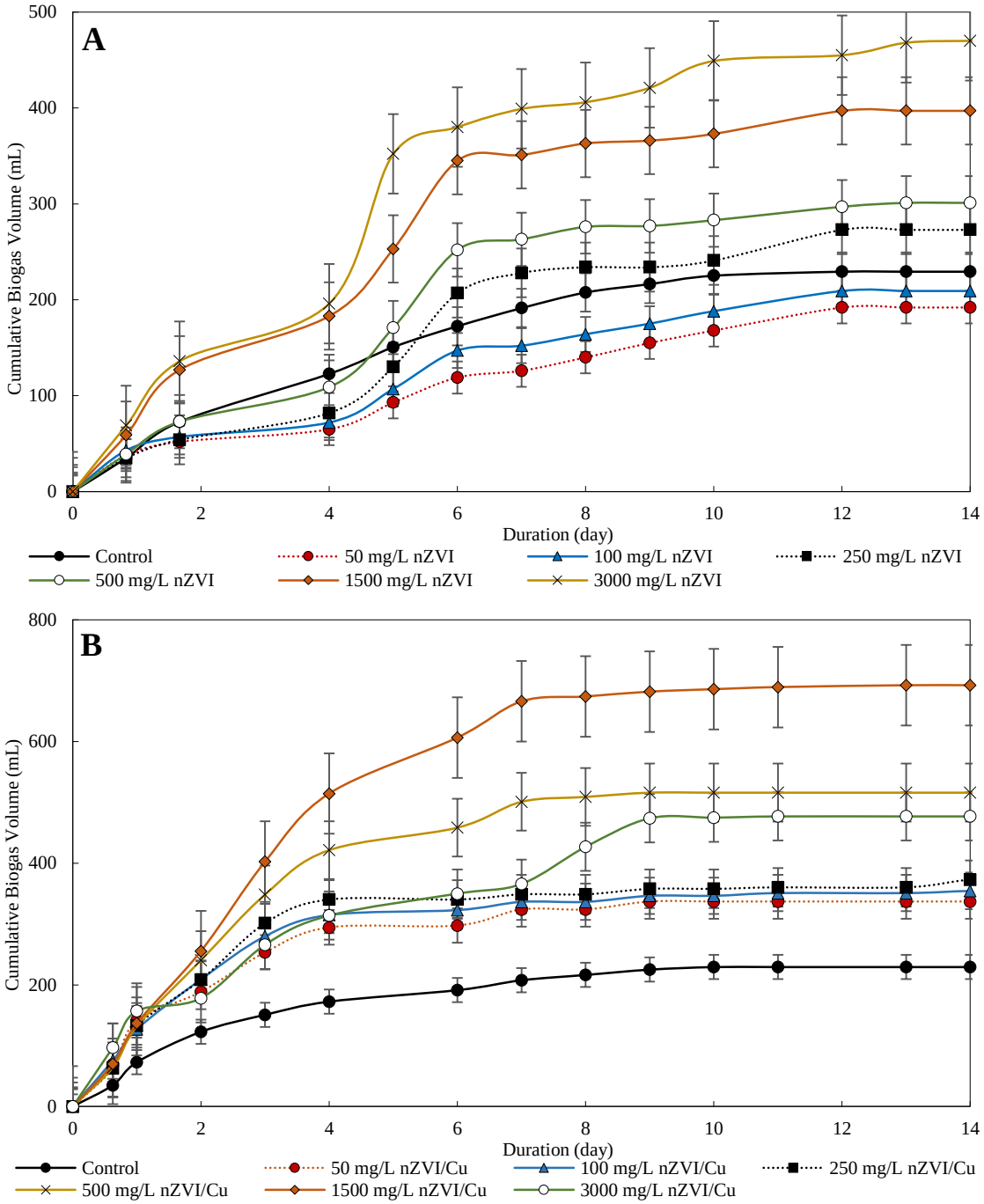

Figure 4.1 Cumulative biogas production profiles affected by the addition of A) nZVI, B) nZVI/Cu^0

$$CO_2 + 4H_2 \rightarrow CH_4 + 2H_2O \quad (4.2)$$

In conclusion, moderate-term (14 days) evaluation of domestic sludge with addition of iron and copper iron-based nanoparticles showed a significant enhancement of anaerobic digestion under mesophilic condition indicating that nZVI and nZVI/Cu^0 nanoparticles can increase the catalytic reactivity and boost anaerobic endogenous metabolism when the concentrations of nZVI were between 250 mg/L to 3,000 mg/L and to 1,500 mg/L of bimetallic nZVI/Cu^0 [106]. If the dosages of nZVI/Cu^0 raised more than 1,500 mg/L, it

would make the bimetallic effect weaker, suggesting that excessive nZVI/Cu^0 doses did not stimulate the methane production further and probably exerted negative effects on microbial activity.

The experimental results obviously indicated that the iron bimetallic relatively had better effects on the stimulated anaerobic digestion of sludge.

4.2 Iron ions release

Generally, hydrogen ions were needed to accomplish the carbon dioxide to methane. The common mechanism for donates the hydrogen electrons from the nZVI particles and its bimetallic forms to microorganisms is via cathodic hydrogen. Under the nitrogen atmosphere, the Fe^0 generates H_2 when it is reduced by the chemical reaction with H_2O as indicated back in Eq. (3.2) [62].

In the present research works, the concentrations of iron ions in the bio-digesters were investigated during the experimental period to show whether the increase of the iron nanoparticles could stimulate the methanogenesis or not. Figure 4.2 shows the changes of iron ions concentrations under the anaerobic condition for both nZVI and nZVI/Cu^0 particles. Almost all iron ions were Fe^{2+} because of the anaerobic ambiance [68].

The concentration of dissolved Fe^{2+} ions gradually increased with increasing the nanoparticles concentrations. For an instant, the Fe^{2+} concentration of 500 mg/L nZVI bio-digester increased to 114.65 mg/L after 24 hours. The similar trend of increase was also observed due to the same dosing concentration of bimetallic nanoparticles as described in Figure 4.2 (A, C).

The Fe^{3+} concentrations were weak and relatively stable, ranging to less than 50.82 mg/L for all bio-digesters exposed to 250 mg/L nanoparticles or less. For the bio-digesters treated with 500 mg/L, the aqueous Fe^{3+} concentrations were around an average of 54.00 and 45.13 mg/L for the nZVI and nZVI/Cu^0 set, respectively.

From day 1 to day 5, the Fe^{2+} concentrations of the bio-digester treated with 3,000 mg/L nZVI increased from 99.99 mg/L to 532.58 mg/L, then it was dramatically dropped until it decreased to the concentration of 285.99 mg/L at day 14. For the 3,000 mg/L nZVI/Cu^0 bio-digester, the Fe^{2+} ions concentration was lower than the 500 and 1500 mg/L nZVI/Cu^0 bio-digesters through the course of experiments and Fe^{2+} concentration has a limit with only 160.72 mg/L (Figure 4.2C). Therefore, the volume of cumulative biogas production as will be discussed in the next section (Figure 4.2B) is attributed to the dissolution trend of the Fe^{2+}.

These results indicated that the additional nZVI and nZVI/Cu^0 could similarly act as electron donors. Moreover, careful tracking of the biogas production rates and the Fe^{2+} ions concentrations showed that biogas production rate was significantly increased in the presence of Fe^{2+} ions Figure 4.2(A, C). Specifically, in case of 3,000 mg/L iron-based bimetallic, the concentration of Fe^{2+} ions increased rapidly until the day 4 and was maintained only between 110.25 and 160.72 mg/L. The generated biogas rate in this duration for 3000 mg/L nZVI/Cu^0 was lower than of the rest of digestion period, whereas with the addition of 3,000 mg/L nZVI nanoparticles, the biogas production raised until the end of digestion period (14 days) and the Fe^{2+} ions reached the maximum. Therefore, the production of biogas with the presence of nZVI and nZVI/Cu^0 was constantly increased with the abundance of Fe^{2+} ions, and these Fe^{2+} ions are considered the main reason for enhancing the methanogenesis, these results were consistent with other studies of Qiao et al. 2015 [107].

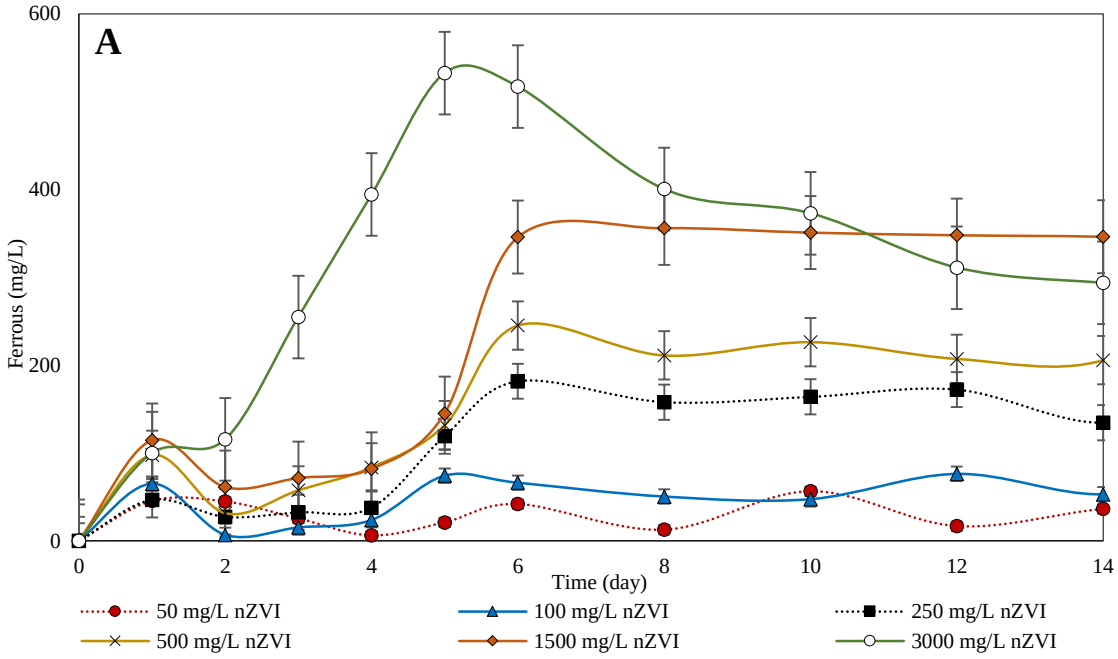
A
Ferrous (mg/L)
600
400
200
0
0
2
4
6
8
10
12
14
Time (day)
50 mg/L nZVI
100 mg/L nZVI
250 mg/L nZVI
500 mg/L nZVI
1500 mg/L nZVI
3000 mg/L nZVI

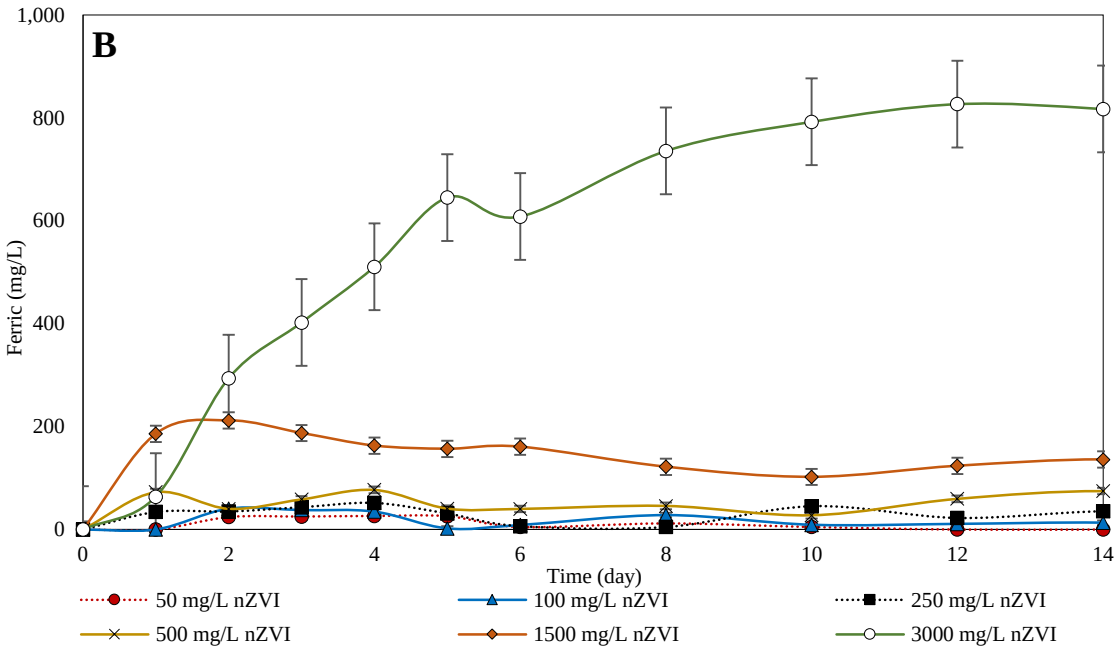
B
Ferric (mg/L)
1,000
800
600
400
200
0
0
2
4
6
8
10
12
14
Time (day)
50 mg/L nZVI
100 mg/L nZVI
250 mg/L nZVI
500 mg/L nZVI
1500 mg/L nZVI
3000 mg/L nZVI

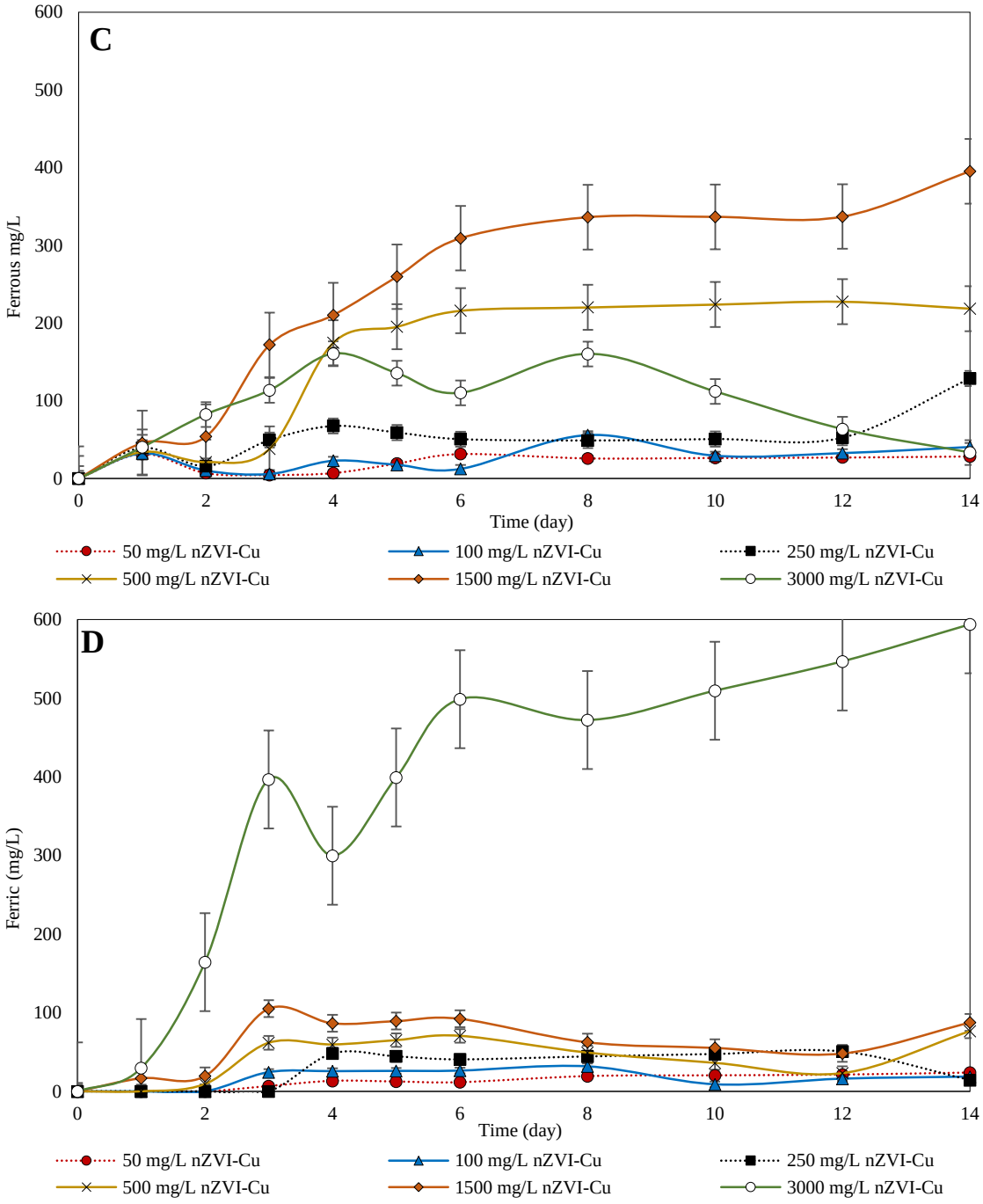

Figure 4.2 Dissolved iron ions concentration change with time A) Ferrous ions of nZVI B) Ferric ions of nZVI C) Ferrous of nZVI/Cu^0 D) Ferric of nZVI/Cu^0.

4.3 Methane Content

From Figure 4.3, despite the nanoparticles concentration, methane content was quite low during the first 24 hours. It was revealed that nZVI with the high concentration (500, 1500 and 300 mg/L) clearly stimulate the methanogenic activity just after 24 hours of anaerobic digestion process in comparison with other concentrations. Furthermore, bio-digesters treated with 250, 500, 1500 and 3000 mg/L nZVI increased the methane content to 62, 57, 59 and 50% compared with 9% as an average content that the control

bio-digester showed on the first day. Additionally, the treatment of activated sludge with 500 mg/L of nZVI or above yielded the highest methane content that exceeds 82% from day 7 until the end of the experiment duration. However, the addition of the same concentration of nZVI/Cu^0 could not attain the same level of methane fraction. All the bio-digesters that were treated with 0, 50 and 100 mg/L nZVI/Cu^0 were close to each other from the beginning of the digestion process.

For comparison, the methane content trend identified two phases in the bio-digesters that were treated with nZVI, but the bimetallic groups showed gradual increase throughout the digestion duration.

In the day 7 and afterward, there was a negligible methane generation in both the control and the bio-digesters treatment with nZVI indicating the completion of methanogenesis. The produced biogas after that (Figure 4.1A) was formed from other gasses mainly carbon dioxide [108].

The interesting results were obtained with bimetallic nanoparticles addition, particularly with the concentration of 3000 mg/L, it did not promote considerable yield, which indicated that 1500 mg/L might be a more appropriate addition concentration for methanogenesis under current research condition.

These results point out that the additional nZVI and nZVI/Cu^0 particles could act as electron donors and the iron dissolution ions could be direct electron transfer, in which methanogenic bacteria work as an iron oxidizer, taking the electron from the nanoparticles to reduce the carbon dioxide to methane. Moreover, precise check about methane rates and Fe^{2+} ions concentrations displayed that the methane content was considerably increased in the presence of iron ions (Figure 4.2). For example, with 3000 mg/l nZVI added, the ions concentration of Fe^{2+} obviously less than that of the 1500 mg/L concentration during the digestion period and with this dosage concentration, the methane contents were particularly less than of the 1500 mg/L bio-digester. Subsequently, the methane increased constantly because of the plenty of iron ions. Thus, there is a reasonable correlation between the methane content and the iron ions and these generated ions should be a reliable cause for the enhancement of methanogenesis.

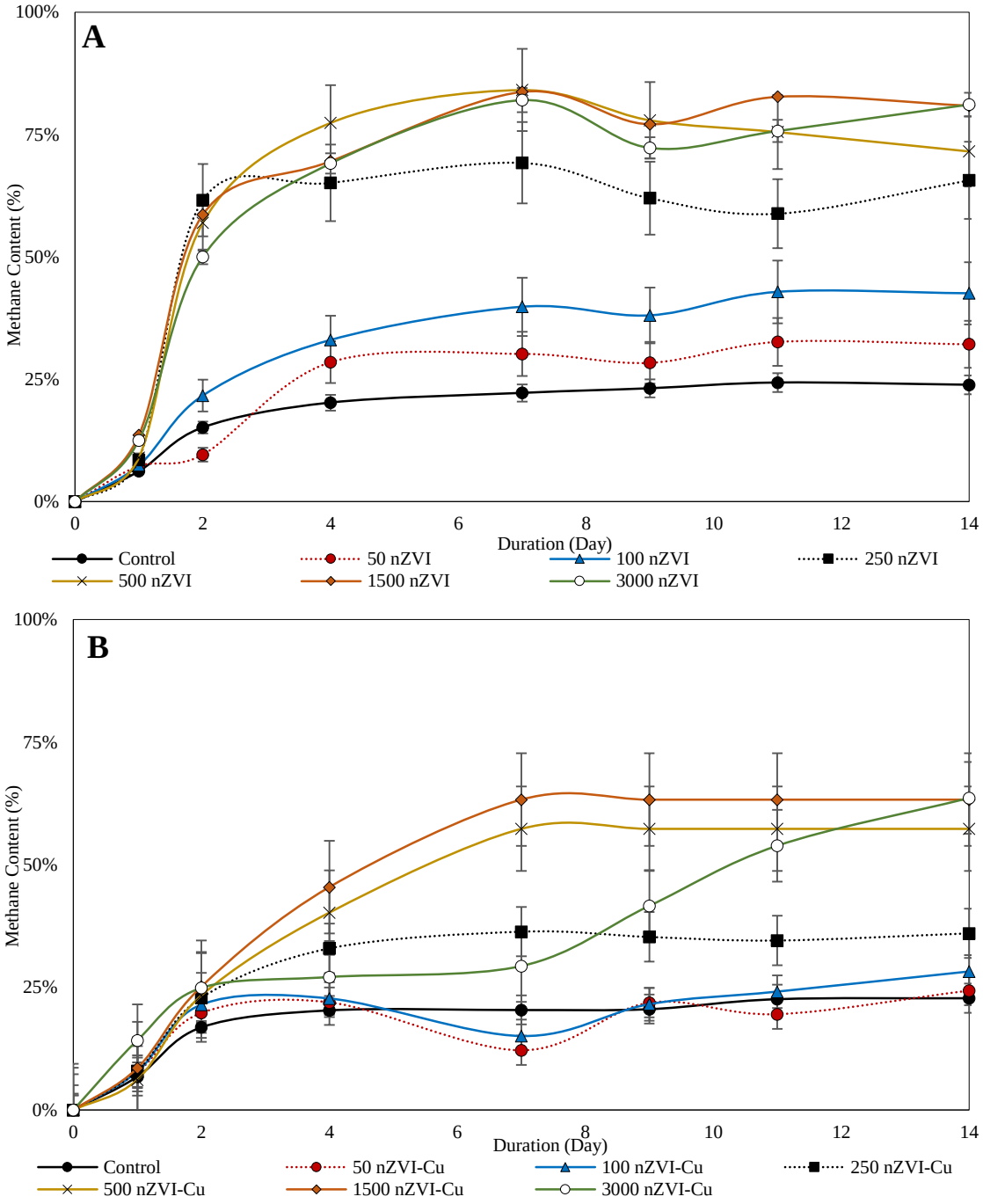

Figure 4.3 Methane Content yielded by A) nZVI, B) nZVI/Cu^0

4.4 Soluble chemical oxygen demand profile

Soluble COD profiles which mainly included soluble forms of protein, volatile fatty acids and carbohydrates [109, 110] are presented in Figure 4.4. The soluble COD concentration started to increase from the beginning of the digestion that confirms the organic matter fermentation. The initial soluble COD concentrations were around 5,453 mg/L for all bio-digesters. The soluble COD was dramatically raised and reached limit concentration from the day 1 with supplementation of the nanoparticles and remained

relatively constant afterward. These trends generally indicate that with the nZVI and nZVI/Cu^0 dose the sludge fermentation was enhanced and the rapid solubilization of sludge was quickly increased during the anaerobic digestion.

For the digestion duration until day 3, the soluble COD in the control bio-digester was 6,888 mg/L which was lower than the concentrations in all other bio-digesters but the soluble COD concentration was increased to 10,591 mg/L at day 9 compared with 8,153, 8,756 and 10,290 mg/L in the bio-digesters exposed to 50, 100 and 250 mg/L nZVI.

From day 2 afterward and regardless of the nanoparticles concentrations, the soluble COD concentrations during the anaerobic digestion period were generally stable in each bio-digesters. This soluble COD was around 9,220 mg/L in control set, while the concentrations were between 7,650 and 21,507 mg/L for the nZVI group and between 11,889 and 21,652 mg/L for the nZVI/Cu^0 bimetallic group. These results indicate that the nZVI/Cu^0 influence the sludge fermentation more than the nZVI.

The maximum soluble COD concentration was obtained at the 1,500 mg/L of nZVI/Cu^0 dose and it reached 22,190 mg/L on day 11 compared with 21,683 mg/L that the 3,000 mg/L nZVI bio-digester reached on day 9. nZVI particles at concentration of 1,500 mg/L prove soluble COD concentration of 21,754 mg/L as maximum, suggesting that the 3,000 mg/L redundant nanoparticles showed no more facilitating effect.

At the end of anaerobic digestion duration, the soluble COD concentrations in the nZVI bio-digesters group were 8,681, 9,404, 11,309, 14,105, 21,380 and 20,848 mg/L and the nZVI/Cu^0 group secured concentration of 15,661, 14,422, 15,304, 16,288, 21,939 and 20,838 mg/L soluble COD. Based on the abovementioned results, the soluble COD on the nZVI and nZVI/Cu^0 generally had increasing trends possibly because of the continued fermentation of sludge and cell lysis that occurred due to disruption of the cell membrane [67, 111].

Compared to untreated bio-digester during the 14 days of anaerobic digestion, it can be concluded that more extracellular polymer and intracellular substances dissolved out of the cell by nZVI or nZVI/Cu^0 treatment and the municipal activated sludge was hence promoted due to the additional easily degradable substrate released with the addition of iron-based nanoparticles [112].

The outcomes demonstrate that the Cu particles which coated the nZVI surface can obviously promote the sludge fermentation capacity because Cu metal can improve the catalytic reactivity of nZVI due to the relatively high reaction potential between Cu and

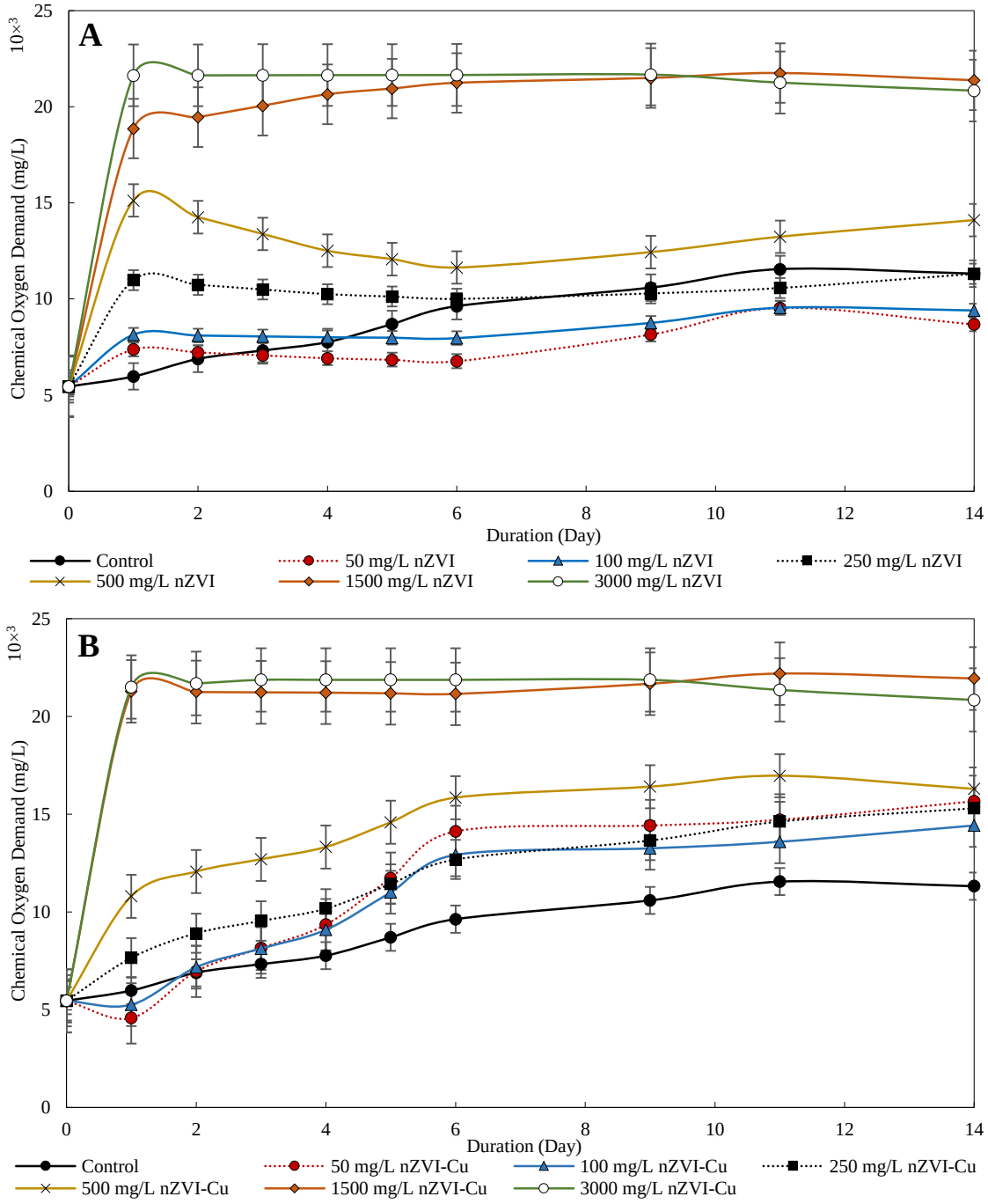

Figure 4.4 Soluble COD with time for A) nZVI bioreactors, B) nZVI/Cu^0 bioreactors

nZVI [49]. More specifically, the Cu can consolidate the production of atomic hydrogen and the reduction capacity of nZVI would be basically improved.

4.5 Bacterial population changes during anaerobic digestion nanoparticles presence

The effects of nZVI and nZVI/Cu^0 particles on the diversity of microbial communities during the fermentation of municipal sludge were estimated. The dynamic population changes during 14 days of anaerobic digestion duration are depicted in Figure 4.5. The CFU counts decreased at the beginning of digestion until they reached the

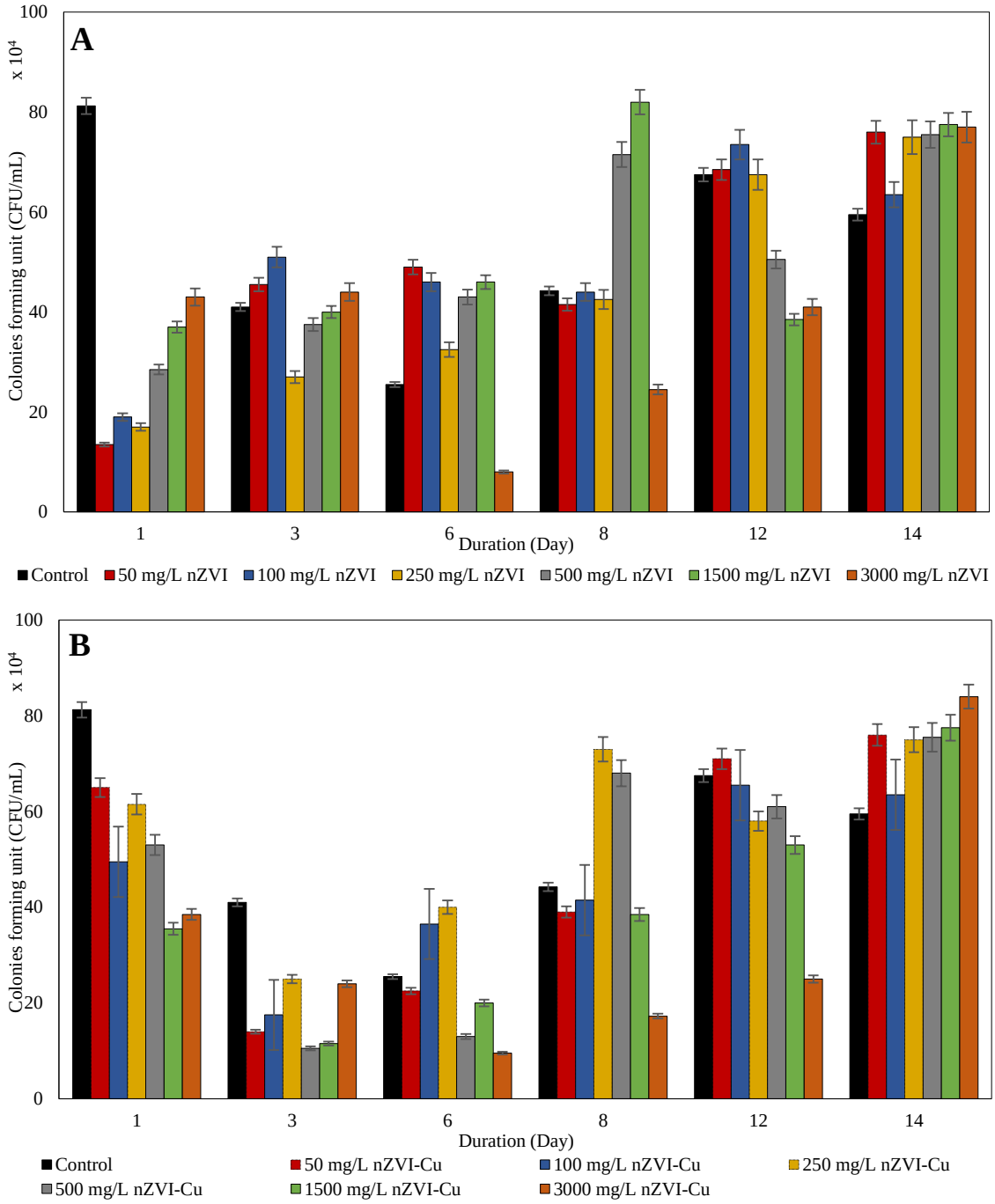

Figure 4.5 Change in bacterial growth rate in presence of A) nZVI, B) nZVI/Cu^0

minimum on day 6 for almost all bio-digesters that exposed to nanoparticles, likely due to the disruption of bacteria membrane cell [111].

In the groups of nZVI, the population was gradually increased and was peaked at day 14 (Figure 4.5). However, the growth rate of survival bacteria in the bio-digesters treated with bimetallic nanoparticles appeared to be much lower in the first 6 days.

The peak bacteria concentrations at day 14 in the groups of nZVI were 76, 64, 75, 76, 78 and 77 CFU/mL respectively, moreover, the groups of nZVI/Cu^0 the CFU numbers were close to the nZVI groups.

The variety of the bacterial community and microorganism analysis involved in the fermentation period might have an influence on the pathways of the biogas production. This was possible due to the biochemical reactions complexity involved in anaerobic digestion. The mechanisms' evidence of methanogenic activities and the relationship between the biogas generation rate and COD trends need to be further revealed in the future study.

4.6 Conclusions

The nZVI and nZVI/Cu^0 bimetallic addition can stimulate the biogas production, methane gas content and can accelerate the sludge fermentation. On the other hand, high nZVI/Cu^0 concentration added did not promote the cumulative volume of the generated biogas or methane content proportion. According to the experimental results, it is advisable to dose the optimum iron-based bimetallic not more than 1500 mg/L, while the cell disruption will occur and other gases such as hydrogen will be rapidly produced hence, the methanogenesis inhibition will be intentionally turned up. This would indicate that using nZVI or nZVI/Cu^0 at appropriate dosing rate could be an effective pathway for improving methane generation.

CHAPTER 5

BIOCHEMICAL METHANE POTENTIAL ENHANCEMENT OF SLUDGE DIGESTION BY ADDING PRISTINE IRON NANOPARTICLES AND IRON COATED ZEOLITE COMPOSITIONS

Chapter 5. Biochemical methane potential enhancement of sludge digestion by adding pristine iron nanoparticles and iron coated zeolite compositions

In this chapter, a new different composites materials were freshly prepared for the anaerobic digestion enhancement of domestic activated sludge. Supporting the nZVI by zeolite to obtain ICZ might promise to increase the biogas cogeneration, methane yielded and degrade the organic matter because ICZ composite compounds facilitate the adsorption capacity. The effect of two different nZVI particles loadings have been examined and the performance on biogas production of this novel composite ICZ was tested based on modified biochemical methane potential test, and compared with that of the bioreactors exposed to only nZVI particles or zeolite material. For comparison, the batch experiments were also carried out with no additive and with the mixture of both nZVI and zeolite.

5.1 Characterization of iron nanoparticles and iron coated zeolite

The prepared nZVI particles were black-colored precipitates, but the color changed to dark brown when coating zeolite with nZVI, indicating the presence of iron particles onto the surface of the zeolite. The particle size of zeolite, nZVI, and ICZ are shown in Table 4.

Table 4 Additives characterization

Experiment	Particle size
Zeolite	7.13 µm
Prepared nZVI	45 nm
ICZ	24.1 µm

These results were confirmed by the TEM images. Figure 5.1 shows a micrograph of zeolite and prepared nZVI. The TEM imaging of nZVI revealed a spherical shape of the particles and it was aggregate into chains (Figure 5.1B)

The chemical structure of zeolite, nZVI and ICZ compositions were determined by the XRD analysis as shown in Figure 5.2. The XRD scanned range of 2θ was from 3° to 90° and the low-intensity peaks of ICZ samples indicate a low crystalline structure. The major constituents of zeolite are silicate, alumina, and sodium. It had a crystalline structure showing predominantly distinguished and multiple diffraction peaks centered at 2θ = 7.17, 10.16, 21.68, 23.99, 27.15, 29.95 and 34.17° corresponding to the reflections of sodium tecto-alumosilicate, which has the chemical composition formula of Na_{92} Si_{92} A_{l00} as seen

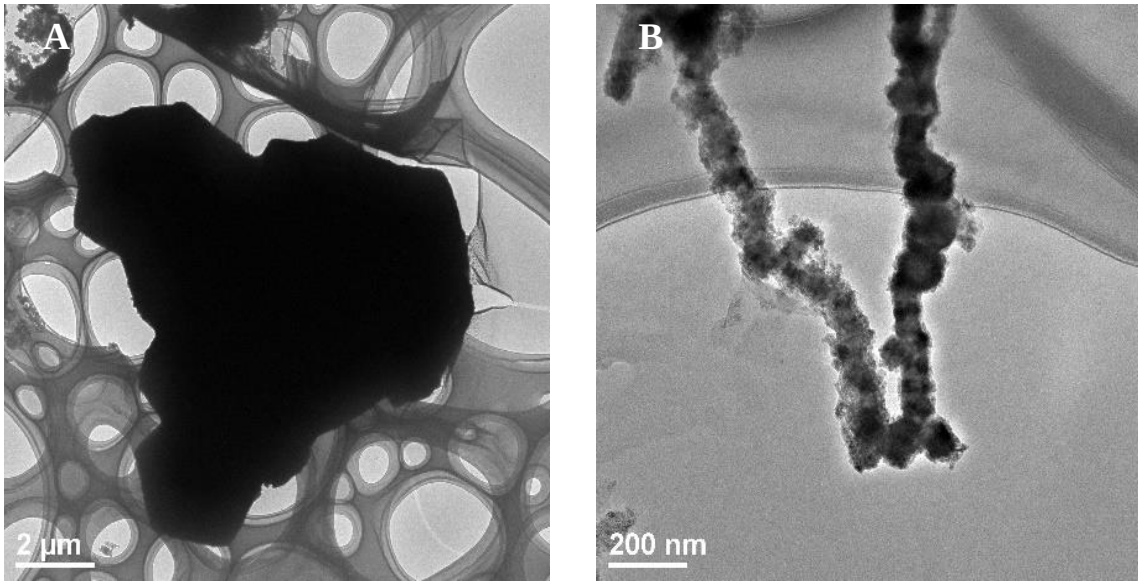

Figure 5.1 Transmission electron micrograph of zeolite (A) and prepared nZVI (B)

in Figure 5.2A. On the other hand, the XRD chart of pure nZVI displayed two diffraction peaks centered at 45.3 and 83.54° owing to the body centered cubic nZVI (Figure 5.2B). The spectrum of ICZ 500 involved the sodium aluminum silicate materials which has a crystal system with notable intensities between 23°-37° (Figure 5.2C). Moreover, with increasing the nZVI loading when preparing the ICZ 1000 spectra (Figure 5.2D) shows amorphous nature when it compared with the zeolite XRD patterns because the basic structure of ICZ 1000 has declined in the intensities. Furthermore, the results indicate that the diffraction peaks of zeolite disappeared owing to the presence of the iron nanoparticles on its framework [113].

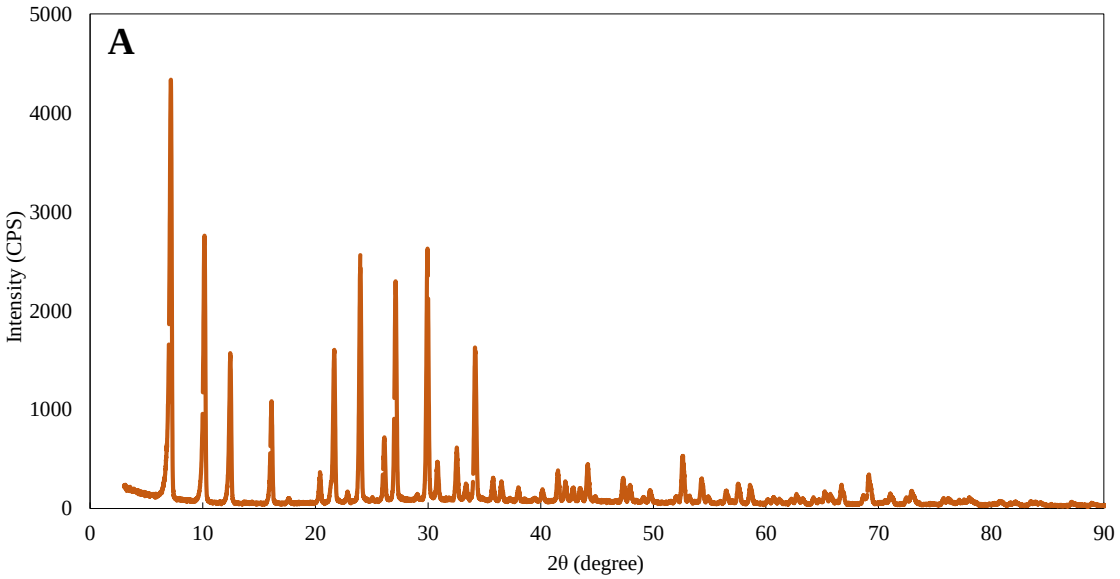

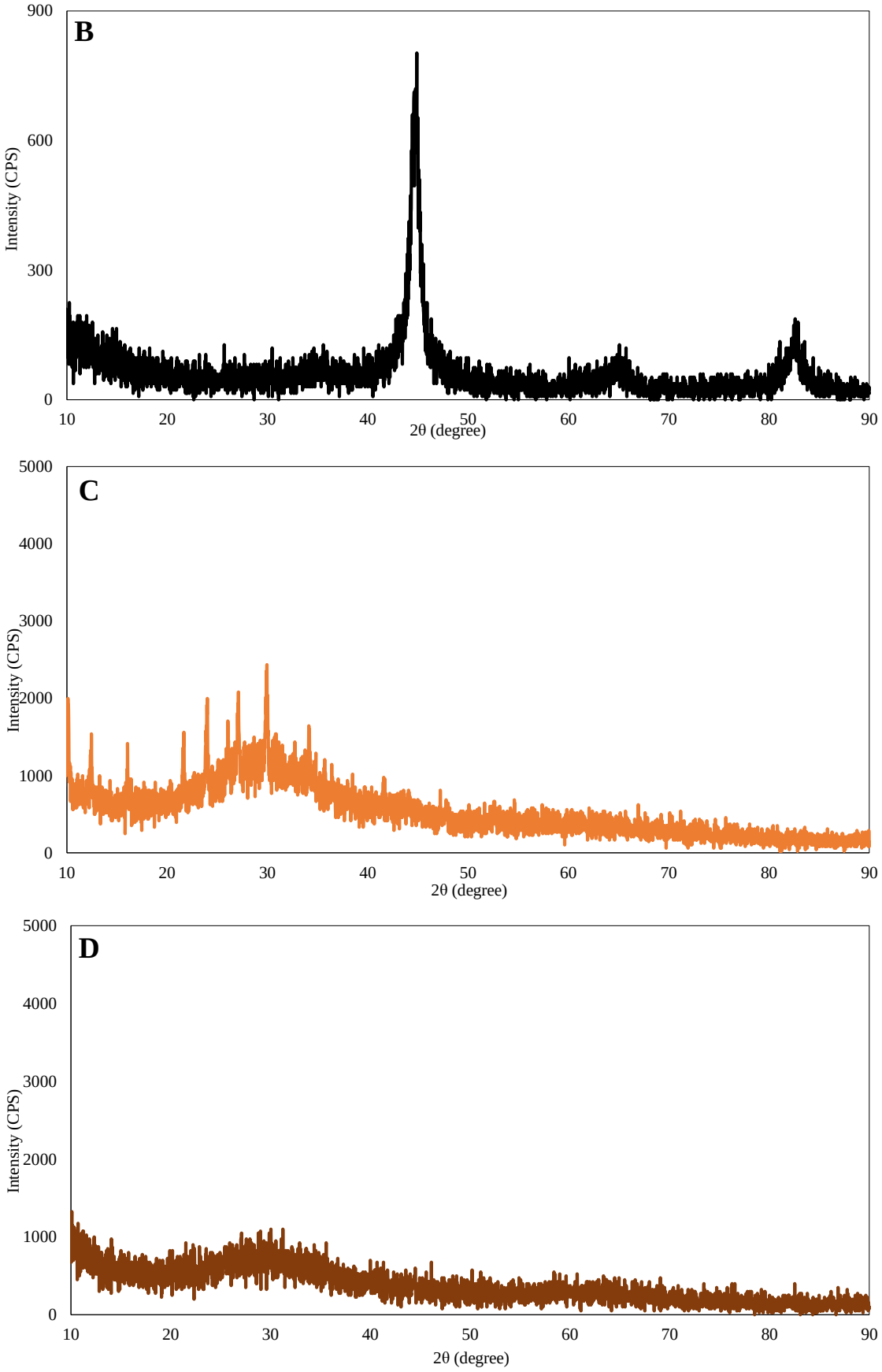

Figure 5.2 X-ray diffraction patterns of zeolite (A), prepared nZVI (B), ICZ 500 (C) and ICZ 1000 (D)

5.2 Kinetics and adsorption isotherm models

5.2.1 Zeolite-iron kinetics

The sorbate amount of ferric was calculated from the concentrations in the aqueous solution before and after sorption and the removal efficiency (R_e) was calculated according to Eq. (5.1).

$$R_e = \frac{(C_0 - C_e)}{C_0} \times 100 \qquad (5.1)$$

Figure 5.3 presents the adsorption kinetics of Fe^{3+} onto zeolite. It shows a momentary uptake of ferric within the first 15 minutes then it approached the equilibrium condition. Therefore, 30 minutes as agitation was selected for the study isotherm experiments to ensure that the maximum iron ions will be adsorbed into the zeolite material.

It can be demonstrated from Figure 5.3 that the adsorption kinetics process included two main phases, a quick adsorption within the first 15 minutes accompanied by a consecutive slow rate of 15-180 minutes. The quick adsorption rate can be allocated to the remarkable number of vacant adsorption sites on the zeolite material surface that could provide abundant binding sites for iron ions. In addition, the large surface area and the appropriate pore size can encourage the internal mass transfer in adsorption process efficiency [83].

The adsorption kinetics of zeolite that has been represented by the pseudo-first-order and pseudo-second-order models were utilized to study the adsorption process of zeolite.

As summarized in Table 5, the features for each model are listed and the highest R^2(=0.9999) indicates that iron ions uptake by zeolite well-fitted to the pseudo-second-order kinetic model. This result suggests that the uptake process of iron ions by zeolite was the rate-controlling limiting step. The value of q_e estimated by the pseudo-second-order kinetic model was 1.00132 mg/g, and the obtained rate constant k_2 was calculated to be 2.706 g/mg×min.

Table 5 Adsorption kinetic equation parameters of ferric ions onto zeolite

Kinetic model	Equation	Parameters	Value
Pseudo-first-order	$\log(q_e - q_t) = \log q_e - \frac{k_1}{2.303} t$	k_1 (1/min)	0.03955
		q_e (mg/g)	1.00
		R^2	0.8386
Pseudo-second-order	$\frac{t}{q_t} = \frac{1}{k_2 q_e^2} + \frac{1}{q_e} t$	k_2 (g/mg×min)	2.706
		q_e (mg/g)	1.00132
		R^2	0.9999

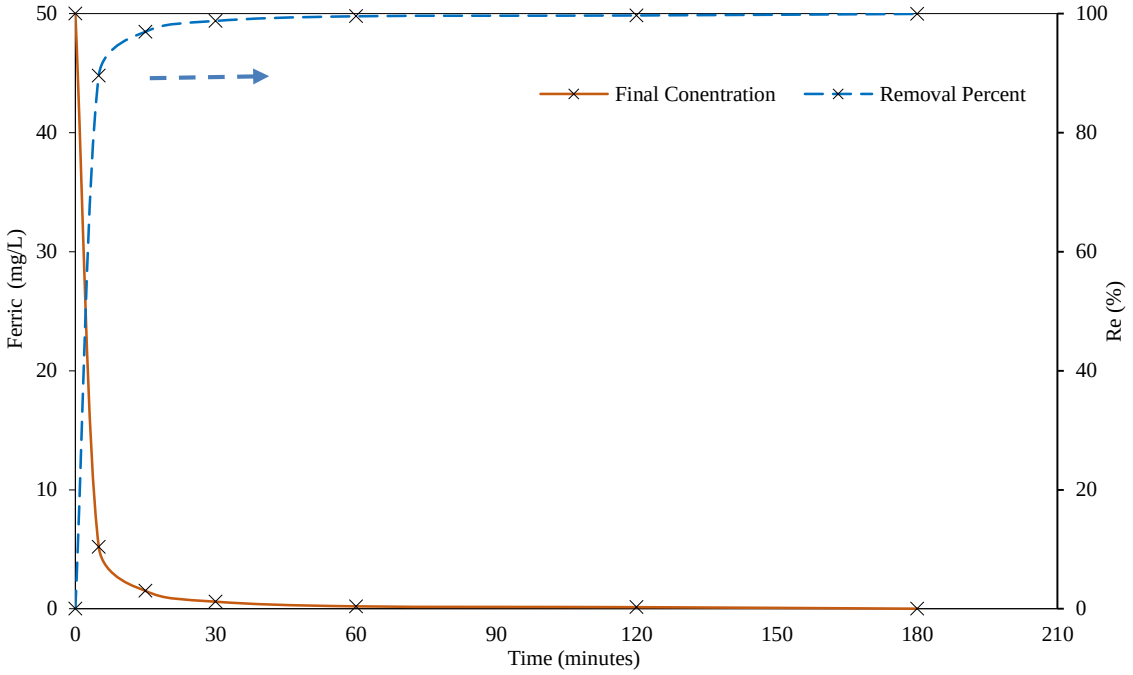

Figure 5.3 Adsorption kinetics of ferric onto zeolite

5.2.2 The Langmuir isotherm model

The Langmuir model considers that the numbers of adsorbent sites are fixed and also assumes that there is only one solute molecule per site. Langmuir model can be applicable for zeolite as adsorbent while zeolite surface has a bounded number of equal sorption sites [114]. The Eq. (**Error! Reference source not found.**) is often used:

$$q_e = \frac{q_{max} K_L C_e}{(1 + K_L C_e)} \qquad (5.2)$$

where q_e is the amount of metal adsorbed per specific amount of adsorbent (mg/g), K_L is Langmuir constant, C_e is the equilibrium concentration of the solution (mg/L), and q_{max} is the maximum amount of adsorbed metal ions (mg/L). q_{max} and K_L can be calculated from the Figure 5.4A.

5.2.3 The Freundlich isotherm model

The Freundlich model is frequently used to describe equilibrium adsorption data. The Freundlich model was used to estimate the distribution of iron between the zeolite solid phase and the solution phase and is can mathematically be expressed in Eq. (5.2).

$$q_e = K_f C_{eq}^{1/n} \qquad (5.2)$$

where K_f and n are the Freundlich coefficients. K_f indicates the adsorption capacity (mg/g), and n is related to the intensity of the Freundlich isotherm.

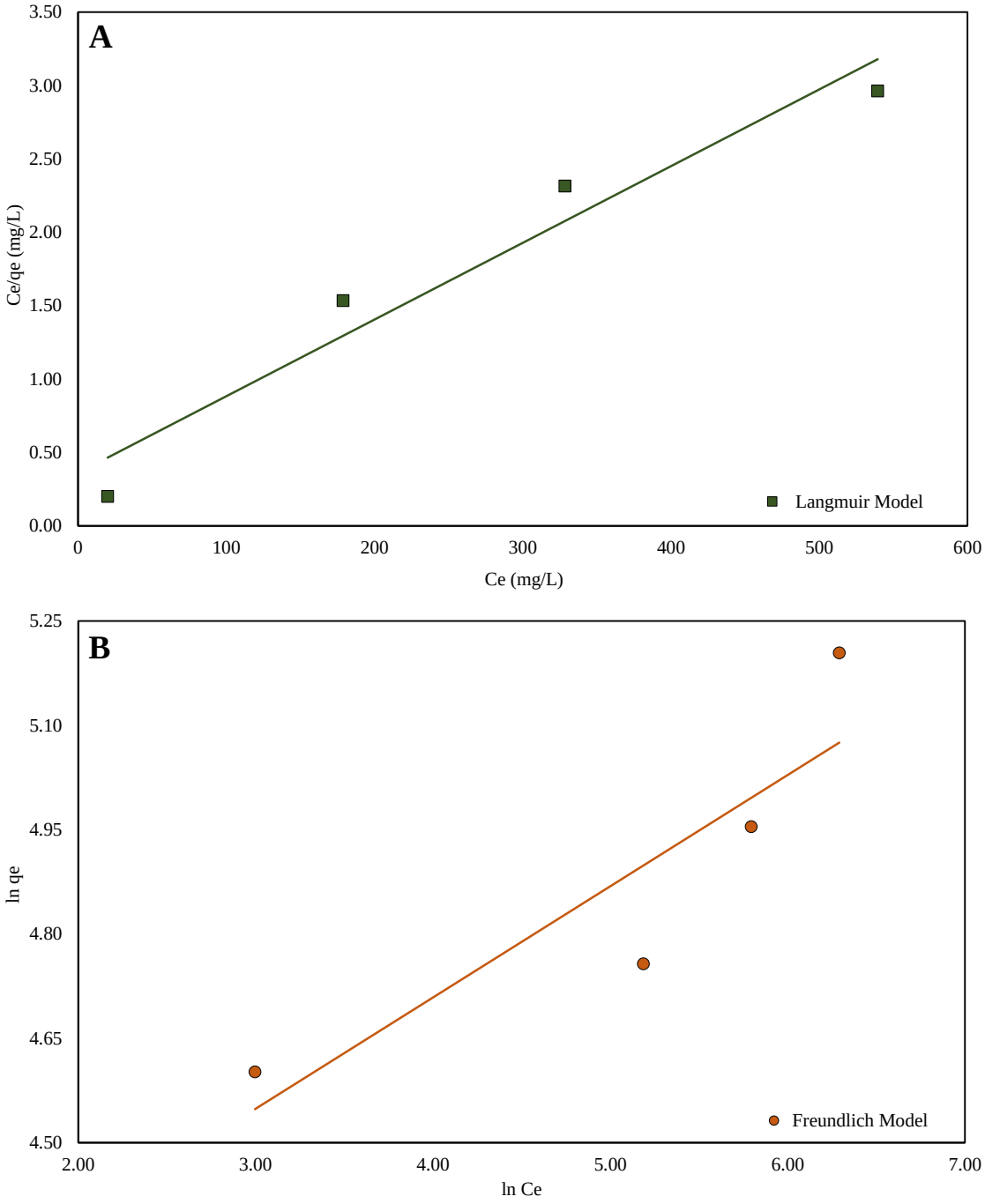

Figure 5.4 Isotherm for sorption of ferric onto zeolite surface by Langmuir isotherm model (A) and Freundlich isotherm model (B)

The Langmuir isotherm model constants were determined by locating the intercept and the slope of the linear plot of log C_e (Figure 5.4A) and log q_e for the Freundlich model (Figure 5.4B).

Figure 5.5 shows the experimental and modeled results of zeolite capacity for adsorbing the ferric ions. It can be noted that the zeolite capacity for adsorption of the iron ions was 182 mg/g when various iron concentrations were processed into 100 mg/L containing 1 gram of zeolite at pH range 2 to 3. It is also depicted that the amount of adsorbed iron

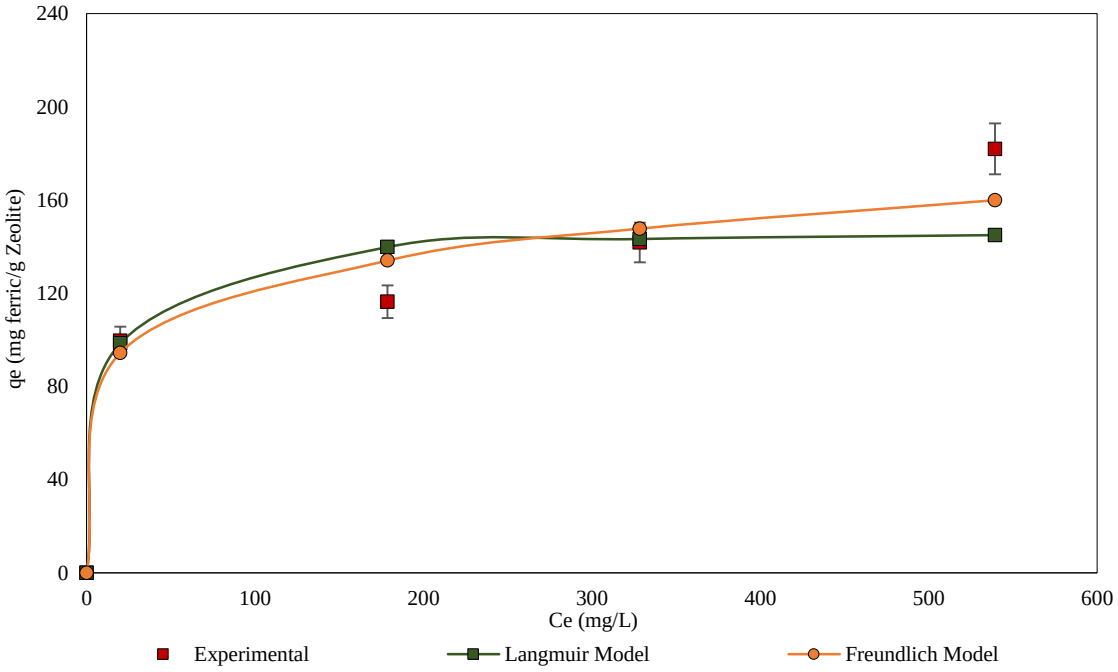

Figure 5.5 Kinetics models of zeolite

ions onto the zeolite increased simultaneously with the increasing of the equilibrium concentration of iron ions (Figure 5.5).

It can be shown from Table 6, the Langmuir model yielded a better fit than Freundlich model when compared to the model parameter to the experimental data and the R^2 was much closer to 1. This shows that zeolite can adsorb the iron ions only via one-layer adsorption. The obtained value of q_{max} was 147.69 mg/g.

Table 6 Isotherm parameters of Langmuir and Freundlich models for ferric sorption onto zeolite surface

Langmuir isotherm			Freundlich isotherm		
$q_e = \frac{q_{max} K_L C_e}{(1 + K_L C_e)}$			$q_e = K_f C_{eq}^{1/n}$		
R^2	q_m(mg/g)	K_L(L/mg)	R^2	n	K_f(L/g)
0.95	147.69	0.10	0.79	6.25	58.5

5.3 Overall anaerobic digestion performance

Figure 5.6A presents the daily biogas profiles under different additives. As demonstrated, both nZVI and zeolite addition played a functional role in daily biogas production and controlled the overall biogas cogeneration during the digestion process. The daily production profile showed a significant increase on the first day for the bioreactors exposed to zeolite, nZVI, and IMZ in addition to the control bioreactor, then

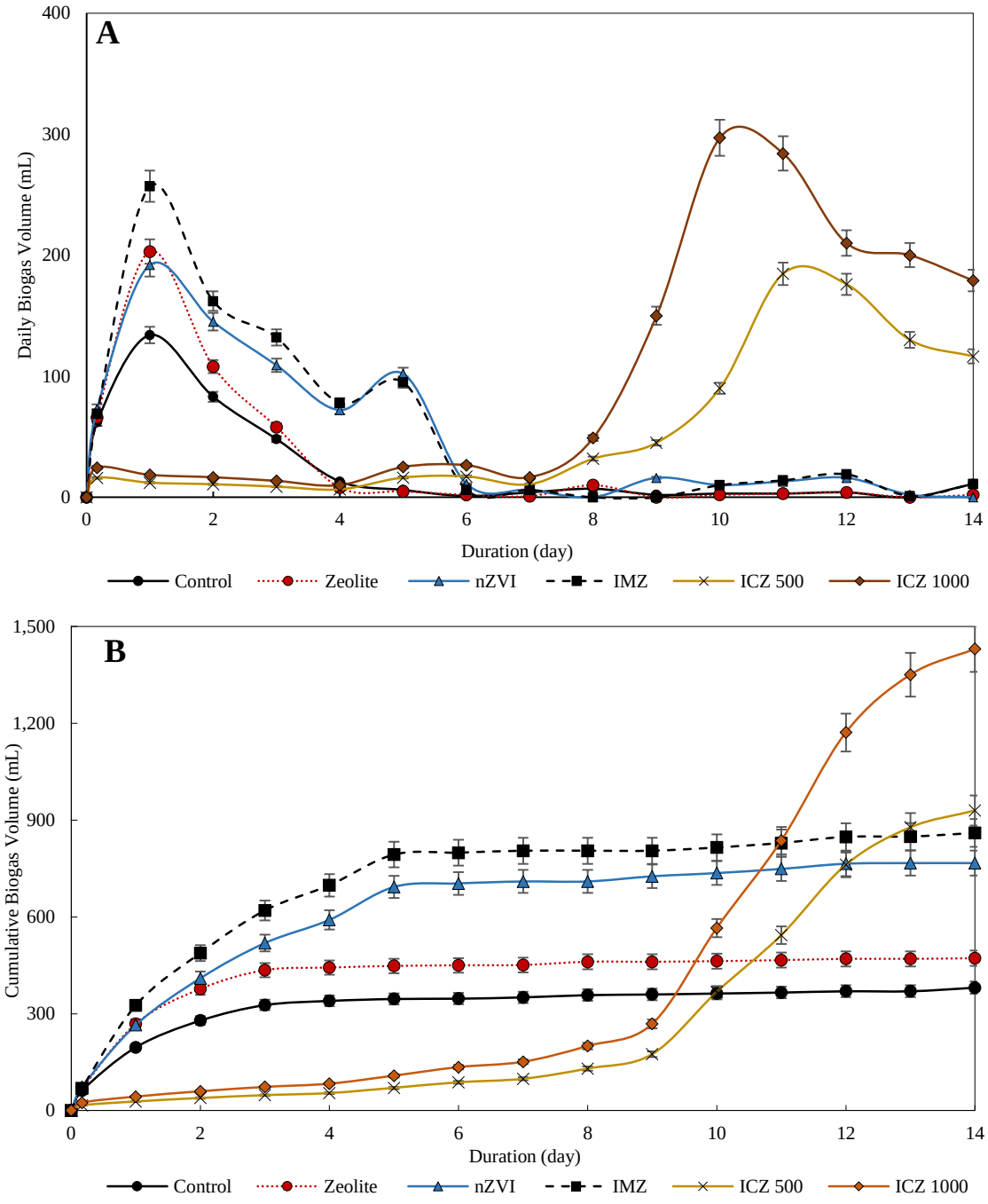

Figure 5.6 Effect of different additives on daily biogas cogeneration (A) and cumulative biogas generation (B)

the daily production was decreased till day 8. The increase at day 1 is assigned mainly to the elector's dissolution of additives into the aqueous medium.

For the sludge treated with ICZ, the generated biogas profiles are divided into two phases. During the first phase (until day 8), the biogas cogeneration showed a slight increase as a result of the weakening activity of the methanogens and the average daily production values were lower than 12 and 19 mL for bioreactors treated with ICZ 500 and ICZ 1000, respectively. This could be attributed to the adaptation process of activated sludge [115]

and it's likely because that the hydrolysis step of anaerobic digestion was almost ceased after exposing the sludge to ICZ materials.

At the second phase, very rapid biogas cogeneration was obtained from day 8 until the end of study duration and the amount of generated biogas was higher than that of the other bioreactors. Moreover, the higher the iron particles coated zeolite were added, the more the biogas generated. As clearly depicted from Figure 5.6B the cumulative biogas was increased by 24.86%, 105.46%, 130.87%, 149.95% and 286.75% for the bioreactors treated with of zeolite, 1 g/L nZVI, IMZ, ICZ 500 and ICZ 1000, respectively. It should be emphasized that the maximum production which was observed at ICZ 1000 bioreactor doubled the maximum production of the ICZ 500 bioreactor and this is may be due to the action of ICZ particles that overcome the uneven dispersion in the digestion media and increase the bioavailability and electron transfer interaction between the ICZ particles and functional microbes.

Furthermore, the average methane contents were 11 and 51% during the increase production period of ICZ 500 and ICZ 1000, respectively (Figure 5.7A)

The diversity of the cumulative biogas cogeneration trend in the different bioreactors could be assigned to the supplementation of the different additives and concentrations. Considering that adding nZVI, zeolite, IMZ or ICZ could support the cogeneration of the biogas, the nZVI coated zeolite was more effective compared to the mixture of zeolite and nZVI. These outcomes suggest that zeolite coated with nZVI has a positive impact in acidogenesis and methanogenesis by the greater bioavailability of iron nanoparticles [116], and by existence as a cofactor for various key enzymatic and co-enzymatic activities into the anaerobic sludge media [117].

The methane content in all bioreactors is summarized in Figure 5.7A and the methane contents were 26, 88, 74, 11 and 59% for the bioreactors exposed to zeolite, nZVI, IMZ, ICZ 500 and ICZ 1000, respectively whereas the methane content could hardly approach only 22% in the control bioreactor.

The two highest methane contents were depicted with the addition of the only nZVI and the IMZ and the methane content was stimulated up to 88 and 74%, respectively. This results might be ascribed to the nanoparticles high reacting capacity which can be attributed to the anaerobic corrosion of nZVI and electrons generation that could be utilized effectively the methanogens utilization and methane production [118, 119].

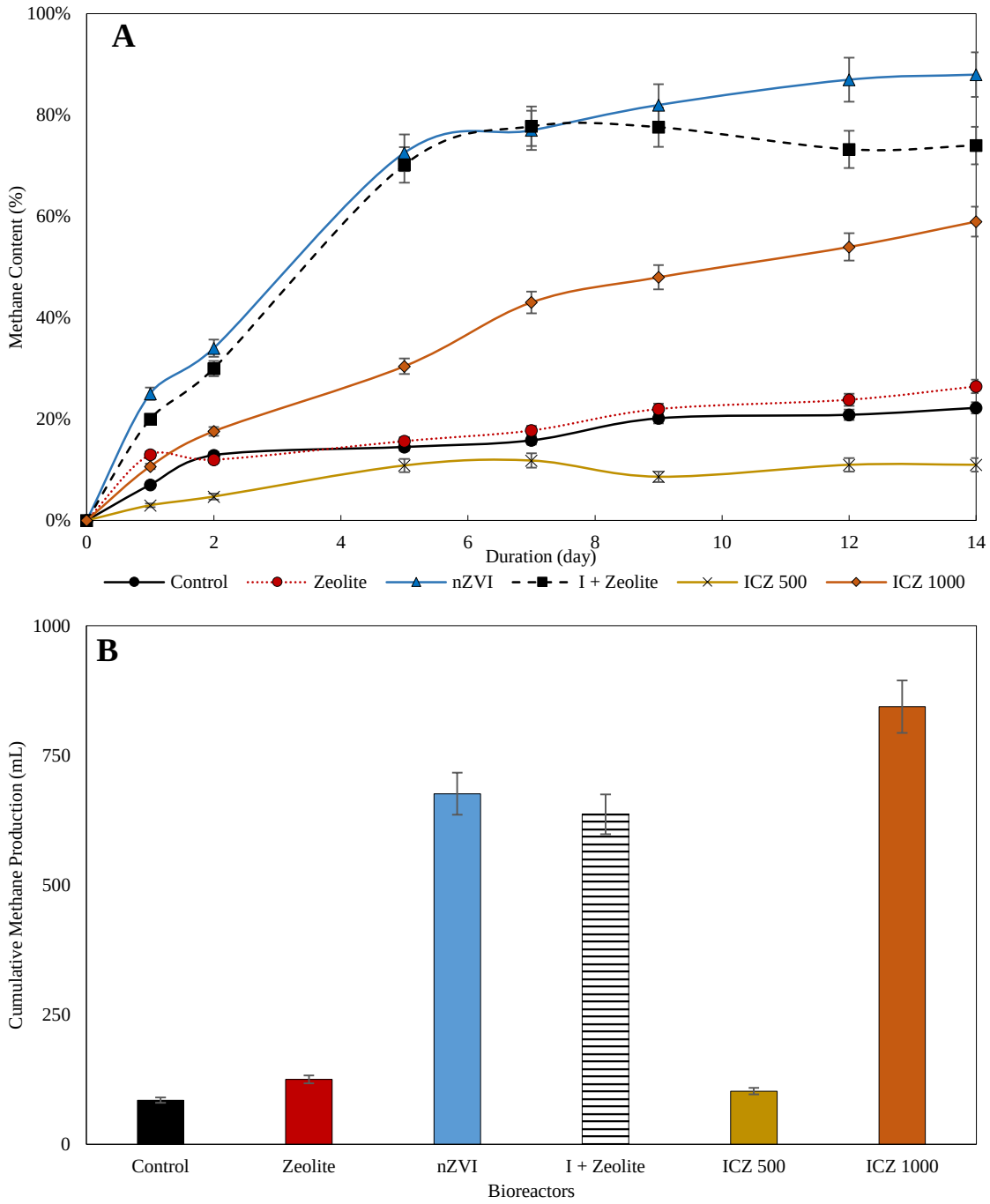

Figure 5.7 Effect of different additives on methane fraction (A) cumulative methane volume by the end of digestion period (B)

As with yielded methane content, the featured pattern was also monitored under the same condition. From Figure 5.7A, methane content at control bioreactor was analogously stable and quite low hence hardly reached 22% throughout the experiment duration. The same profile trend was detected with adding only zeolite material, however, nZVI particles supplemented with a high concentration (1000 mg/L) gave the maximum methane content in the first 5 days, and then there was little methane cogeneration over

the digestion time. This means that the methane cogeneration due to methanogenic activities was weak 5 days from the start of the anaerobic digestion.

Comparing the IMZ dosed bioreactor with the nZVI bioreactor, there was a little decrease in the methane content. In contrast, the methane content in the ICZ 500 bioreactor declined but further increase of the iron loading during the ICZ synthesis resulted in a notable of the methane content at the ICZ 1000 bioreactor. This is likely due to the adsorption capacity of zeolite and the quantities of free nZVI particles that cannot be adsorbed onto the zeolite materials and used in order to form nZVI particles throughout the ICZ synthesis, therefore pure nZVI nanoparticles that founded into the ICZ 1000 with much amount compared with ICZ 500 is responsible for the high methane content. Considering the methane production, the maximum cumulative methane was acquired with the addition of ICZ 1000 and its amount was more than 844 mL of methane by the end of day 14 of digestion period as clarified in Figure 5.7B. In contrast, the bioreactor of ICZ 500 only produced 102.3 mL of methane and the rest of biogas production as illustrated in the Figure 5.7A is mainly carbon dioxide and other gases.

5.4 Ammonium nitrogen and soluble COD

High concentration of ammonium nitrogen is recognized as an inhibitory factor in the sludge anaerobic digestion throughout inhabitation of a specific enzyme reaction [25, 116]. The variations of the total ammonium nitrogen in each bioreactor are displayed in Figure 5.8A. The total ammonium nitrogen concentration was 150 mg/L at the beginning of digestion period and along the digestion period, it increased steadily for the control, zeolite, nZVI and IMZ bioreactors and by the end of digestion period, the total ammonium concentrations were reduced by 13.34, 18.64 and 3.53%, respectively compared with no additives bioreactor. However, the total ammonium concentrations at the early 8 days of digestion period were raised dramatically in the bioreactors exposed to ICZ. Moreover, the final total ammonium concentration in the ICZ 1000 bioreactor was about 11.3% lower than that in the ICZ 500.

Furthermore, by the end of day 14, there was no significant difference in ammonium concentration among the different bioreactors which ranged between 488 and 670 mg/L, were far away below the concentration of inhabitation level [105], all bioreactors exposed to study additives showed low ammonium concentration compared with the control. These outcomes might be due to the characterization of both zeolite and iron nanoparticles as ion exchangers for ammonium removal as a result of cations presence [120]. For the

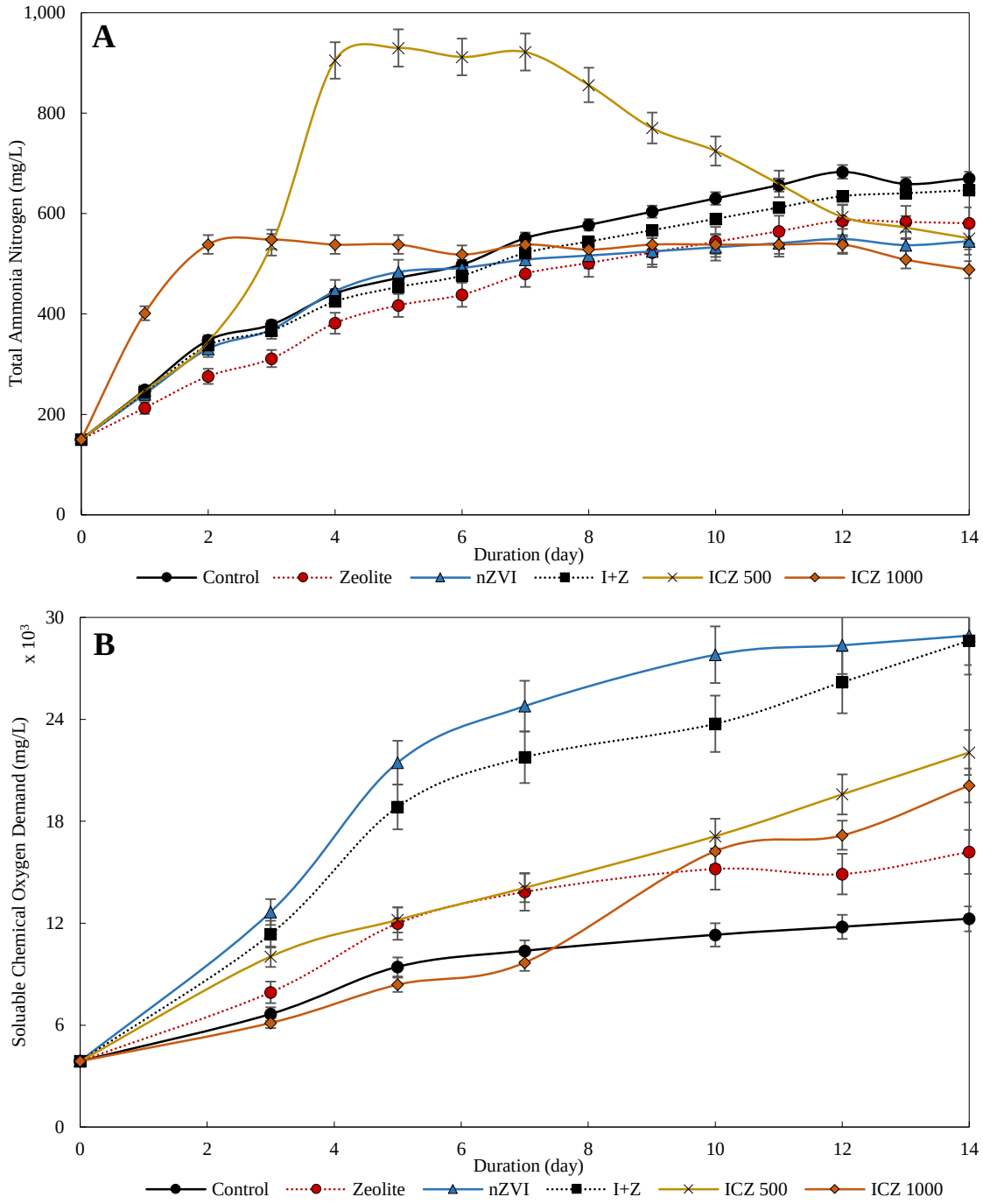

Figure 5.8 Variation of total ammonia nitrogen (A) and soluble COD (B) of the bioreactors with supplementation of different additives

ammonium nitrogen profile in the ICZ 500 and ICZ 1000 bioreactors, it can be said that the ammonium accumulation at the beginning of digestion period is the main reason for the lag period of biogas production and the decreasing of the cumulative cogeneration of biogas as shown in Figure 5.6 (A, B).

The variations in the soluble COD concentrations of different bioreactors are shown in Figure 5.8B. The soluble COD of the sludge increased quickly and the gradual increasing trends were maintained along the digestion period for all bioreactors. The rapid increase

of soluble COD, which was observed at the early digestion stage, is due to the rapid organic material degradation through the hydrolysis process where the organic materials solubilized hydrolytic enzymes [121].

The average soluble COD concentration was 3,873 mg/L at the beginning of anaerobic digestion and at the completion of digestion duration, the soluble COD concentrations raised to 12,256, 16,195, 28,936, 28,640, 22,050 and 20,110 mg/L for control, zeolite, nZVI, IMZ, ICZ 500 and ICZ 1000, respectively. Generally, the soluble COD in bioreactors exposed to this study additives had increasing trends, due to the continued endogenous biomass decay and the release of cellular components as a result of the disruption of cell membranes [67], particularly in bioreactors exposed to only nZVI or IMZ.

5.5 pH limits and total alkalinity profile

pH and total alkalinity are crucial indicators, therefore monitoring their values is substantial in controlling the sludge treatment and ensuring the process stability of anaerobic digestion as well as the metabolic status [116].

According to Figure 5.10A, all bioreactors have final pH values within the neutral pH range, thus indicating that nZVI, zeolite or its compositions resist the pH changes during the anaerobic digestion. Normally, zeolite systems tend to neutralize the aqueous solutions, acting either as proton donors or as proton acceptors thus exhibiting an amphoteric character [122].

The final pH variations for all bioreactors with the supplementation of different additives are between 5.81 and 7.32. These pH values are close to initial pH 6.2 which reflect that two successive pathways occurred during the digestion period. The first pathway includes a decrease in the sludge pH due to the conversion of easily degradable organic matters to fatty acids during the hydrolysis and acidogenesis at the beginning of digestion period and formation of ammonia took place. Subsequently, the increasing pH value to get back to the initial values presented in the Figure 5.10A are due to the hydrogen ions uptake by cation site of nZVI particles via ion exchange or adsorption via zeolite pores structure. The bioreactor with no additives had a relatively slower final pH, which was possibly due to relatively slow organic acids degradation [105].

The dynamic changes in total alkalinity during the anaerobic digestion reflected a positive impact of the study additives on consuming the volatile fatty acids. On the whole, a dramatical increase of total alkalinity has been detected from the beginning duration of

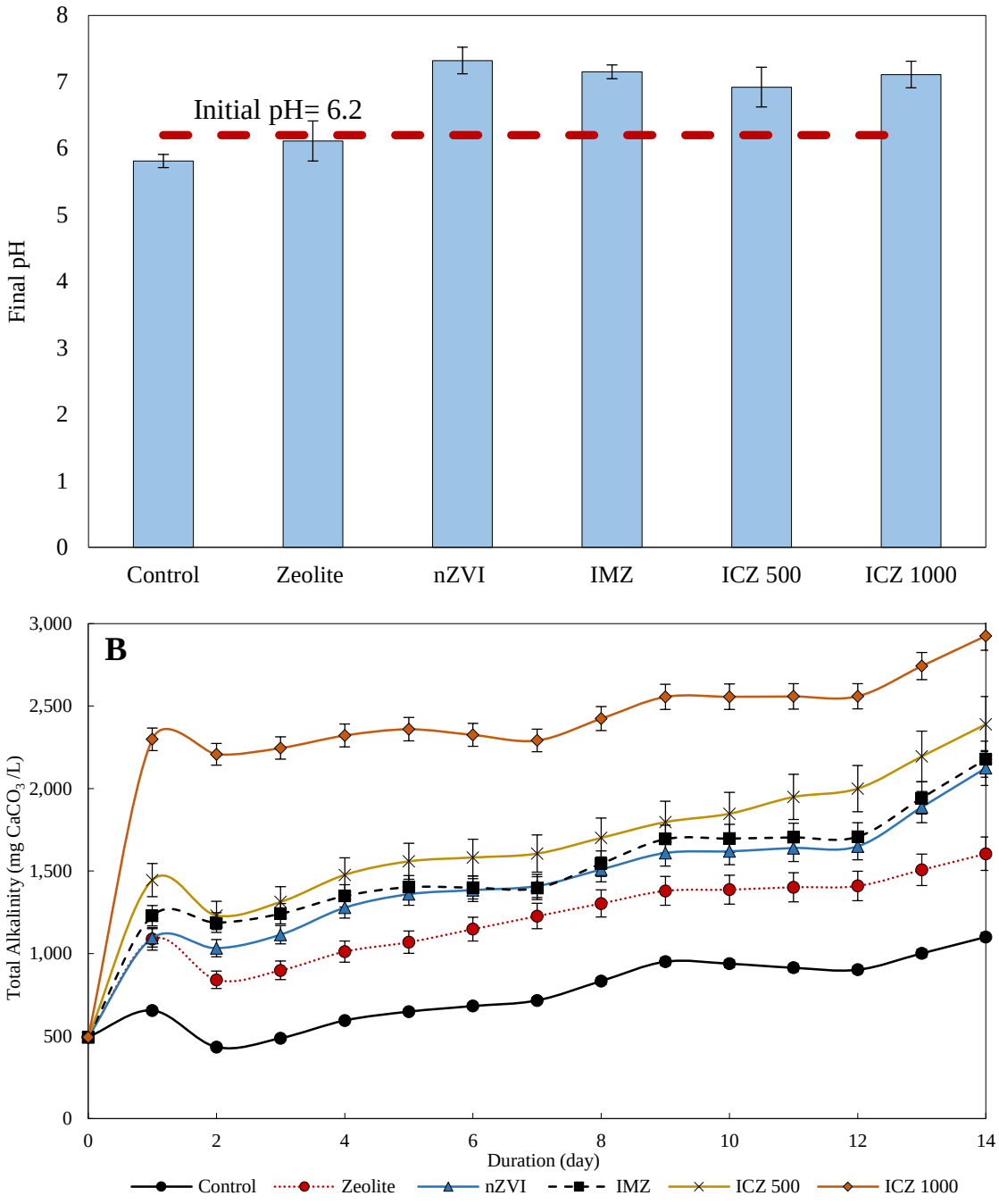

Figure 5.9 Initial pH and variations of final pH (a) and total alkalinity (b) during the overall digestion duration

anaerobic digestion, supposedly as a result of biomass fermentation as shown in the Figure 5.10B. The initial concentration of total alkalinity was 494 mg $CaCO_3$/L and the profile trend for each bioreactor was maintained until the end of the experiment. For example, the average total alkalinity concentrations in the groups of control, zeolite, nZVI, IMZ, ICZ 500 and ICZ 1000 were 776, 1234, 1480, 1549, 1721 and 2456 mg $CaCO_3$/L, respectively. The distinguished increment of total alkalinity was particularly observed in the bioreactor exposed to ICZ 1000. The increase in the total alkalinity of sludge reflected

the consumption of volatile fatty acids by methanogens microbes or other microbes [123] and the promotion of the biogas production was due to the consumption of volatile fatty acids and the alkalinity production increase effect.

5.6 Fate of iron ions release

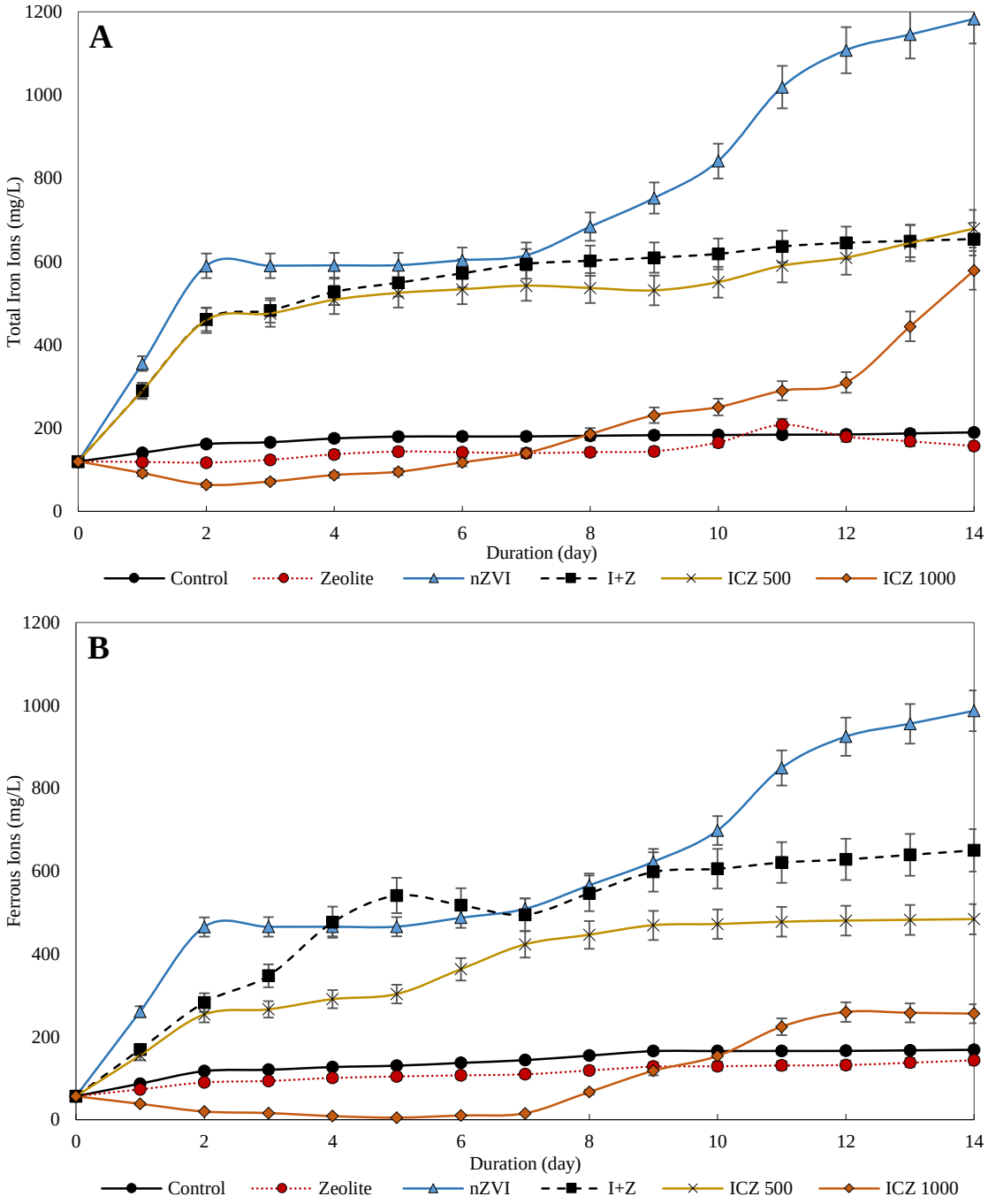

Figure 5.10 Variations of total dissolved iron concentrations (A) and ferrous iron concentrations (B) of the bioreactors

As shown in the Figure 5.10, in general, all the dissolved iron ions species were in the form of ferrous ions. The bioreactors of control, zeolite and ICZ 1000 had relatively

low quantities of dissolved iron concentrations during the digestion period, which were at 173.4, 147.3 and 205.2 mg/L, respectively.

The high total iron concentrations in the nZVI and IMZ bioreactors pointed out to the high iron-containing cellular components were released throughout the endogenous digestion [67]. These results come in accordance with the increasing trends of the soluble COD in the bioreactors (Figure 5.8B).

In the group of zeolite and along the digestion period, the dissolved iron concentration was less than the control implying that this decrease is due to the adsorption properties of zeolite. Moreover, the ICZ 1000 bioreactor offered a reduction in dissolved iron concentration until the day 8 then the iron concentrations increased gradually exceeding the control bioreactors by the end of digestion period.

The highest released concentration of total iron resulted from the nZVI bioreactor and it was much more than that generated by both IMZ or ICZ 500 bioreactor and the volume of cumulative biogas production as described in the Figure 5.7A is attributed to the dissolution trend of the nZVI.

To summarize, adding zeolite to anaerobic sludge plays a workable role in the dissolved iron ions levels and the quick increasing trends of iron dissolution were attributed to sludge fermentation that leads to decrease the pH values.

5.7 Conclusions

In this work, six bioreactors with different additives of nZVI particles and zeolite were tested to evaluate the overall anaerobic digestion performance under mesophilic temperature and the main results are:

The kinetics of iron ions uptake by zeolite are well-fitted to the pseudo-second-order model and the Langmuir model yielded a better fit than the Freundlich model regarding the adsorption equilibrium isotherm.

Zeolite material, due to its cation exchange properties, presented a high performance in adsorption of dissolved iron ions from the activated sludge. Consequently, zeolite shows varying iron selectivity and competitive adsorption for bi-component bioreactors.

The addition of ICZ causes a lag period before starting to produce a significant biogas cogeneration that reached a maximum value compared with the other bioreactors, and the higher the iron particles coated zeolite were added the more the biogas was generated.

The preferable results of cumulative methane production were obtained when supplementing ICZ 1000 particles, which gave the maximum methane production volume.

CHAPTER 6

EVALUATION OF SULFATE-CONTAINING SLUDGE STABILIZATION AND THE ALLEVIATION OF METHANOGENESIS INHIBITATION AT MESOPHILIC TEMPERATURE

Chapter 6. Evaluation of sulfate-containing sludge stabilization and the alleviation of methanogenesis inhibitation at mesophilic temperature

In this chapter, and based on the questions as to whether and how the nZVI will affect the biochemical process and over the inhibitation of methanogenesis in anaerobic digestion of sulfate-containing sludge. By focusing on observation of the anaerobic digestion performance of domestic activated sludge with various sulfate concentration and various nZVI dosing under a fixed condition. The chapter main objective is to assess the performance of anaerobic digestion process for the treatment of sulfate-containing sludge in presence of nZVI. Accurately, here, the impact of various concentrations of nZVI on methanogenesis activities in anaerobic digestion will be determined.

6.1 Removal characteristics of dissolved sulfates in aqueous solution by nZVI

6.1.1 Removal kinetics

The adsorption kinetic line-graph of sulfate by nZVI is presented in Figure 6.1. Within the first 20 minutes, the amount of sulfate adsorption increased sharply and almost the maximum adsorption capacity was reached after 30 minutes with adsorption capacity of 15.45 mg/g. The adsorption capacity was increased sharply due to the available adsorption sites on nZVI particles at the beginning of interaction time indicating that the adsorption sites on the nZVI particles gradually interacted with the sulfates. Thus, the adsorption capacity decreased with increasing reaction time. Therefore, 30 minutes duration was selected for the following adsorption isotherm experiments. The pseudo-

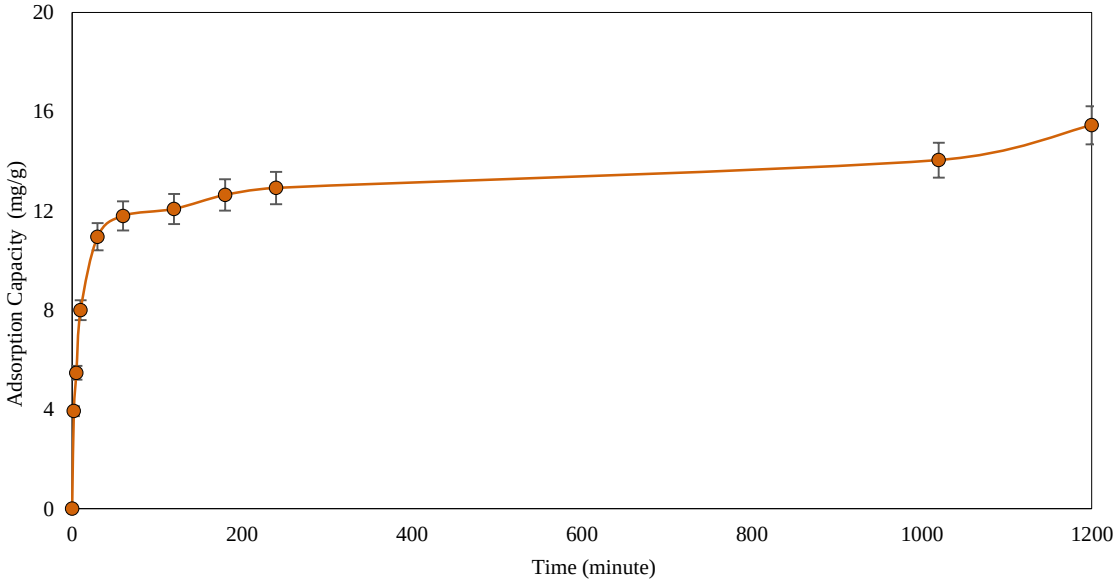

Figure 6.1 Kinetics plot for the kinetics of sulfate on nZVI

first order, pseudo-second order, Elovich, and intraparticular diffusion models were employed to study the adsorption process and the correlation coefficients (R^2) were listed in Table 7. R^2 coefficient of the pseudo-second order model (R^2 = 0.9960) was higher than the other models, indicated that the removal of sulfate followed the pseudo-second order kinetic model. This result suggests that the uptake process of sulfate can be broken down into two or more steps. The first step is the adsorption onto the nZVI surface whereas the second step is the gradual adsorption step and the final step is the equilibrium step.

Table 7 Kinetics models of sulfate on nZVI

Kinetic model	Equation	R^2 Value
Pseudo-first order	$\log(q_e - q_t) = \log q_e - \frac{k_1}{2.303} t$	0.7083
Pseudo-second order	$\frac{t}{q_t} = \frac{1}{k_2 q_e^2} + \frac{1}{q_e} t$	0.9960
Elovich	$\frac{q_e}{q_e - q_t} = 1 + k_2 t$	0.9256
Intraparticular diffusion	$\log q_t = \log K + 0.5 \log t$	0.6022

6.1.2 Adsorption Isotherm

The adsorption of sulfate by nZVI results provide obviously better fitting to the three-parameter isotherm model of Redlich-Peterson, among the various isotherm models which show the maximum agreement with the experimental data, which is indicated by the highest value of R^2 which exceeded 0.994 as listed in Table 8. Redlich–Peterson isotherm consists of both Langmuir and Freundlich isotherms, therefore the sulfate isotherm on nZVI can be applied either in heterogeneous and homogeneous systems due to its adaptability [124].

Table 8 Adsorption isotherm models

Isotherm Model	Equation	R^2	Parameters
Langmuir	$q_e = \frac{q_{max} K_L C_e}{(1 + K_L C_e)}$	0.9700	$q_{max} = 22.258;\ K_L = 0.068$
Freundlich	$q_e = K_f C_e^{\frac{1}{n}}$	0.7933	$K_f = 8.558;\ \mathrm{n} = 7.152$
Redlich-Peterson	$q_e = \frac{K_R C_e}{(1 + a_R C_e^g)}$	0.9942	$K_R = 11;\ a_R = 1.007;\ \mathrm{g} = 0.876$
Hill	$q_e = \frac{\mathrm{qH} C_e^{n_H}}{(K_D + C_e^{n_H})}$	0.7933	$q_H = 39.19;\ n_H = 0.322;\ K_D = 2.397$
Koble-Corrigan	$q_e = \frac{A C_e^D}{(1 + B C_e^D)}$	0.9707	$\mathrm{A} = 0.977;\ D = 1.140;\ \mathrm{B} = 0.046$
Sips	$q_e = \frac{Q_S K_S C_e^{n_S}}{(1 + K_S C_e^{n_S})}$	0.7942	$Q_S = -36.11;\ K_S = -0.210;\ n_S = 0.1$
Temkin	$q_e = q_m \ln(K_T C_e)$	0.8215	$q_m = 22.21;\ K_T = 18.786$

6.1.3 Affecting factors at equilibrium

In order to study the factors affecting the adsorption of sulfates onto nZVI particles, adsorption experiments were repeated with changing various parameters. The adsorption experiments were conducted under various temperatures of 5 °C, 25°C, 50°C and 90°C; initial pH 3, 5, 7, 10 and 12; initial sulfates concentration of 50 mg/L, 100 mg/L, 250 mg/L, 500 mg/L and 1000 mg/L; and agitating speed of 50 rpm, 100 rpm, 150 rpm and 200 rpm.

The above mentioned different key factors were applied in order to study their effects on the amounts of adsorbed sulfate at equilibrium time. The effects of changing the initial pH on the amount of sulfate were investigated by changing the pH in the range from 3 to 12 (Figure 6.2A). Over the aqueous solutions, the pH value was considered as an important factor that controlling the adsorption process of sulfate by nZVI due to ions competitive adsorption [125]. The highest adsorption capacity was observed at strong acidic conditions, in contrast, both strong and weak alkaline conditions are unfavorable for nZVI to adsorb sulfate ions. At pH equal to 10 and 12, the adsorption capacities were decreased to 3.1 and 2.8 mg/g, respectively. This phenomenon is due to the existence of hydroxyl ions that compete with sulfide ions. However, at the same time, the sulfate

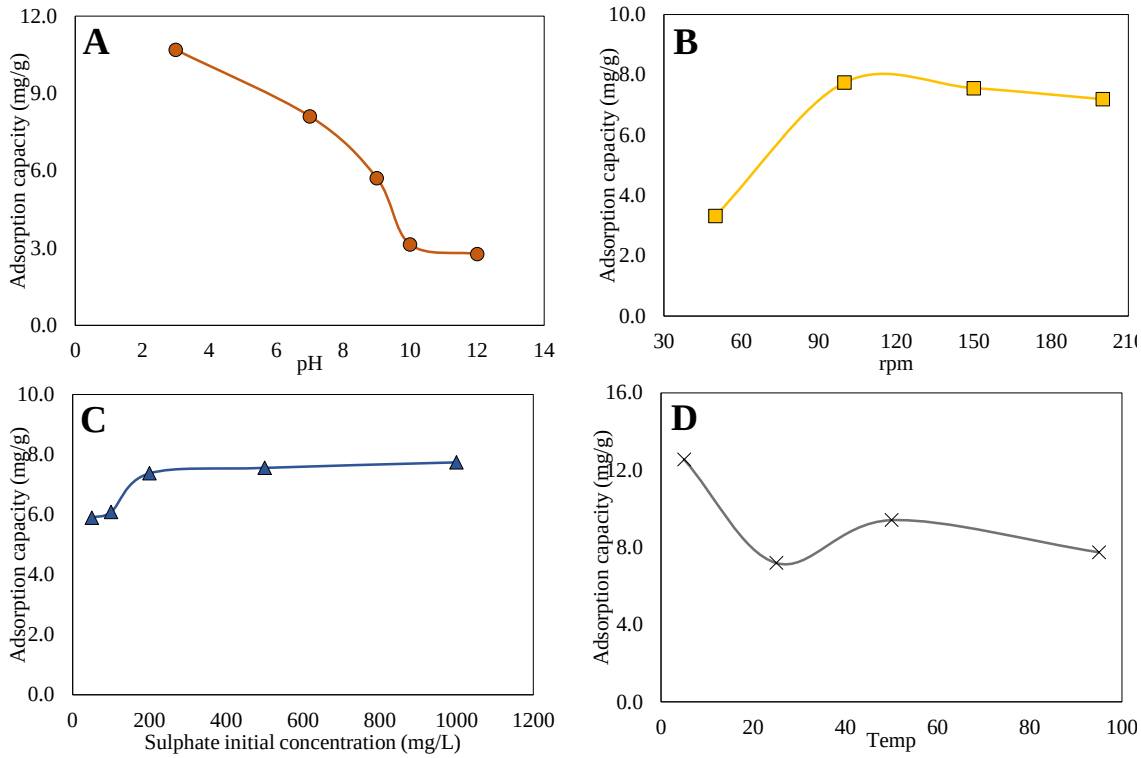

Figure 6.2 Effect of adsorption conditions on the amounts of adsorbed sulfates

adsorption amounts increased clearly to 10.7 mg/g at pH 3. Moreover, the results of changing the agitation speed on the adsorption capacity of nZVI particles were depicted in Figure 6.2B. The agitation speed was raised from 50 to 200 rpm and the adsorption capacities were increased notably when the speed increased to 100 rpm, giving 7.7 mg/g sulfate ions adsorbed by nZVI compared with 3.3 mg/g that can be adsorbed under the low agitating speed of 50 rpm. This is because that increases the agitation speed boost the species transfer between the sulfate ions and nZVI as adsorbent [126].

Figure 6.2C exhibits the adsorption capacity under modifying the initial sulfate concentrations. The adsorption amounts of sulfate by nZVI were increased by increasing the initial sulfate concentration to a certain extent. The equilibrium nZVI adsorption capacity of sulfate was 5.9, 6.1, 7.4, 7.6 and 7.7 mg/g at initial sulfate concentrations of 50, 100, 200, 500 and 1000 mg/L, respectively. These outcomes are due to the increase of active molecules with higher sulfides concentrations [127].

Eventually, the influence of varying the reaction temperature on the amounts of adsorbed sulfate at equilibrium time is shown in Figure 6.2D. The temperature range was from 5 to 90 °C and the adsorbed sulfate amounts were 12.5, 7.2, 9.4 and 7.7 mg/g at 5, 25, 50 and 90 °C, respectively. It can be said that the adsorption capacity decreased with increasing the temperature. Therefore, the negative correlation between the adsorption capacity and

temperature guides that the sulfate ions adsorption onto nZVI is a physical adsorption process rather than chemical adsorption process.

6.2 Overall anaerobic digestion performance

The roles of nZVI particles in controlling the methanogenic inhabitation of the sulfate-containing sludge were investigated based on conducting the anaerobic digestion experiments. The activated sludge samples that enriched with sulfate concentration were treated with various concentrations of nZVI based on Table 9.

Table 9 Various bioreactors setup

Reactor Label	nZVI (mg/L)	Sulfate (mg/L)	pH
R1	0.00	0.00	-
R2	0.00	500	-
R3	1000	1000	-
R4	500	500	-
R5	100	500	-
R6	1000	500	3
R7	1000	500	12

Figure 6.3A shows the cumulative biogas production over 20 days of anaerobic digestion experiments operation. Compared with control bioreactor (R1), the generated biogas of R2 was inhibited significantly when the influent sulfate was 500 mg/L and the nZVI particles were not added. Specifically, the cumulative biogas production decreased from 293 to 249 mL. Comparatively, the sulfate-containing sludge bioreactors were exposed to nZVI particles were less affected by the increase in sulfate concentrations, with biogas production fluctuating at 389, 368, 266, 448 and 492 mL for R3, R4, R5, R6, and R7, respectively.

Overall, the presence of sulfate anions dramatically decreased the biogas production and the decrease in the generated biogas volume of sulfate-containing sludge was due to the competition status between the methanogenic bacteria and SRB for the same substrate degradation [69]. Moreover, the sulfate existence in the sludge would increase the production of H_2S which is considered as a toxic gas to anaerobic microorganisms and later it caused a decrease in biogas production as in bioreactor R2. The fewer effects of sulfate present in the other bioreactors are attributed to the function of nZVI when preventing the negative effects on sulfate anions by buffering the pH value and subsequently, decreased the un-dissociated H_2S concentrations [69, 128].

Concretely, during the operation period, no significant differences were detected between the bioreactors R3 and R4. Nevertheless, over the 20-day period, a substantial increase from 293 mL to 492 mL (68%) was detected when the nZVI concentration was increased to a concentration of 1000 mg/L and the pH was fixed at 12 (in bioreactor R7). On the other hand, comparing with R7 the biogas production decreased by 9.8% when the initial pH was controlled to be not more than 3 (in bioreactor R6).

Generally, for all the operated bioreactors, from the day 4, there was negligible biogas production in the treated bioreactors, indicating the completion of methanogenesis while it was strongly inhibited with the sulfate ions.

Various biogas samples were withdrawn from each bioreactor and then analyzed in order to determine the methane and carbon dioxide contents. It was found that the major components of biogas in the anaerobic sludge were nitrogen, carbon dioxide, methane and a small amount of hydrogen [108]. The content of methane and carbon dioxide produced are shown respectively in Figure 6.3B, C. The amended bioreactors R2, R3. R4, R5, R6, and R7 released respectively more carbon dioxide with 82, 76, 64, 66, 68 and 68% than the bioreactor without the addition of neither sulfate nor nZVI particles. By the end of biogas production period, the carbon dioxide concentration in the treated bioreactors was almost the same (Figure 6.3B), which were in the range of 75–90%.

In contrast, there was a little methane generated during the digestion period which points out the low methanogenic activities particularly at the low nZVI dosage as in R4 and R5 or R2 (without nZVI dosage). However, when further increasing the nZVI dosage, the methane yield was relatively high which indicate that the nZVI particles decrease the inhabitation of methanogenic activities of sulfate-containing sludge and sulfate plays a clear role in the inhabitation of methanogenic bacteria.

As a result of sulfate addition, two forms (primary and secondary) of inhibition existed. Primary inhibition form exists due to the competition of different microorganisms for the same substrate besides, secondary inhibition form was observed from the toxicity of sulfide ions to various bacteria groups [25].

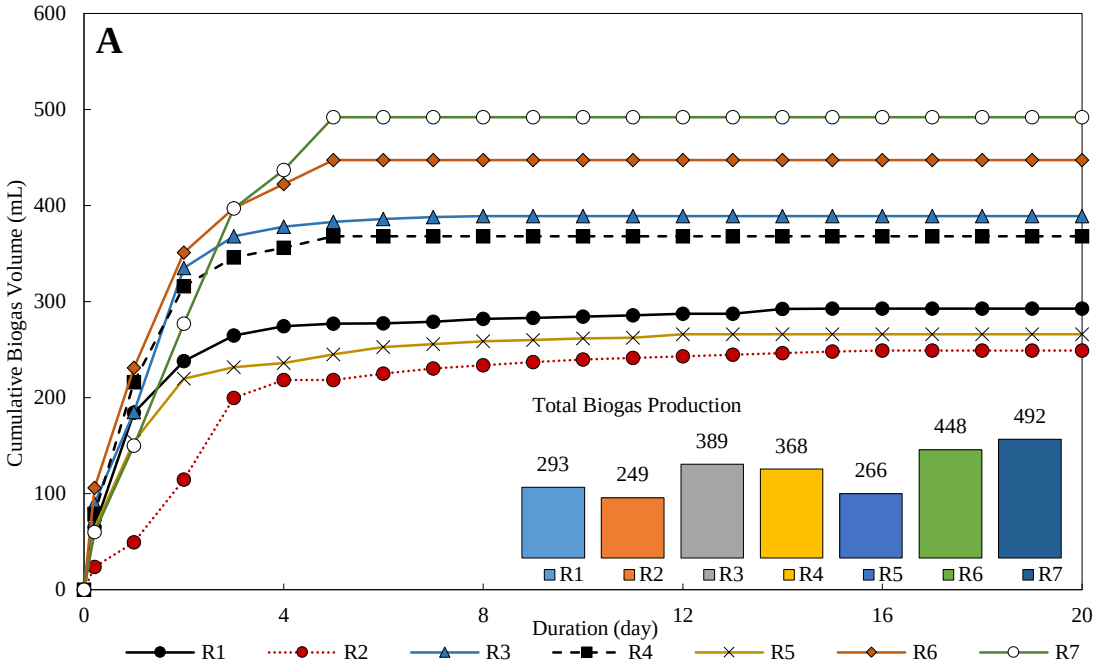
A
Cumulative Biogas Volume (mL)
Duration (day)
Total Biogas Production
293
249
389
368
266
448
492
R1
R2
R3
R4
R5
R6
R7

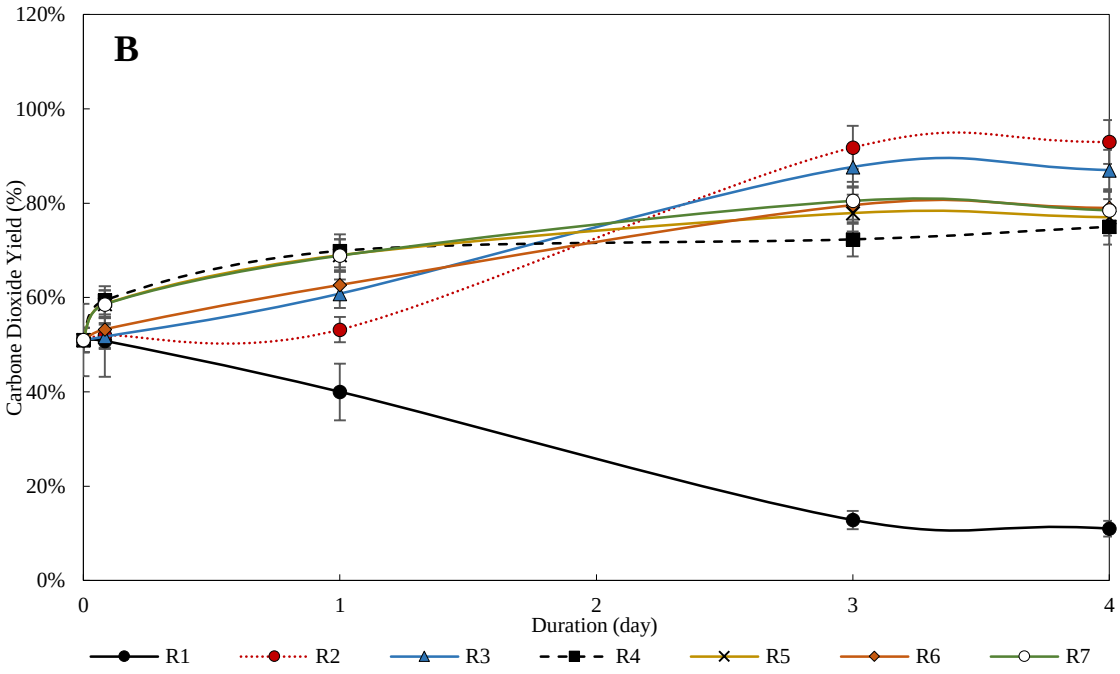
B
Carbone Dioxide Yield (%)
Duration (day)
R1
R2
R3
R4
R5
R6
R7

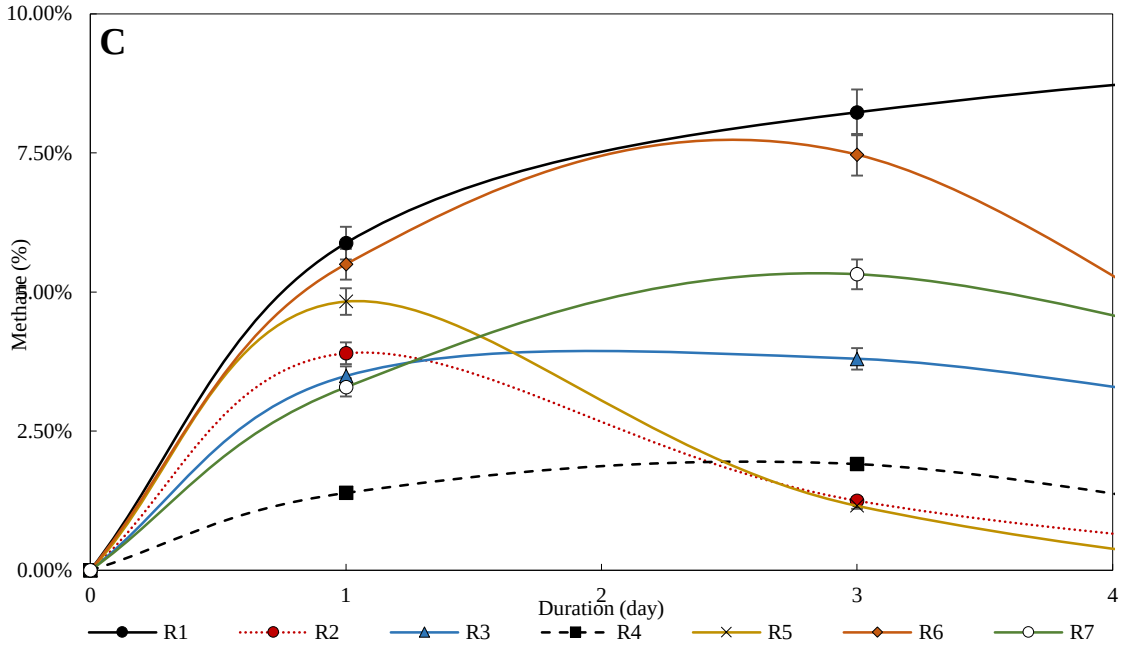

Figure 6.3 Cumulative Biogas volume (A), Carbon dioxide (B) Mathane yeild (C)

6.3 Dynamic changes in pH and Alkalinity

pH is considered as one of the substantial indicators for marking the anaerobic digestion status stability [129]. The pH measurements exhibit that the final pH values were not appropriate for generating methane as listed in Table 10, the methane is produced in the pH range 7.0 – 8.5 [130]. Thus, the final pH dropped to values between 5.2 and 5.5 since the volatile fatty acids were accumulated and the activities of acidogenic and methanogenic bacteria were inhibited and subsequently, the whole anaerobic digestion performance may be disrupted. Therefore, when the medium is not favorable to methanogenesis, the volatile fatty acids consequently will be accumulated and the alkalinity will be raised as it will be clearly discussed in Figure 6.4. The no additive bioreactor R1 has the lowest final pH due to the relatively slow organic acids degradation [105].

Table 10 Initial and Final of pH

Bioreactor	Initial pH	Final pH
R1		5.17
R2		5.26
R3		5.45
R4	7.2	5.20
R5		5.25
R6		5.45
R7		5.42

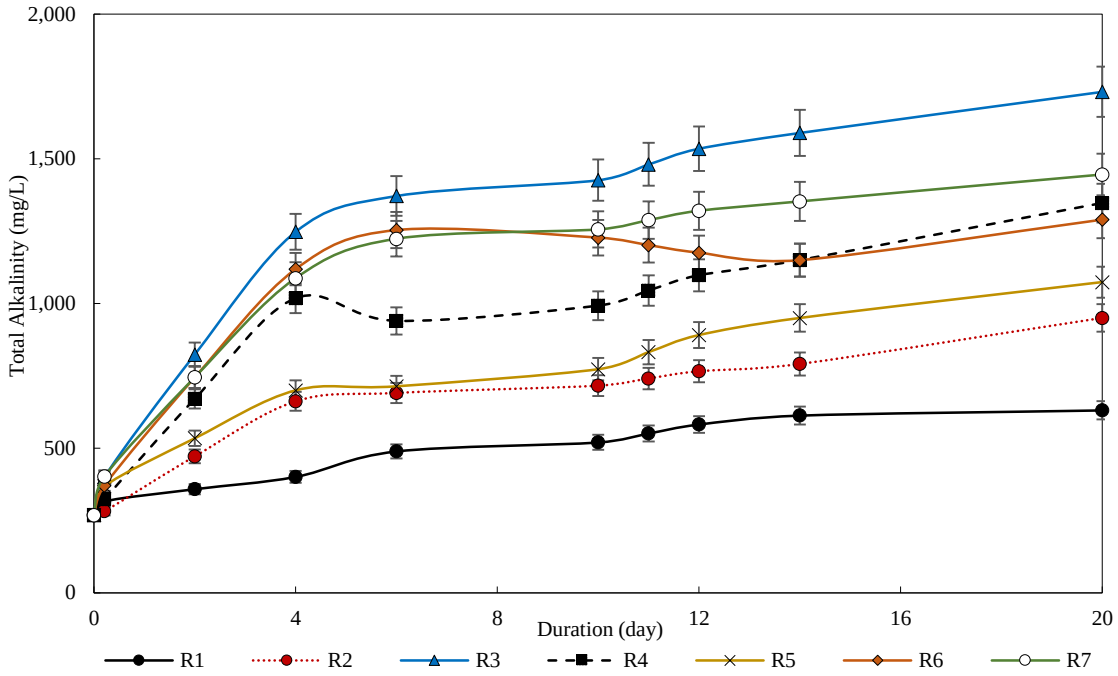

Figure 6.4 Total alkalinity

Ordinarily, alkalinity rate increased together with the volatile fatty acids accumulation due to incomplete of methanogenic activities, therefore all the bioreactors showed total alkalinity values more than the blank bioreactor R1 (Figure 6.4). From the beginning of anaerobic digestion until day 4, the apparent raise in total alkalinity in R3, R6 and R7, which achieved 2.11, 1.79 and 1.71 times more than what R1 achieved, points out to the accumulation of volatile fatty acids [131]. It can be clearly seen that the alkalinity shows a similar trend for all the bioreactors regardless the sulfate or nZVI concentrations, reaching the highest level of 950, 1732, 1347, 1074, 1290 and 1447 mg $CaCO_3$/L on the last day of digestion process duration for the bioreactors R2, R3, R4, R5, R6, and R7, respectively.

6.4 Fate of iron ions release

To a large extent, the formation of various Fe^{2+} or Fe^{3+} species at most controls the reactivity of nZVI [132]. As seen in Figure 6.5, the iron release was mainly in Fe^{2+} form, and raising the nZVI load resulted in an increase of iron ions concentration in the sludge samples. During microbial sulfate reduction, iron sulfides (FeS) are also expected to form. Obviously, the Fe^{2+} concentration decreased as the concentration of the sulfate increased. This occurred distinctly at bioreactor R5 with only 100 mg/L nZVI, where Fe^{2+} was precipitated into FeS which indicate that the addition of nZVI to precipitate sulfide could relieve the inhibition of sulfide [69, 133]. Therefore, the existence of Fe^{2+}

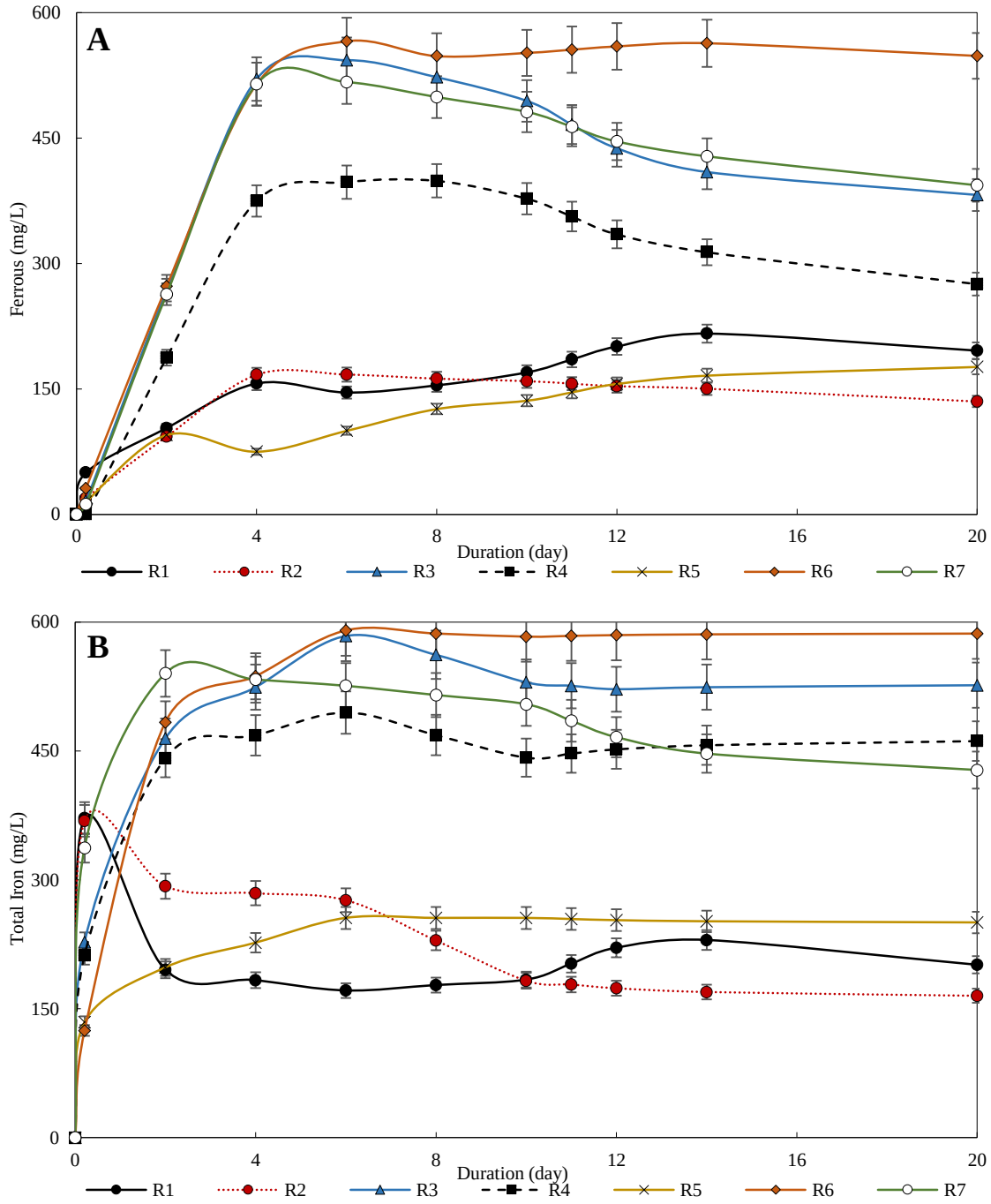

Figure 6.5 Iron ions release

and the formation of FeS in some extent were benefited for anaerobic bacteria [34] and the formation of an optimized environment for the microbial activities in the reactor might be responsible for the enhanced performance of methanogensis that was reflected by increasing the methane yeild (Figure 6.3C). According to Yang Y. et al. [67], the higher dissolved iron concentrations as in the bioreactors R3, R6, and R7, pointed out the iron-containing cellular component emissions during the fermentation process of anaerobic sludge in which the COD trends are increased undoubtedly (Figure 6.7).

6.5 Ammonia nitrogen and COD

Ammonia is produced mainly by the biological degradation of proteins as nitrogenous matter and it has been assigned to be the main inhibition cause of anaerobic digestion performance and responsible for ceasing the methanogenesis process. Ammonia can disturb the methanogenic bacteria via the bacterial cell membrane pentration causing proton imbalance and ions deficiency into the bacterial cells [134].

Ammonia concentrations were gradually increased for the blank reactor, and the ammonia concentration was increased from 85 mg NH_3-N/L to reach more than 400 mg NH_3-N/L as an average concentration from the day 6. Bioreactors R2 and R5 showed a remarkable ammonia generation from the beginning of digestion period which reflects the reduction in biogas production (Figure 6.3A). Generally, when the ammonia concentrations were below 200 mg/L, the anaerobic digestion process was enhanced as in bioreactors R6 and R7. The low ammonia concentrations express nitrogen as a necessary nutrient for the methanogenic microorganisms. The high methane production could be related to the SRB and methanogenic bacteria kinetics variations in acetate and hydrogen utilization because SRB has kinetic advantages over methanogenic bacteria on their common substrates [128, 135].

As ammonia concentrations were increased in the range of 313–581 mg NH_3–N/L after 6 days of digestion and the methanogenic bacteria simultaneously lost most of its activity. These outcomes come in agreement with methanogenesis inhibitation by facilitating the reactions between the hydrochloric acid and amino acid and may be increasing the ammonium release [136]. The likely explanation is that SRB is anaerobic bacteria that utilize sulfate as an electron acceptor resulting in an increase in alkalinity, this is in agreement of Dar S. A. et al. outcomes[137].

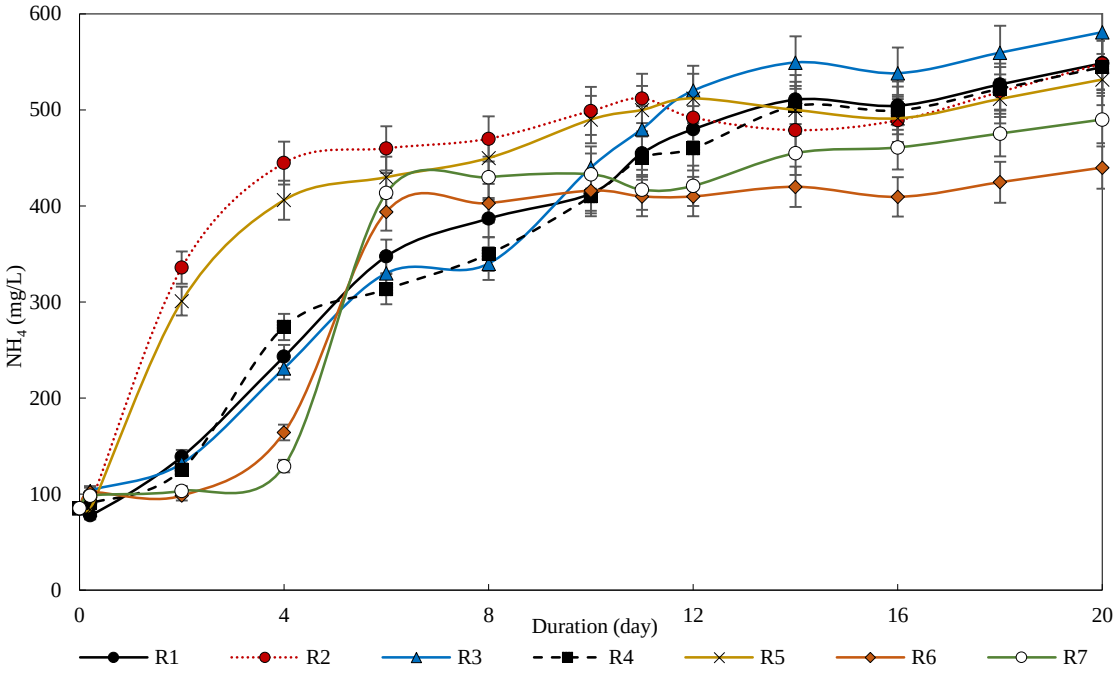

Figure 6.6 Ammonia release

Figure 6.7 shows COD concentrations for all bioreactors. The initial COD concentration was increased effectually to reach the average of 7.51 times at day 20. Compared to the amended bioreactors, the R2 bioreactor was less affected by the existence of sulfate and its COD increasing ranging was from 11.6 to 20.34% over the digestion period. During the anaerobic digestion treatment of sulfate-containing sludge, the presence of sulfate would increase the H_2S which caused toxicity to the anaerobic microorganisms, therefore, the performance declination of bioreactors exposed to sulfate concentrations.

It was observed that the COD concentrations were maintained higher than the initial COD (1954 mg/L) for all the bioreactors along the batch test period, which suggests a rapid accumulation of partially stabilizied organic materials [121] which indicates that the whole anaerobic digestion process was ceased.

During anaerobic digestion, the dynamic kinetics of the COD reflected a negative performance of methanogenic bacteria. By the end of anaerobic digestion, the COD concentrations in all bioreactors increased to 10,156; 11,764; 18,768; 15,228; 12,310; 16,333 and 17,684 mg/L for R1; R2; R3; R4; R5; R6 and R7 probably as a result of the continued endogenous biomass decay [67].

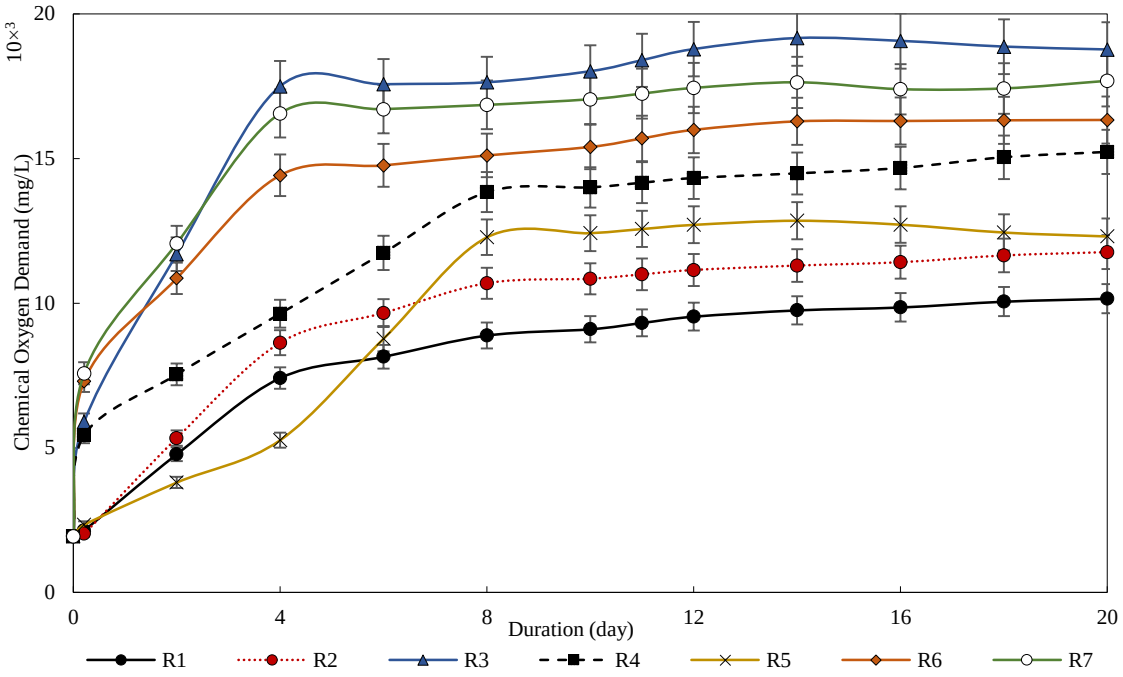

Figure 6.7 Chemical oxygen demand release

6.6 Sulfate reduction

Under anaerobic conditions and because nZVI particles in water oxidized, nZVI produce Fe^{2+} and two electrons (Eq. (6.1)). SRB use these electrons to reduce the sulfate via hydrogen formation (Eq.(6.2)).

$$Fe^0 + 2H_2O \rightarrow Fe^{2+} + H_2 + 2OH^- \quad (6.1)$$

$$SO_4^{2-} + 4H_2 + H^+ \rightarrow HS^- + 4H_2O \quad (6.2)$$

Sulfide ions in the aqueous medium have various forms (S^{2-}, HS^-, dissolved H_2S), and these forms are appeared due to the sulfate reduction process and are considered as toxic species to SRB and methanogenic bacteria. Therefore, controlling and precipitating sulfide forms in the sludge media will enhance the methane production.

Figure 6.8 clarifies the time-course of the sulfate concentration for each amended bioreactor. It can be seen that sulfate concentrations were eliminated slowly from the bioreactors exposed to small amounts of nZVI as in R2, R3, and R4. However, a more rapid removal rate of sulfate was detected in the highest nZVI concentration bioreactors R6 and R7. These experimental results clearly reveal that SRB can utilize nZVI.

The reaction between iron and sulfate species can take these following reaction pathways:

$$2CH_2O + SO_4^{2-} \rightarrow H_2S + 2HCO_3^- \quad (6.3)$$

$$Fe^{2+} + H_2S \rightarrow FeS + 2H^+ \quad (6.4)$$

$$2Fe^{3+} + HS^- \rightarrow 2Fe^{2+} + S^0 + H^+ \quad (6.5)$$

$$Fe^{2+} + HS^- \rightarrow FeS + H^+ \quad (6.6)$$

$$FeS + H_2S \rightarrow FeS_2 + H_2 \quad (6.7)$$

During the biodegradation of sulfate, SRB can react with sulfate to produce sulfide and alkalinity (Eq. (6.3)) whereas Fe^{2+} can remove sulfide by precipitation and form FeS according to Eq. (6.4) or Fe^{3+} can remove sulfide by oxidizing it chemically to elemental sulfur while being reduced to Fe^{2+}, which can subsequently produce FeS (Eq. ((6.5)) and (Eq. (6.6)). The FeS can further react with H_2S and form iron disulfide precipitate (FeS_2),

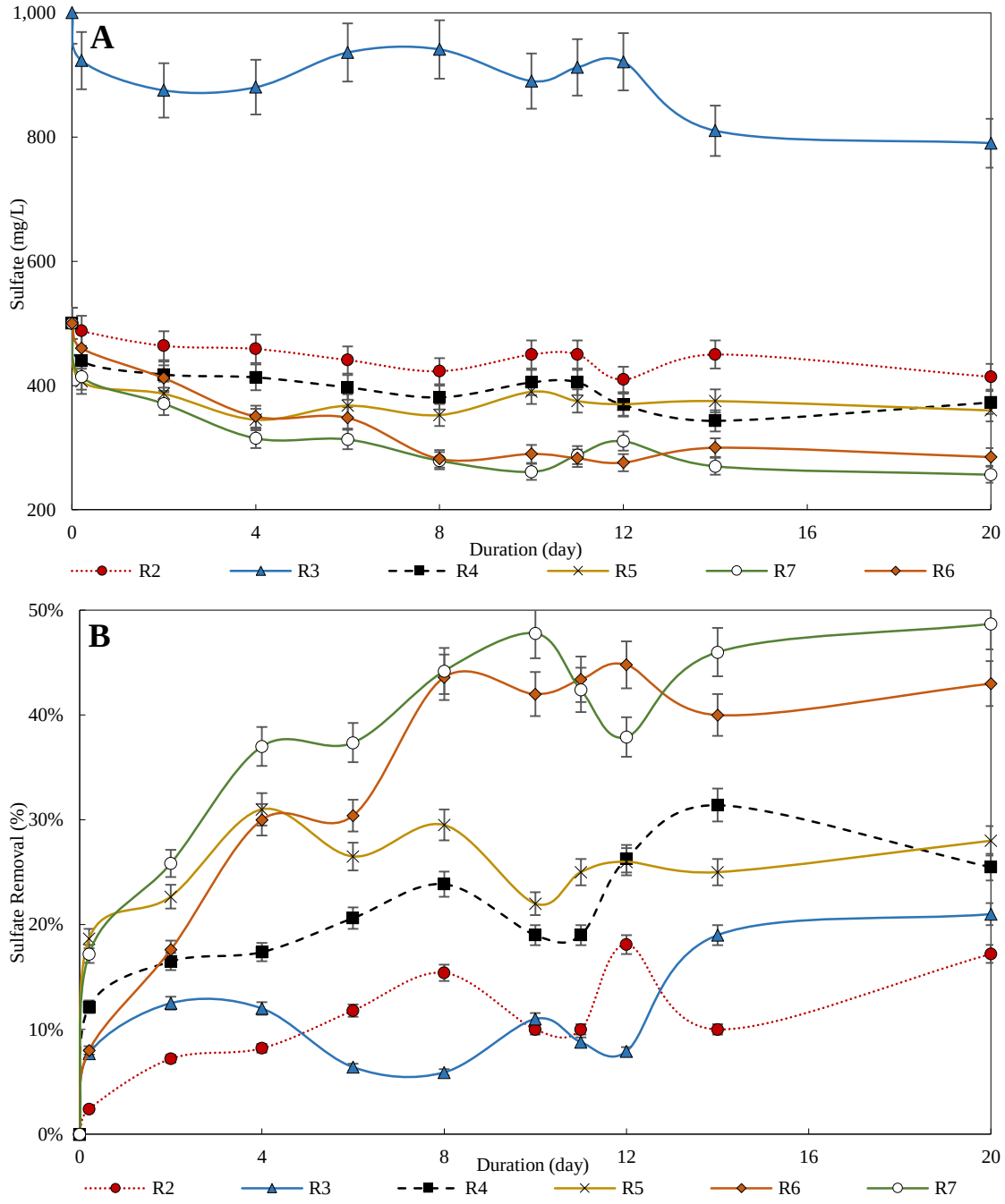

Figure 6.8 Sulfate concentration (A), Sulfate removal rate (B)

Eq. (6.7). These results were confirmed by Rickard D. et al. study that clearly demonstrates that sulfate is attached to the phosphate of adenosine triphosphate forming adenosine phosphosulfate and subsequently sulfate moiety is reduced to sulfide [138]. This process involves a noticeable fractionation of the sulfur forms and most of the sulfate ions present in the activated sludge can be precipitated as iron insoluble sulfides using biogenic sulfide produced due to the sulfate reduction by nZVI. It was indicated that SRB played a major role in the sulfate reduction and the sulfate removal by nZVI is mainly due to biodegradation rather than adsorption [62].

6.1 Conclusions

Mesophilic anaerobic digestion of waste activated sludge is clearly affected by the increasing concentration of sulfate. The nZVI presence in a reactor could effectively improve the performance of sulfate-containing sludge digestion because it can serve as an electron donor that could mitigate the competition between SRB and methanogenic bacteria for the same substrates. Also, it can precipitate the content of un-dissociated H_2S that is the main factor inhibiting anaerobic digestion of sulfate-containing sludge.

We predicted that this kind of treatment technology may hold promise to be applied in the anaerobic treatment of sulfate-containing wastewater and decrease the high costs of construction and operation of normal treatment plants and these outcomes are very interesting for carrying out the full-scale treatment of sludge substrates with a high concentration of sulfate.

CONCLUSIONS AND RECOMMENDATIONS

Chapter 7. Conclusions and recommendations

7.1 Conclusions

The main objective of this research study was to examine the addition of nZVI and its modifications as an efficient method for wastewater treatment and sludge stabilization which could be more useful and cost-effective technology.

The results of the experimental works allow outlining the following conclusions:

- The addition of high concentrations of bimetallic nZVI/Cu^0 nanoparticles to the wastewater mixed cultures enhances the microbial life regardless the availability of oxygen while the copper plated onto the nZVI can produce more Fe^{2+} ions specifically under anaerobic condition which plays a crucial role in limitation ammonia production and phosphorus concentrations during biological and chemical degradation processes in the domestic wastewater.
- The nZVI addition can stimulate the biogas production, methane gas content and can accelerate the sludge fermentation. Whereas, high nZVI/Cu^0 bimetallic concentration did not promote the cumulative volume of the generated biogas or methane content proportion while the cell disruption will occur to methanogenesis bacteria.
- The addition of ICZ causes a lag period before starting to produce a significant biogas cogeneration that reached a maximum value compared with the other bioreactors, and the higher the iron particles coated zeolite were added the more the biogas was generated.
- The preferable results of cumulative methane production were obtained when supplementing ICZ 1000 particles, which gave the maximum methane production volume.
- The nZVI presence in a reactor of mesophilic anaerobic digestion of WAS could effectively improve the performance of sulfate-containing sludge digestion because it can serve as an electron donor that could mitigate the competition between SRB and methanogenic bacteria for the same substrates. Also, it can precipitate the content of un-dissociated H_2S that is the main factor inhibiting anaerobic digestion of sulfate-containing sludge.

On the whole, it is predicted that the addition of nZVI holds a promising technology to be applied in the anaerobic treatment of activated sludge and hence decrease the high costs of construction and operation of normal treatment plants. This will open

many new doors for our better understanding and application of iron nanoparticles on wastewater treatment and sustainable resource recovery.

7.2 Recommendations

Based on the research findings, here are some suggestions and recommendations:

- Its essential to ensure an anaerobic atmosphere for more COD concentration reduction by NZVI/Cu^0
- It is advisable to dose the optimum nZVI/Cu^0 bimetallic not more than 1500 mg/L, while the cell disruption will occur and other gases such as hydrogen will be rapidly produced hence, the methanogenesis inhibition will be intentionally turned up. This would indicate that using nZVI or nZVI/Cu^0 at appropriate dosing rate could be an effective pathway for improving methane generation.
- Due to its greater biogas generation, its recommended to employ the high concentration of iron nanoparticles coated zeolite materials rather than the only the mixture of iron nanoparticles and zeolite.

7.3 Future outlook and research needs

This work represents the forthcoming stage of my research in a further continuation of the accomplishments of this thesis. The proposed title is integration of nano Fe for developing the next generation of double-stage digestion process

7.3.1 Background of proposed research plan

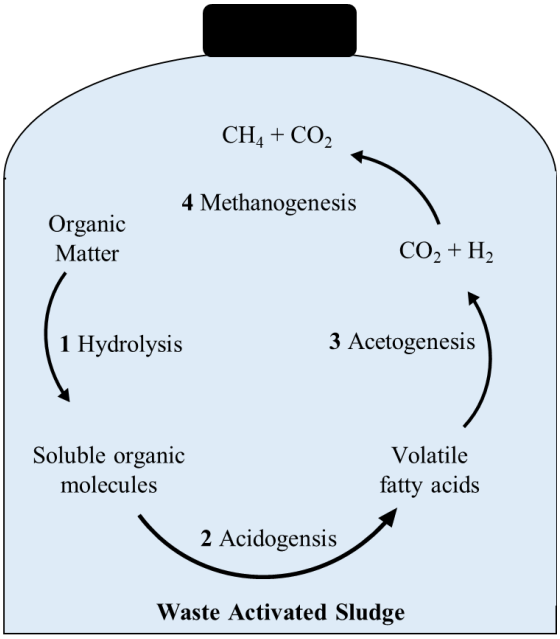

Figure 7.1 Anaerobic digestion

Due to limit supply of fossil fuel, the waste activated sludge as biomass resource is considered as an important renewable and clean energy sources. Anaerobic digestion is a biological process that converts complex substrates into biogas and digestate by microbial action in the absence of oxygen [139] through four consecutive steps, namely hydrolysis, acidogensis, acetogenesis and methanogenesis (Figure 7.1).

Generally, double-stage fermentation process which is present in the early stages of development means the phase separation of acetogenesis (Hydrogen production) from methanogenesis (methane production) in anaerobic digestion. It has been proposed recently to increase overall process performances, in terms of stability, degradation efficiencies in both acetogenesis and methanogenesis phases and thereby in terms of overall energy recovery from biomass.

Conventionally, single-stage anaerobic digestion is used for digesting the biomass and produce methane. The double-stage anaerobic digestion system consists of a acidogenic stage followed by the methanogenic stage [140].

The supplementation of iron nanoparticles known as nZVI onto double-stage anaerobic digestion process is not yet investigated and the integration of nZVI supplementation into double-stage anaerobic digestion system is promised to stimulate the energy recover compared with traditional single-phase digestion [141].

nZVI have a core−shell structure and exhibit characteristics of both hydrous iron oxides (as a sorbent) and metallic iron (as a reductant), and it have a relatively low standard potential, an inexpensive, efficient, and environmentally friendly electron donor [101].

This study is a first attempt to create a new methodology for comprehensively demonstrate the potentialities of the double-stage anaerobic digestion system with the addition of nZVI.

7.3.2 Double-stage digestion versus conventional technology

Recently, the double-stage anaerobic digestion process has often been reported as a viable way to produce bio-hydrogen and bio-methane separately. The double-stage anaerobic fermentation process is in early stages of development consisting of (a hydrogen reactor) where acidogenic process produce hydrogen gas, and (a methane reactor) where methanogenic microbes produce methane gas (Figure 7.2). This new technology is an effective system with highly efficient energy recovery.

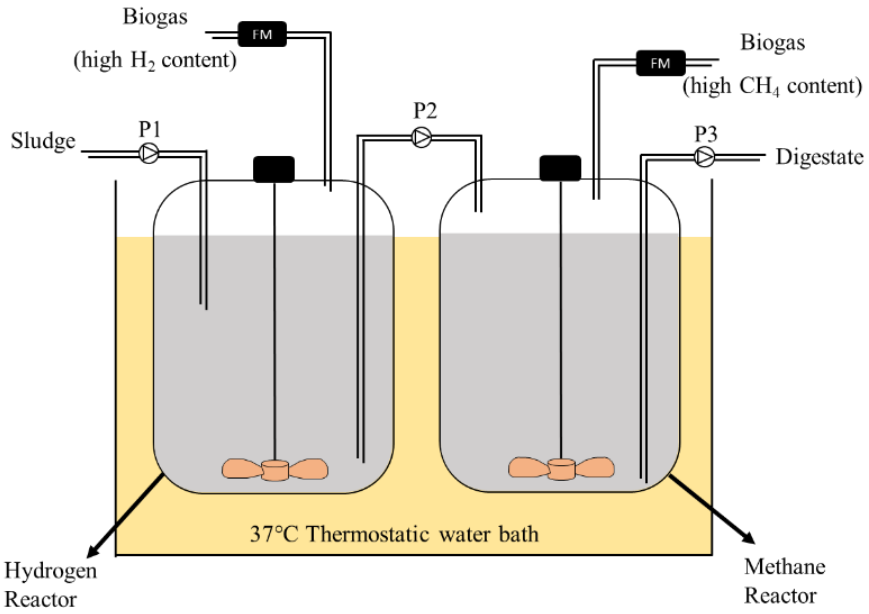

Figure 7.2 Double-stage lab-scale fermenters

The development of bio-hythane –The entire bio-hydrogen and bio-methane– production appears inevitable as the direction for future energy emerges while bio-hydrogen production is considered more environmentally friendly.

In single-stage process, the generated bio-hydrogen in the single-phase digestion is rapidly consumed by methanogenic bacteria in order to produce bio-methane.

7.3.3 Iron nanoparticles supplementation in sludge digestion

While the nZVI is very strong reducing character and it have a superior reactivity, it was successfully used for the enhancement of methane yield, elimination and diminution of inhibitory gases such as H_2S, and better sludge stabilizer during the one-stage anaerobic digestion process.

During one-stage process, comparable hydrogen amounts are produced, while concurrently hydrogen-trophic microbes convert the produced hydrogen into methane, this reaction requires a fraction of energy for microbial metabolism [3]. On the other hand, in the double-stage process, all the produced hydrogen can be recovered.

7.3.4 Setup and operation of double-stage lab-scale fermenters

Double-stage and single-stage anaerobic digestion will be assembled in lab-scale. Each setup will be supplied with waste activated sludge as substrate and will be run in semi-continuous mode. The bio-hythane productions will be optimized by varying the feeding condition in two parameters: (i) nZVI concentration and (ii) hydraulic retention time (HRT).

The optimized process was performed in batch mesophilic reactors and adapted from standard procedures of biochemical methane potential (BMP) and the energy recovery from both single and double-stage systems were compared to look for possible increase in performance of the double-stage concept.

7.3.5 Objectives of proposed research

The following objectives are proposed:

- Understand the conditions that can drive the double-stage anaerobic digestion to higher performance;
- Develop a new strategy to increase the overall anaerobic digestion process performances, in terms of stability, degradation efficiencies and increase the specific activity of methanogens in order to reach a higher methane yield;
- Investigate the effect of nZVI supplementations and determine its enhancement roles with various concentrations;
- Clarify the effect of HRTs and temperature on methane and hydrogen production;
- Optimized the lab-scale of both hydrogen and methane generation with the addition on iron nanoparticles.

7.3.6 Proposed plan

Activity description	from	to
Review, purchase, prepare, sampling and data collection: Conduct a critical literature review. Sample the activated sludge, purchase both the apparatuses used for assembling the bioreactors and the reagents for the analysis.	Oct, 2018	Nov, 2018
Research design, experimental setup and operation: Synthesis the most effective nZVI based additive. Setup both single and double-stage lab scale bioreactors. Operate the digestion process based on biochemical methane potential (BMP) test with various HRTs and several additives concentrations.	July, 2018	Sep, 2019
Data analysis: Characterize the sludge samples, digested sludge and produced biogas using several analysis instruments.	Oct, 2019	Dec, 2019
Optimization and modeling: Establish a comprehensive model to simulate and further apply the nZVI double-stage anaerobic digestion for treating waste activated sludge in which abiotic processes such as nZVI corrosion and bio-hythane production occur.	Jan, 2020	April, 2020

Future works, publication and reporting: Propose a pilot project of nZVI-double-stage process based on the works results with a cooperation with Japanese company. Write research manuscripts in order to publish it into leading scientific journals. Submit various reports to Japan society for the promotion of science.	May, 2020	Sep, 2020

7.3.7 Expected results and impacts

From all described above and based on research activities and outcomes, it's expected to:

- Develop a nZVI double-stage anaerobic digesters for co-digestion of waste activated sludge.
- Determine the most adequate concentration of nZVI, best temperature and the sufficient HRT for each bioreactor.
- Making a very attractive bio-hythane producing system.
- Increase the energy recovery from waste activated sludge.
- Expanding the biogas potential by the co-digestion of the biodegradable substrate.
- Develop a general mathematic model to simulate all the process in nZVI-based double-stage anaerobic bioreactors.

References

[1] F.L. Burton, H.D. Stensel, G. Tchobanoglous, Wastewater engineering: treatment and Resource recovery, McGraw-Hill2014.
[2] H. Akbaş, B. Bilgen, A.M. Turhan, An integrated prediction and optimization model of biogas production system at a wastewater treatment facility, Bioresour. Technol. 196 (2015) 566-576.
[3] T.W. Amen, O. Eljamal, A.M. Khalil, N. Matsunaga, Biochemical methane potential enhancement of domestic sludge digestion by adding pristine iron nanoparticles and iron nanoparticles coated zeolite compositions, J. Environ. Chem. Eng. 5 (2017) 5002-5013.
[4] H. Li, D. Si, C. Liu, K. Feng, C. Liu, Performance of direct anaerobic digestion of dewatered sludge in long-term operation, Bioresour. Technol. (2017).
[5] E. Abdelsalam, M. Samer, Y. Attia, M. Abdel-Hadi, H. Hassan, Y. Badr, Comparison of nanoparticles effects on biogas and methane production from anaerobic digestion of cattle dung slurry, Renewable Energy 87 (2016) 592-598.
[6] Y.-X. Huang, J. Guo, C. Zhang, Z. Hu, Hydrogen production from the dissolution of nano zero valent iron and its effect on anaerobic digestion, Water Res. 88 (2016) 475-480.
[7] L. Appels, J. Baeyens, J. Degrève, R. Dewil, Principles and potential of the anaerobic digestion of waste-activated sludge, Prog. Energy Combust. Sci. 34 (2008) 755-781.
[8] I.S. Horváth, M. Tabatabaei, K. Karimi, R. Kumar, Recent updates on biogas production-a review, Bio. Res. J. 3 (2016) 394-402.
[9] D. Copetti, K. Finsterle, L. Marziali, F. Stefani, G. Tartari, G. Douglas, K. Reitzel, B.M. Spears, I.J. Winfield, G. Crosa, Eutrophication management in surface waters using lanthanum modified bentonite: a review, Water Res. 97 (2016) 162-174.
[10] A.A. Badejo, D.O. Omole, J.M. Ndambuki, W.K. Kupolati, Municipal wastewater treatment using sequential activated sludge reactor and vegetated submerged bed constructed wetland planted with Vetiveria zizanioides, Ecolo.l Eng. 99 (2017) 525-529.
[11] J. Zhang, W. Li, J. Lee, K.-C. Loh, Y. Dai, Y.W. Tong, Enhancement of biogas production in anaerobic co-digestion of food waste and waste activated sludge by biological co-pretreatment, Energy (2017).
[12] C. Liu, H. Li, Y. Zhang, C. Liu, Improve biogas production from low-organic-content sludge through high-solids anaerobic co-digestion with food waste, Bioresour. Technol. 219 (2016) 252-260.
[13] V.K. Tyagi, S.-L. Lo, Sludge: a waste or renewable source for energy and resources recovery?, Renewable and Sustainable Energy Reviews 25 (2013) 708-728.
[14] J.-H. Tay, K.-Y. Show, D.-J. Lee, S.-Y. Hong, Reuse of wastewater sludge with marine clay as a new resource of construction aggregates, Water Science and Technology 50 (2004) 189-196.
[15] H. Wang, S.L. Brown, G.N. Magesan, A.H. Slade, M. Quintern, P.W. Clinton, T.W. Payn, Technological options for the management of biosolids, Environmental Science and Pollution Research-International 15 (2008) 308-317.
[16] Y. Lin, S. Zhou, F. Li, Y. Lin, Utilization of municipal sewage sludge as additives for the production of eco-cement, J. Hazard Mater. 213 (2012) 457-465.
[17] L. Spinosa, From sludge to resources through biosolids, Water science and technology 50 (2004) 1-9.
[18] C. Vongvichiankul, J. Deebao, W. Khongnakorn, Relationship between pH, Oxidation Reduction Potential (ORP) and Biogas Production in Mesophilic Screw Anaerobic Digester, Energy Procedia 138 (2017) 877-882.
[19] M.H. Gerardi, The microbiology of anaerobic digesters, John Wiley & Sons2003.

[20] A. Wellinger, J.D. Murphy, D. Baxter, The biogas handbook: science, production and applications, Elsevier2013.
[21] S. Wei, Y. Guo, Comparative study of reactor performance and microbial community in psychrophilic and mesophilic biogas digesters under solid state condition, J. Biosci Bioeng. (2018).
[22] C. Da Ros, C. Cavinato, P. Pavan, D. Bolzonella, Mesophilic and thermophilic anaerobic co-digestion of winery wastewater sludge and wine lees: An integrated approach for sustainable wine production, J. Environ. Manage. (2016).
[23] S.A. Ghanimeh, D.N. Al-Sanioura, P.E. Saikaly, M. El-Fadel, Correlation between system performance and bacterial composition under varied mixing intensity in thermophilic anaerobic digestion of food waste, J. Environ. Manage. 206 (2018) 472-481.
[24] P. Kongjan, O. Sompong, I. Angelidaki, Performance and microbial community analysis of two-stage process with extreme thermophilic hydrogen and thermophilic methane production from hydrolysate in UASB reactors, Bioresour. Technol. 102 (2011) 4028-4035.
[25] Y. Chen, J.J. Cheng, K.S. Creamer, Inhibition of anaerobic digestion process: a review, Bioresour. Technol. 99 (2008) 4044-4064.
[26] B. Kanokwan, Online monitoring and control of the biogas process, Phd Thesis Institute of Environment & Resouces, Technical University of Denmark, 2006.
[27] I.S. Turovskiy, P. Mathai, Wastewater sludge processing, John Wiley & Sons2006.
[28] M.H. Hwang, N.J. Jang, S.H. Hyun, I.S. Kim, Anaerobic bio-hydrogen production from ethanol fermentation: the role of pH, J. Biotechnol. 111 (2004) 297-309.
[29] I.H. Franke-Whittle, A. Walter, C. Ebner, H. Insam, Investigation into the effect of high concentrations of volatile fatty acids in anaerobic digestion on methanogenic communities, Waste management 34 (2014) 2080-2089.
[30] P.F. Pind, I. Angelidaki, B.K. Ahring, K. Stamatelatou, G. Lyberatos, Monitoring and control of anaerobic reactors, Biomethanation II, Springer2003, pp. 135-182.
[31] D. Deublein, A. Steinhauser, Biogas from waste and renewable resources: an introduction, John Wiley & Sons2011.
[32] H.B. Møller, S.G. Sommer, B.K. Ahring, Methane productivity of manure, straw and solid fractions of manure, Biomass and bioenergy 26 (2004) 485-495.
[33] K. Yadav, J. Singh, N. Gupta, V. Kumar, A Review of Nanobioremediation Technologies for Environmental Cleanup: A Novel Biological Approach, (2017).
[34] M.C. Roco, The emergence and policy implications of converging new technologies integrated from the nanoscale, J. Nanopart. Res. 7 (2005) 129-143.
[35] R. Dastjerdi, M. Montazer, A review on the application of inorganic nano-structured materials in the modification of textiles: focus on anti-microbial properties, Colloids Surf. B Biointerfaces 79 (2010) 5-18.
[36] G.L. Hornyak, J.J. Moore, H.F. Tibbals, J. Dutta, Fundamentals of nanotechnology, CRC press2008.
[37] F. Fu, D.D. Dionysiou, H. Liu, The use of zero-valent iron for groundwater remediation and wastewater treatment: a review, J. Hazard Mater. 267 (2014) 194-205.
[38] C.-B. Wang, W.-X. Zhang, Synthesizing nanoscale iron particles for rapid and complete dechlorination of TCE and PCBs, J. Environ. Sci. Technol 31 (1997) 2154-2156.
[39] X. Guo, Z. Yang, H. Dong, X. Guan, Q. Ren, X. Lv, X. Jin, Simple combination of oxidants with zero-valent-iron (ZVI) achieved very rapid and highly efficient removal of heavy metals from water, Water Res. 88 (2016) 671-680.
[40] A. Khan, S.M. Prabhu, J. Park, W. Lee, C.-M. Chon, J.S. Ahn, G. Lee, Azo dye decolorization by ZVI under circum-neutral pH conditions and the characterization of

ZVI corrosion products, Journal of Industrial and Engineering Chemistry 47 (2017) 86-93.
[41] Y. Zhang, G.B. Douglas, L. Pu, Q. Zhao, Y. Tang, W. Xu, B. Luo, W. Hong, L. Cui, Z. Ye, Zero-valent iron-facilitated reduction of nitrate: Chemical kinetics and reaction pathways, Sci. Total Environ. 598 (2017) 1140-1150.
[42] Z. Yang, X. Ma, C. Shan, Z. Fang, B. Pan, Enhanced Nitrobenzene reduction by zero valent iron pretreated with H 2 O 2/HCl, Chemosphere (2018).
[43] I.-H. Yoon, G. Yoo, H.-J. Hong, J. Kim, M.G. Kim, W.-K. Choi, J.-W. Yang, Kinetic study for phenol degradation by ZVI-assisted Fenton reaction and related iron corrosion investigated by X-ray absorption spectroscopy, Chemosphere 145 (2016) 409-415.
[44] B.D. Yirsaw, M. Megharaj, Z. Chen, R. Naidu, Environmental application and ecological significance of nano-zero valent iron, J. Environ. Sci. 44 (2016) 88-98.
[45] Y. Liu, G.V. Lowry, Effect of particle age (Fe0 content) and solution pH on NZVI reactivity: H2 evolution and TCE dechlorination, J. Environ. Sci. Technol 40 (2006) 6085-6090.
[46] F. Fu, J. Ma, L. Xie, B. Tang, W. Han, S. Lin, Chromium removal using resin supported nanoscale zero-valent iron, J. Environ. Manage. 128 (2013) 822-827.
[47] X.-q. Li, W.-x. Zhang, Sequestration of metal cations with zerovalent iron nanoparticles a study with high resolution X-ray photoelectron spectroscopy (HR-XPS), J. Phys. Chem. C 111 (2007) 6939-6946.
[48] R. Crane, T. Scott, Nanoscale zero-valent iron: future prospects for an emerging water treatment technology, J. Hazard. Mater. 211 (2012) 112-125.
[49] B. Lai, Y. Zhang, Z. Chen, P. Yang, Y. Zhou, J. Wang, Removal of p-nitrophenol (PNP) in aqueous solution by the micron-scale iron–copper (Fe/Cu) bimetallic particles, Appl. Catal., B. 144 (2014) 816-830.
[50] N. Fernández, S. Montalvo, F. Fernández-Polanco, L. Guerrero, I. Cortés, R. Borja, E. Sánchez, L. Travieso, Real evidence about zeolite as microorganisms immobilizer in anaerobic fluidized bed reactors, Process Biochem. 42 (2007) 721-728.
[51] S. Bhowmick, S. Chakraborty, P. Mondal, W. Van Renterghem, S. Van den Berghe, G. Roman-Ross, D. Chatterjee, M. Iglesias, Montmorillonite-supported nanoscale zero-valent iron for removal of arsenic from aqueous solution: Kinetics and mechanism, Chem. Eng. J. 243 (2014) 14-23.
[52] M. Sarioglu, Removal of ammonium from municipal wastewater using natural Turkish (Dogantepe) zeolite, Sep. Purif. Technol. 41 (2005) 1-11.
[53] Z. Li, L. Wang, J. Meng, X. Liu, J. Xu, F. Wang, P. Brookes, Zeolite-supported nanoscale zero-valent iron: New findings on simultaneous adsorption of Cd (II), Pb (II), and As (III) in aqueous solution and soil, J. Hazard Mater. 344 (2018) 1-11.
[54] Y. Zeng, H. Walker, Q. Zhu, Reduction of nitrate by NaY zeolite supported Fe, Cu/Fe and Mn/Fe nanoparticles, J. Hazard Mater. 324 (2017) 605-616.
[55] N. Arancibia-Miranda, S.E. Baltazar, A. García, D. Munoz-Lira, P. Sepúlveda, M.A. Rubio, D. Altbir, Nanoscale zero valent supported by zeolite and montmorillonite: template effect of the removal of lead ion from an aqueous solution, J. Hazard Mater. 301 (2016) 371-380.
[56] A.-B. InBev, A. Worldwide, B. Auto, C. Chance, D.P. DHL, S. Embraer, E. SpA, G.I. SA, S. Iberdrola, N. Mining, World Economic Forum, (2015).
[57] A.M. Khalil, O. Eljamal, S. Jribi, N. Matsunaga, Promoting nitrate reduction kinetics by nanoscale zero valent iron in water via copper salt addition, Chem. Eng. J. 287 (2016) 367-380.

[58] N. Efecan, T. Shahwan, A.E. Eroğlu, I. Lieberwirth, Characterization of the uptake of aqueous Ni 2+ ions on nanoparticles of zero-valent iron (nZVI), Desalination 249 (2009) 1048-1054.
[59] M.S. Mak, P. Rao, I.M. Lo, Effects of hardness and alkalinity on the removal of arsenic (V) from humic acid-deficient and humic acid-rich groundwater by zero-valent iron, Water Res. 43 (2009) 4296-4304.
[60] I.A. Katsoyiannis, T. Ruettimann, S.J. Hug, pH dependence of Fenton reagent generation and As (III) oxidation and removal by corrosion of zero valent iron in aerated water, J. Environ. Sci. Technol 42 (2008) 7424-7430.
[61] Y. Feng, Y. Zhang, X. Quan, S. Chen, Enhanced anaerobic digestion of waste activated sludge digestion by the addition of zero valent iron, Water Res. 52 (2014) 242-250.
[62] S. Karri, R. Sierra‐Alvarez, J.A. Field, Zero valent iron as an electron‐donor for methanogenesis and sulfate reduction in anaerobic sludge, Biotechnol. Bioeng. 92 (2005) 810-819.
[63] B. Marsalek, D. Jancula, E. Marsalkova, M. Mashlan, K. Safarova, J. Tucek, R. Zboril, Multimodal action and selective toxicity of zerovalent iron nanoparticles against cyanobacteria, J. Environ. Sci. Technol 46 (2012) 2316-2323.
[64] C. Lee, J.Y. Kim, W.I. Lee, K.L. Nelson, J. Yoon, D.L. Sedlak, Bactericidal effect of zero-valent iron nanoparticles on Escherichia coli, Environ. Sci. Technol 42 (2008) 4927-4933.
[65] Y. Yang, C. Zhang, Z. Hu, Impact of metallic and metal oxide nanoparticles on wastewater treatment and anaerobic digestion, Environ. Sci. Process. Impact 15 (2013) 39-48.
[66] L. Su, X. Shi, G. Guo, A. Zhao, Y. Zhao, Stabilization of sewage sludge in the presence of nanoscale zero-valent iron (nZVI): abatement of odor and improvement of biogas production, J. Mater. Cycles Waste Manage. 15 (2013) 461-468.
[67] Y. Yang, J. Guo, Z. Hu, Impact of nano zero valent iron (NZVI) on methanogenic activity and population dynamics in anaerobic digestion, Water Res. 47 (2013) 6790-6800.
[68] Y. Zhang, Y. Feng, Q. Yu, Z. Xu, X. Quan, Enhanced high-solids anaerobic digestion of waste activated sludge by the addition of scrap iron, Bioresour. Technol. 159 (2014) 297-304.
[69] J. Zhang, Y. Zhang, X. Quan, Y. Liu, X. An, S. Chen, H. Zhao, Bioaugmentation and functional partitioning in a zero valent iron-anaerobic reactor for sulfate-containing wastewater treatment, Chem. Eng. J. 174 (2011) 159-165.
[70] Y. Zhang, Y. Jing, J. Zhang, L. Sun, X. Quan, Performance of a ZVI‐UASB reactor for azo dye wastewater treatment, J. Chem. Technol. Biotechnol. 86 (2011) 199-204.
[71] T.L. Kirschling, K.B. Gregory, J. Minkley, Edwin G, G.V. Lowry, R.D. Tilton, Impact of nanoscale zero valent iron on geochemistry and microbial populations in trichloroethylene contaminated aquifer materials, J. Environ. Sci. Technol 44 (2010) 3474-3480.
[72] Y. Xie, H. Dong, G. Zeng, L. Tang, Z. Jiang, C. Zhang, J. Deng, L. Zhang, Y. Zhang, The interactions between nanoscale zero-valent iron and microbes in the subsurface environment: A review, J. Hazard. Mater. 321 (2017) 390-407.
[73] A.B. Cundy, L. Hopkinson, R.L. Whitby, Use of iron-based technologies in contaminated land and groundwater remediation: a review, Sci. Total Environ. 400 (2008) 42-51.

[74] P. Bardos, B. Bone, P. Daly, D. Elliott, S. Jones, G. Lowry, C. Merly, A risk/benefit appraisal for the application of nano-scale zero valent iron (nZVI) for the remediation of contaminated sites, WP9 NanoRem (2014).
[75] F. Obiri-Nyarko, S.J. Grajales-Mesa, G. Malina, An overview of permeable reactive barriers for in situ sustainable groundwater remediation, Chemosphere 111 (2014) 243-259.
[76] S. Li, W. Wang, F. Liang, W.-x. Zhang, Heavy metal removal using nanoscale zero-valent iron (nZVI): theory and application, J. Hazard Mater. 322 (2017) 163-171.
[77] J. Kumpiene, S. Ore, G. Renella, M. Mench, A. Lagerkvist, C. Maurice, Assessment of zerovalent iron for stabilization of chromium, copper, and arsenic in soil, Envi. pollu. 144 (2006) 62-69.
[78] D. Mohan, C.U. Pittman, Arsenic removal from water/wastewater using adsorbents—a critical review, J. Hazard Mater. 142 (2007) 1-53.
[79] X. Meng, G.P. Korfiatis, Removal of arsenic from Bangladesh well water using a household filtration system, BUETUNU International Workshop on Technologies for Arsenic Removal from Drinking Water, Dhaka, Bangladesh, 2001.
[80] M. Stefaniuk, P. Oleszczuk, Y.S. Ok, Review on nano zerovalent iron (nZVI): from synthesis to environmental applications, Chem. Eng. J. 287 (2016) 618-632.
[81] G.N. Glavee, K.J. Klabunde, C.M. Sorensen, G.C. Hadjipanayis, Chemistry of borohydride reduction of iron (II) and iron (III) ions in aqueous and nonaqueous media. Formation of nanoscale Fe, FeB, and Fe2B powders, Inorg. Chem. 34 (1995) 28-35.
[82] P.H. Rieger, Electrochemistry, Second Edition ed., Chapman & Hall1994.
[83] Y. Guo, W. Huang, B. Chen, Y. Zhao, D. Liu, Y. Sun, B. Gong, Removal of tetracycline from aqueous solution by MCM-41-zeolite A loaded nano zero valent iron: Synthesis, characteristic, adsorption performance and mechanism, J. Hazard Mater. (2017).
[84] K.Y. Foo, B.H. Hameed, Insights into the modeling of adsorption isotherm systems, Chem. Eng. J. 156 (2010) 2-10.
[85] W.E. Federation, A.P.H. Association, Standard methods for the examination of water and wastewater, American Public Health Association (APHA): Washington, DC, USA (2012).
[86] K.A. Schug, I. Sawicki, D.D. Carlton Jr, H. Fan, H.M. McNair, J.P. Nimmo, P. Kroll, J. Smuts, P. Walsh, D. Harrison, Vacuum ultraviolet detector for gas chromatography, J Analyt. Chem. 86 (2014) 8329-8335.
[87] R. Li, Y. Gao, X. Jin, Z. Chen, M. Megharaj, R. Naidu, Fenton-like oxidation of 2, 4-DCP in aqueous solution using iron-based nanoparticles as the heterogeneous catalyst, J. Colloid Interface Sci. 438 (2015) 87-93.
[88] Metcalf, Eddy, Wastewater Engineering: Treatment and Resource Recovery, McGraw-Hill international ed.2014.
[89] R.J. Barnes, C.J. van der Gast, O. Riba, L.E. Lehtovirta, J.I. Prosser, P.J. Dobson, I.P. Thompson, The impact of zero-valent iron nanoparticles on a river water bacterial community, J. Hazard Mater. 184 (2010) 73-80.
[90] C. Lee, J.Y. Kim, W.I. Lee, K.L. Nelson, J. Yoon, D.L. Sedlak, Bactericidal effect of zero-valent iron nanoparticles on Escherichia coli, Environ. Sci. Technol. 42 (2008) 4927-4933.
[91] J. Bosch, K. Heister, T. Hofmann, R.U. Meckenstock, Nanosized iron oxide colloids strongly enhance microbial iron reduction, Appl. Environ. Microbiol. 76 (2010) 184-189.
[92] N. Fujioka, M. Suzuki, S. Kurosu, Y. Kawase, Linkage of iron elution and dissolved oxygen consumption with removal of organic pollutants by nanoscale zero-valent iron:

effects of pH on iron dissolution and formation of iron oxide/hydroxide layer, Chemosphere 144 (2016) 1738-1746.
[93] T. Harada, T. Yatagai, Y. Kawase, Hydroxyl radical generation linked with iron dissolution and dissolved oxygen consumption in zero-valent iron wastewater treatment process, Chem. Eng. J. (2016).
[94] J. Chen, X. Qiu, Z. Fang, M. Yang, T. Pokeung, F. Gu, W. Cheng, B. Lan, Removal mechanism of antibiotic metronidazole from aquatic solutions by using nanoscale zero-valent iron particles, Chem. Eng. J. 181 (2012) 113-119.
[95] D.-G. Kim, Y.-H. Hwang, H.-S. Shin, S.-O. Ko, Kinetics of nitrate adsorption and reduction by nano-scale zero valent iron (NZVI): Effect of ionic strength and initial pH, KSCE J. Civ. Eng. 20 (2016) 175-187.
[96] L. Peng, Y. Liu, S.-H. Gao, X. Chen, P. Xin, X. Dai, B.-J. Ni, Evaluation on the nanoscale zero valent iron based microbial denitrification for nitrate removal from groundwater, Scientific reports 5 (2015) 12331.
[97] W. Zhao, Y. Zhang, D. Lv, M. Wang, Y. Peng, B. Li, Advanced nitrogen and phosphorus removal in the pre-denitrification anaerobic/anoxic/aerobic nitrification sequence batch reactor (pre-A 2 NSBR) treating low carbon/nitrogen (C/N) wastewater, Chem. Eng. J. 302 (2016) 296-304.
[98] O. Eljamal, J. Okawauchi, K. Hiramatsu, M. Harada, Phosphorus sorption from aqueous solution using natural materials, Environ. Earth Sci. 68 (2013) 859-863.
[99] S. Mahdavi, D. Akhzari, The removal of phosphate from aqueous solutions using two nano-structures: copper oxide and carbon tubes, Clean Technol. Environ. Policy 18 (2016) 817-827.
[100] C. He, J. Yang, L. Zhu, Q. Zhang, W. Liao, S. Liu, Y. Liao, M.A. Asi, D. Shu, pH-dependent degradation of acid orange II by zero-valent iron in presence of oxygen, Sep. Purif. Technol. 117 (2013) 59-68.
[101] O. Eljamal, A.M. Khalil, Y. Sugihara, N. Matsunaga, Phosphorus removal from aqueous solution by nanoscale zero valent iron in the presence of copper chloride, Chem. Eng. J. 293 (2016) 225-231.
[102] Y.-J. Tu, C.-F. You, Phosphorus adsorption onto green synthesized nano-bimetal ferrites: equilibrium, kinetic and thermodynamic investigation, Chem. Eng. J. 251 (2014) 285-292.
[103] Y. Lee, S.G. Zimmermann, A.T. Kieu, U. von Gunten, Ferrate (Fe (VI)) application for municipal wastewater treatment: a novel process for simultaneous micropollutant oxidation and phosphate removal, Environ. Sci. Technol. 43 (2009) 3831-3838.
[104] K. Chaithawiwat, A. Vangnai, J.M. McEvoy, B. Pruess, S. Krajangpan, E. Khan, Impact of nanoscale zero valent iron on bacteria is growth phase dependent, Chemosphere 144 (2016) 352-359.
[105] Y. Yang, S. Gajaraj, J.D. Wall, Z. Hu, A comparison of nanosilver and silver ion effects on bioreactor landfill operations and methanogenic population dynamics, Water Res. 47 (2013) 3422-3430.
[106] Y. Yang, Q. Chen, J.D. Wall, Z. Hu, Potential nanosilver impact on anaerobic digestion at moderate silver concentrations, Water Res. 46 (2012) 1176-1184.
[107] S. Qiao, T. Tian, B. Qi, J. Zhou, Methanogenesis from wastewater stimulated by addition of elemental manganese, Scientific reports 5 (2015).
[108] Y. Yang, M. Xu, J.D. Wall, Z. Hu, Nanosilver impact on methanogenesis and biogas production from municipal solid waste, Waste Manage. (Oxford) 32 (2012) 816-825.

[109] Y. Zhang, Y. Feng, X. Quan, Zero-valent iron enhanced methanogenic activity in anaerobic digestion of waste activated sludge after heat and alkali pretreatment, Waste Manage. (Oxford) 38 (2015) 297-302.
[110] B. Yu, Z. Lou, D. Zhang, A. Shan, H. Yuan, N. Zhu, K. Zhang, Variations of organic matters and microbial community in thermophilic anaerobic digestion of waste activated sludge with the addition of ferric salts, Bioresour. Technol. 179 (2015) 291-298.
[111] Z. Li, K. Greden, P.J. Alvarez, K.B. Gregory, G.V. Lowry, Adsorbed polymer and NOM limits adhesion and toxicity of nano scale zerovalent iron to E. coli, Environ. Sci. Technol. 44 (2010) 3462-3467.
[112] R. Sun, D. Xing, J. Jia, A. Zhou, L. Zhang, N. Ren, Methane production and microbial community structure for alkaline pretreated waste activated sludge, Bioresour. Technol. 169 (2014) 496-501.
[113] M. Danish, X. Gu, S. Lu, A. Ahmad, M. Naqvi, U. Farooq, X. Zhang, X. Fu, Z. Miao, Y. Xue, Efficient transformation of trichloroethylene activated through sodium percarbonate using heterogeneous zeolite supported nano zero valent iron-copper bimetallic composite, Chem. Eng. J. 308 (2017) 396-407.
[114] H. Javadian, F. Ghorbani, H.-a. Tayebi, S.H. Asl, Study of the adsorption of Cd (II) from aqueous solution using zeolite-based geopolymer, synthesized from coal fly ash; kinetic, isotherm and thermodynamic studies, Arab J Chem. 8 (2015) 837-849.
[115] S.-L. Yang, Y.-Q. Tang, M. Gou, X. Jiang, Effect of sulfate addition on methane production and sulfate reduction in a mesophilic acetate-fed anaerobic reactor, Appl. Microbiol. Biotechnol. 99 (2015) 3269-3277.
[116] X. Lu, H. Wang, F. Ma, G. Zhao, S. Wang, Enhanced anaerobic digestion of cow manure and rice straw by the supplementation of iron oxide-zeolite system, Energy & Fuels (2016).
[117] M. Romero-Güiza, J. Vila, J. Mata-Alvarez, J. Chimenos, S. Astals, The role of additives on anaerobic digestion: a review, Rene. Sus. Eng. Rev. 58 (2016) 1486-1499.
[118] Y.-g. Liang, X.-j. Li, J. Zhang, L.-g. Zhang, B. Cheng, Effect of microscale ZVI/magnetite on methane production and bioavailability of heavy metals during anaerobic digestion of diluted pig manure, Environ. Sci. Poll. Res. 24 (2017) 12328-12337.
[119] G. Zhen, X. Lu, Y.-Y. Li, Y. Liu, Y. Zhao, Influence of zero valent scrap iron (ZVSI) supply on methane production from waste activated sludge, Chem. Eng. J. 263 (2015) 461-470.
[120] S. Montalvo, L. Guerrero, R. Borja, E. Sánchez, Z. Milán, I. Cortés, M.A. de la la Rubia, Application of natural zeolites in anaerobic digestion processes: A review, Applied Clay Sci. 58 (2012) 125-133.
[121] H.K. Ahn, M. Smith, S. Kondrad, J. White, Evaluation of biogas production potential by dry anaerobic digestion of switchgrass–animal manure mixtures, Appl. Biochem. Biotechnol. 160 (2010) 965-975.
[122] M.K. Doula, Removal of Mn 2+ ions from drinking water by using clinoptilolite and a clinoptilolite–Fe oxide system, Water Res. 40 (2006) 3167-3176.
[123] F. Suanon, Q. Sun, M. Li, X. Cai, Y. Zhang, Y. Yan, C.-P. Yu, Application of nanoscale zero valent iron and iron powder during sludge anaerobic digestion: Impact on methane yield and pharmaceutical and personal care products degradation, J. Hazard. Mater. 321 (2017) 47-53.
[124] H. Shahbeig, N. Bagheri, S.A. Ghorbanian, A. Hallajisani, S. Poorkarimi, A new adsorption isotherm model of aqueous solutions on granular activated carbon, World J. Model. Simul 9 (2013) 243-254.

[125] B.-W. Pang, C.-H. Jiang, M. Yeung, Y. Ouyang, J. Xi, Removal of dissolved sulfides in aqueous solution by activated sludge: mechanism and characteristics, J. Hazard. Mater. 324 (2017) 732-738.
[126] J. Zhang, Q. Ping, M. Niu, H. Shi, N. Li, Kinetics and equilibrium studies from the methylene blue adsorption on diatomite treated with sodium hydroxide, Applied Clay Sci. 83 (2013) 12-16.
[127] S. Larous, A.-H. Meniai, M.B. Lehocine, Experimental study of the removal of copper from aqueous solutions by adsorption using sawdust, Desalination 185 (2005) 483-490.
[128] J. Sun, X. Dai, Q. Wang, Y. Pan, B.-J. Ni, Modelling Methane Production and Sulfate Reduction in Anaerobic Granular Sludge Reactor with Ethanol as Electron Donor, Scientific reports 6 (2016).
[129] X. Lu, H. Wang, F. Ma, G. Zhao, S. Wang, Enhanced Anaerobic Digestion of Cow Manure and Rice Straw by the Supplementation of an Iron Oxide–Zeolite System, Energy & Fuels 31 (2016) 599-606.
[130] A. Mshandete, L. Björnsson, A.K. Kivaisi, M.S. Rubindamayugi, B. Mattiasson, Effect of particle size on biogas yield from sisal fibre waste, Renew. Energy 31 (2006) 2385-2392.
[131] T.W. Amen, O. Eljamal, A.M. Khalil, N. Matsunaga, Biochemical methane potential enhancement of domestic sludge digestion by adding pristine iron nanoparticles and iron nanoparticles coated zeolite compositions, Journal of Environmental Chemical Engineering (2017).
[132] Z. Shi, D. Fan, R.L. Johnson, P.G. Tratnyek, J.T. Nurmi, Y. Wu, K.H. Williams, Methods for characterizing the fate and effects of nano zerovalent iron during groundwater remediation, J. Contam. Hydrol. 181 (2015) 17-35.
[133] A.H. Nielsen, P. Lens, J. Vollertsen, T. Hvitved-Jacobsen, Sulfide–iron interactions in domestic wastewater from a gravity sewer, Water Res. 39 (2005) 2747-2755.
[134] J. Siles, J. Brekelmans, M. Martin, A. Chica, A. Martin, Impact of ammonia and sulphate concentration on thermophilic anaerobic digestion, Bioresour. Technol. 101 (2010) 9040-9048.
[135] L. Raskin, B.E. Rittmann, D.A. Stahl, Competition and coexistence of sulfate-reducing and methanogenic populations in anaerobic biofilms, Appl. Environ. Microbiol. 62 (1996) 3847-3857.
[136] D. Strik, A. Domnanovich, P. Holubar, A pH-based control of ammonia in biogas during anaerobic digestion of artificial pig manure and maize silage, Process Biochem. 41 (2006) 1235-1238.
[137] S.A. Dar, R. Kleerebezem, A.J. Stams, J.G. Kuenen, G. Muyzer, Competition and coexistence of sulfate-reducing bacteria, acetogens and methanogens in a lab-scale anaerobic bioreactor as affected by changing substrate to sulfate ratio, Appl. Microbiol. Biotechnol. 78 (2008) 1045-1055.
[138] D. Rickard, G.W. Luther, Chemistry of iron sulfides, Chem. Rev. 107 (2007) 514-562.
[139] R. Rafieenia, F. Girotto, W. Peng, R. Cossu, A. Pivato, R. Raga, M.C. Lavagnolo, Effect of aerobic pre-treatment on hydrogen and methane production in a two-stage anaerobic digestion process using food waste with different compositions, Waste management 59 (2017) 194-199.
[140] T. Kobayashi, K.-Q. Xu, Y.-Y. Li, Y. Inamori, Effect of sludge recirculation on characteristics of hydrogen production in a two-stage hydrogen–methane fermentation process treating food wastes, international journal of hydrogen energy 37 (2012) 5602-5611.

[141] A. Schievano, A. Tenca, S. Lonati, E. Manzini, F. Adani, Can two-stage instead of one-stage anaerobic digestion really increase energy recovery from biomass?, Applied Energy 124 (2014) 335-342.

Appendices

A.1 List of Publications

Amen, T., Eljamal O., Khalil, A., Matsunaga, N., Evaluation of nano zero valent iron effects on fermentation of municipal anaerobic sludge and inducing biogas production, IOP Conference Series: Earth and Environmental Science, Vol. 67, article number 012004, (June, 2017).

Amen, T., Eljamal O., Khalil, A., Matsunaga, N., Biochemical methane potential enhancement of domestic sludge digestion by adding pristine iron nanoparticles and iron nanoparticles coated zeolite composition, Journal of Environmental Chemical Engineering, Vol. 5, Issue. No. 5, 5002-5013. (Oct., 2017).

Amen, T., Eljamal O., Khalil, A., Matsunaga, N., Wastewater degradation by iron/copper nanoparticles and the microorganism growth rate, Journal of Environmental Sciences, Accepted, Corrected proof, Available online 7. (Feb, 2018).

Amen, T., Eljamal O., Khalil, A., Matsunaga, N., Methane yield enhancement by the addition of new novel of iron and copper-iron bimetallic nanoparticles, Chemical Engineering and Processing: Process Intensification Journal, Vol. 130, 253-261. (June, 2018).

Amen, T., Eljamal O., Khalil, A., Matsunaga, N., Evaluation of sulfate-containing sludge stabilization and the alleviation of methanogenesis inhibitation at mesophilic temperature, Journal of Water Process Engineering, Vol. 25, 212-221. (October, 2018).

Amen, T., Eljamal O., Application of bimetallic nanoparticles during activated sludge digestion at high iron concentrations, International Symposium on Earth Science and Technology, Fukuoka, Japan, December, 2017.

Amen, T., Eljamal O., Anaerobic Digestion Enrichment by Iron-Coated Zeolite, The 19th cross straits symposium on energy and environmental science and technology (CSS-EEST19), Fukuoka, Japan, November 2017.

Amen, T., Eljamal O., Khalil, A., Matsunaga, N., Potential catalytic effect of bimetallic nanoparticles on digestion of anaerobic activated sludge, 3rd International Exchange and Innovation Conference on Engineering and Sciences (IEICES), Fukuoka, Japan, October, 2017.

Amen, T., Eljamal O., Khalil, A., Matsunaga, N., Evaluation of nano zero valent iron effects on fermentation of municipal anaerobic sludge and inducing biogas production, 7th International Conference on Environment and Industrial Innovation (ICEII), Kuala Lumpur, Malaysia, April 2016.

Amen, T., Eljamal O., Khalil, A., Sugihara Y., Matsunaga, N., Functionality of nanoscale zero-valent iron into domestic wastewater treatment and the role of microorganisms, IV.

International Chemical Engineering and Technologies Conference (CHEMTECH '16), Istanbul, Turkey, November 2016.

Amen, T., Eljamal O., Khalil, A., Sugihara Y., Matsunaga, N., Effects of iron metal on the chemical oxygen demand removal, phosphorus adsorption, and viable bacteria in domestic wastewater, 2nd International Exchange and Innovation Conference on Engineering and Sciences (IEICES), Fukuoka, Japan, October 2016.

A.2 About the author

Tareq Amen was born in 1985 in Gaza City, Palestine. He received the BSc., and MSc. degrees in Engineering from the Islamic University of Gaza, Palestine, in 2008, and 2014, respectively. Amen have gained work experience in different regional projects at the Ministry of Local Government.

In October 2015, he joined the intellectual exchange and innovation program as PhD researcher with the MEXT scholarship, Kyushu University, Japan. His main areas of research interest are environmental and chemical engineering and his PhD research focus mainly to develop a novel treatment enhancement system for waste activated sludge based on assembling and operate biochemical methane potential setup. He also worked partially as a teacher assistant at the environment and fluid science laboratory at Kyushu University.

During his PhD research, Mr. Amen consolidated useful skills and he becomes excellent time manager with the ability to work independently and he has experience in working as part of the multidisciplinary research team. As you are finished to read this thesis, his PhD research focus was mainly to develop a novel treatment enhancement system for waste activated sludge based on assembling and operate biochemical methane potential setup. In his study, nZVI was selected as a promising catalytic reactive material for wastewater treatment and sludge stabilization enhancement.

Amen succeed as a conference coordinator for the second International Exchange and Innovation Conference on Engineering & Sciences (IEICES 2016) and he also makes a lot of technical reviews for several international refereed journal and conferences.